IN VITRO STUDIES OF SEX PHEROMONE BIOSYNTHESIS IN THE YELLOW MEALWORM BEETLE, TENEBRIO MOLITOR (COLEOPTERA: TENEBRIONIDAE)

BY

RAY BACALA

A thesis submitted in partial fulfillment of the requirements for the degree of

MASTER OF SCIENCE

Department of Biochemistry and Medical Genetics
Faculty of Medicine, University of Manitoba
Winnipeg, Manitoba

THE UNIVERSITY OF MANITOBA

FACULTY OF GRADUATE STUDIES

*****

COPYRIGHT PERMISSION PAGE

In Vitro Studies of Sex Pheromone Biosynthesis in the Yellow Mealworm Beetle, *Tenebrio Molitor* (Coleoptera: Tenebrionidae)

BY

Ray Bacala

A Thesis/Practicum submitted to the Faculty of Graduate Studies of The University of Manitoba in partial fulfillment of the requirements of the degree of Master of Science

ACKNOWLEDGEMENT

I would like to express my appreciation to my thesis supervisor, Dr. Désirée Vanderwel, for her guidance and wisdom both in and outside the lab. She has been an asset both to my research and to the writing of this thesis. I would also like to thank Dr. Rob Currie for guidance through the 'statistical underworld'.

I also wish to express my gratitude towards my committee members, Dr. Barb Triggs-Raine and Dr. Jim Peeling for reviewing this thesis.

I wish to thank the students, faculty and staff (notably the omniscient office staff) in the University of Manitoba Department of Biochemistry and Medical Genetics for making my educational experience pleasant and enjoyable. I would also like to thank the students, faculty and staff of the University of Winnipeg Department of Chemistry for being supportive of my endeavors and providing a productive work environment.

TABLE OF CONTENTS

TABLE OF CONTENTS

LIST OF FIGURES

ABSTRACT

The mature female yellow mealworm beetle, *Tenebrio molitor*, uses 4-methylnonanol as a sex attractant pheromone. Data from *in vivo* studies suggest that the terminal biosynthetic step, reduction of 4-methylnonanoic acid (or derivative) to 4-methylnonanol, is regulated by Juvenile Hormone (JH) III. The goals of this study were (i) to develop synthetic routes to commercially unavailable substrates and standards required to study the reduction of 4-methylnonanoic acid (or derivative); (ii) to develop an *in vitro* assay for the reduction of 4-methylnonanoic acid (or derivative) to 4-methylnonanol in the yellow mealworm beetle; (iii) and to confirm that the reduction of 4-methylonanoic acid is regulated by JH. A facile synthetic route to racemic 4-methylnonanoic acid and 4-methylnonanol was developed. As the overall yields were low (11.8% and 10.1%, respectively), a second route involving a Claisen orthoester rearrangement was developed, producing racemic 4-methylnonanol in 21.2% overall yield. [^{3}H]-4-Methylnonanoyl-CoA was synthesized in yields ranging from 10% to 20% using an enzymatic method. The *in vitro* assay was performed by incubating crude or partially purified (by differential centrifugation) enzyme in the presence of tritium labeled 4-methylnonanoyl-CoA and reducing cofactor (NADH and/or NADPH). Products were solvent extracted, resolved by silica gel chromatography and quantified by liquid scintillation counting. Activity was increased by incorporating protease inhibitors during the protein isolation, and increased further by decreasing the ionic strength of the isolation/assay buffer. The activity in the crude protein experiments was largely compromised by an extremely active thioesterase activity, which destroyed the substrate. This problem was reduced dramatically by sub-cellular fractionation, as the majority of the thioesterase activity was localized in the soluble fraction, while the reductase was in the 10 000 x g pellet. Localization of reductase activity in the 10 000 x g pellet was unexpected, as all known eukaryotic acyl-CoA reductases are microsomal. Higher activity was observed in crude protein

assays using NADH as reducing cofactor. However, there was no detectable difference between NADH and NADPH when using protein isolated from the 10 000 x g pellet. Although the assay was optimized for time and protein concentration, NADH and NADPH activity curves must yet be determined to find the preferred reducing cofactor and optimal concentration. Preliminary results suggest that females and not males are able to perform the conversion. The inability of males to reduce 4-methylnonanoyl-CoA implies that the conversion is a regluated step of sex pheromone biosynthesis in the yellow mealworm beetle.

1.0.0. INTRODUCTION

Pheromones are chemicals used by individuals to convey specific messages to others of the same species. Pheromone use is highly evolved in insects, and mediates processes such as mating, aggregation/anti-aggregation, alarm signaling, foraging, and trail marking. The many molecules used by insects as pheromones are structurally diverse and may be of fatty acid, terpenoid, amino acid or unknown origin (Vanderwel and Oehlschlager, 1987). Such a wide spectrum of pheromone molecules no doubt involves an equally wide spectrum of biosynthetic pathways, which have only begun to be explored. A greater understanding of the biochemistry of pheromone production may eventually lead to the development of environmentally friendly pest monitoring or control strategies.

Although pheromone biosynthesis has been studied extensively in moths, the process in beetles has received much less attention. Furthermore, what is known of beetle pheromone biosynthesis mostly concerns aggregation pheromones, while little is known about sex pheromone biosynthesis. The yellow mealworm beetle, *Tenebrio molitor*, serves as an attractive model for studies on sex pheromone biosynthesis as it is commercially available, easily reared and many aspects of its physiology have been characterized. The goal of our lab is to further the knowledge of sex pheromone biosynthesis and regulation in beetles using *T. molitor* as a model for study. A better understanding of sex pheromone biosynthesis in *T. molitor* would aid future studies of similar processes in other beetle species.

Early investigations found the adult female yellow mealworm beetle produced a sex attractant pheromone and studied its regulation using behavioral assays, long before the pheromone's chemical identity was elucidated. Sex pheromone levels are extremely low in

newly eclosed (emerged as an adult from the pupal state) females, who usually do not mate and are not attractive to males for the first three days of adult life (Gerber, 1973). Female attractiveness to males increases over time, reaching a maximum between 4 days (Happ and Wheeler, 1969; Happ, 1970) and 7 days (Tschinkel, *et al.*, 1967) post-eclosion. Activity remains relatively constant until between 9 days (Tschinkel, *et al.*, 1967; Menon and Nair, 1976) and 11 days (Happ and Wheeler, 1969), at which point it decreases over the life of the beetle (Tschinkel *et al.*, 1967). This female-produced male attractant pheromone was later identified as (4*R*)-(+)-4-methylnonanol (Tanaka *et al.*, 1986; Tanaka *et al.*, 1989). Recently, through stable isotope labeling studies, the biosynthetic route to 4-methylnonanol was elucidated (Islam *et al.*, 1999). As summarized in Figure 1, the pathway is basically a modification of normal fatty acid biosynthesis. Production is initiated with a propionyl moiety (presumably propionyl-CoA), to which a two-carbon unit (presumably via malonyl-CoA) is added, followed by a three-carbon unit (presumably via methylmalonyl-CoA) to create the methyl branch, followed by another two-carbon unit (again, presumably via malonyl-CoA). The pathway is completed by reduction of the 4-methylnonanoyl moiety (possibly as an acyl carrier protein or CoA conjugate, or as the free acid) to the behaviorally active alcohol.

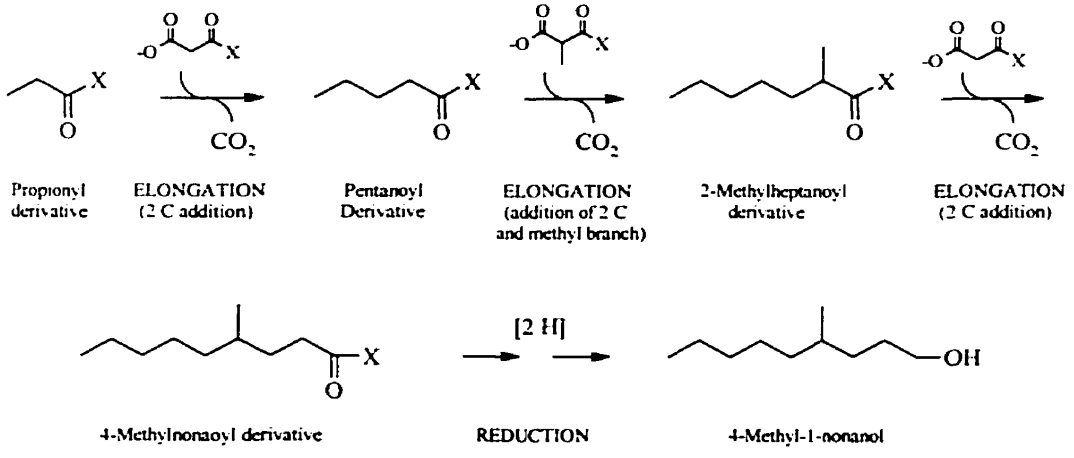

Figure 1: Biosynthetic route to 4-methyl-1-nonanol in female *T. molitor* (Islam *et al.*, 1999). X is likely coenzyme A or acyl carrier protein, although species may also be present as the free acid.

1.1.0. LITERATURE REVIEW

The levels of 4-methylnonanol in the female yellow mealworm are regulated by Juvenile Hormone (JH) III (Menon, 1970). JH III is produced in the corpora allata (a pair of glands in the head, associated with the brain) and stored and released from the corpora cardiaca (two glands closely associated with the corpora allata). Removal of the corpora allata and corpora cardiaca greatly diminishes pheromone production in mature female yellow mealworms when compared to sham operated controls (Menon, 1970). This decrease, however, is reversed by injection or topical treatment with the JH analogues (JHA) farnesyl methyl ether and *trans*, *trans*,-N,N-diethyl-3,7,11-trimethyl-10-11-epoxydodeca-2,6-dienamide. Menon and Nair (1976) demonstrated that the latter JHA can also increase pheromone levels in immature females (which do not produce pheromone) to levels above those of mature females. Furthermore, corpora allata from adult *T. molitor* specimens produce JH III *in vitro*, while those from immature females do not (Judy *et al.*, 1975). This suggests a model where as JH III levels increase during maturity, pheromone activity is gradually up-regulated. At the physiological level, it is as yet unclear how pheromone levels are modulated. The simplest explanation would be that JH mediates the stimulation of pheromone biosynthesis at the cellular level by increasing the levels of one or more enzymes involved in the 4-methylnonanol biosynthetic pathway. However, other explanations are possible. For example, JH might regulate pheromone release (where pheromone transport to or release from a pheromone gland is regulated by JH). Alternatively, pheromone production may be constitutively active and a degradative pathway may be present that modulates pheromone titre. This degradative pathway may be inhibited by JH, slowly being 'turned off' as the beetle matures and JH levels increase, thus allowing pheromone levels to rise. JH III generally acts as a transcriptional regulator, although the events from hormone reception

to transcriptional activation or repression have not been well-defined (Laufer and Borst, 1983; Jones, 1995). JH mediates events by one of two distinct mechanisms: either by binding to high affinity nuclear receptors; or by binding to cell surface receptors and activating an inositol triphosphate-mediated second message system (Nijhout, 1994). Exactly how JH III modulates 4-methylnonanol levels, however, remains to be elucidated.

1.1.1. *JH Regulation of Pheromone Biosynthesis in Other Insects*

JH has been implicated in the regulation of pheromone biosynthesis in over a dozen species of beetle in addition to *T. molitor* (Vanderwel and Oehlschlager, 1987; Vanderwel, 1994). Unfortunately, only preliminary investigations have been completed in most systems and many of the biosynthetic pathways involved are poorly defined. In the boll weevil, *Anthonomis grandis*, biosynthesis of the male-produced four-component aggregation pheromone blend is stimulated when beetles are fed a JH III-supplemented diet (Hedin *et al.*, 1982) or treated topically with the JHA methoprene (Dickens *et al.*, 1988). Wiygul *et al.* (1990) subsequently determined that pheromone biosynthesis occurs in the fat body and that JH III stimulates pheromone production when the fat body is incubated *in vitro* along with ß-bisabolol (a major terpenoid volatile of cotton, the natural boll weevil host). Since JH III is terpenoid in origin as are the aggregation pheromones of the boll weevil, it is possible that JH III is simply acting as a precursor (*i.e.*, more substrate may yield more activity), rather than a hormone. Further study, such as the development of a cell-free *in vitro* assay or use of a non-terpenoid JHA (which could act as a hormone, but not as a pheromone precursor) are necessary before the true mode of JH action may be elucidated. If JH is indeed functioning hormonally, it must be acting directly at the site of pheromone biosynthesis (Wiygul *et al.*, 1990) and not through a secondary brain

hormone, as JH is sufficient to increase activity in fat body incubations (where the brain and other brain factors are absent).

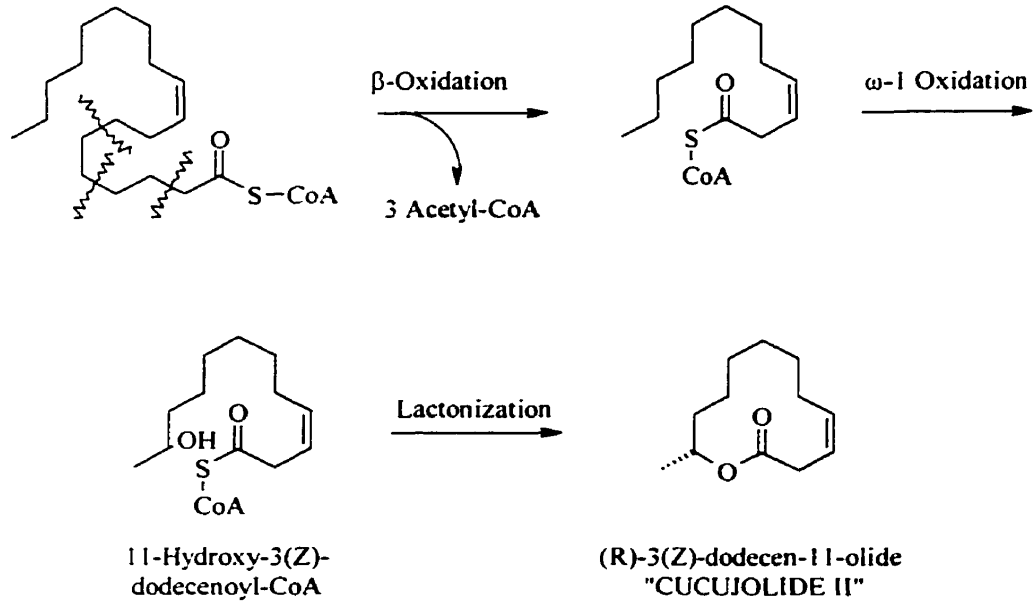

Figure 2: Biosynthetic route to Cucujolide II, *Orzaephilus mercator* aggregation pheromone (Vanderwel *et al.*, 1992).

Production of the male-produced aggregation pheromones of the grain beetles *Orzaephilus mercator*, *O. surinamensis*, *Cryptolestes ferrugineus* and *Tenebrio casteneum* is stimulated by feeding on oats treated with the JHA methoprene (Pierce *et al.*, 1986). The biosynthetic route to cucujolide II [3(Z)-dodecen-11-olide], the fatty acid derived aggregation pheromone of the merchant grain beetle, was elucidated through stable isotope labeling studies (Figure 2) (Vanderwel *et al.*, 1992). Biosynthesis consists of chain-shortening of a fatty acid, such as oleic acid (likely through ß-oxidation as the CoA derivative), to 3(Z)-dodecenoyl-CoA, followed by hydroxylation of the penultimate carbon (second to last in the chain), and finally stereospecific cyclization. Pheromone biosynthesis is drastically reduced in starved merchant grain beetles (Pierce *et al.*, 1986). The biosynthetic point for this regulation seems to be the

hydroxylation of 3(Z)-dodecenoyl-CoA (Vanderwel, 1991; Vanderwel 1994). It is also possible that this step is the target for JH regulation as well, though this remains to be proven.

In the female western pine beetle *Dendroctonus brevicomis*, aggregation pheromone biosynthesis is stimulated by either JH treatment or by ingestion of a polar factor from the host tree (Hughes and Renwick, 1977a). JH likely works directly at the site of pheromone production in *D. brevicomis*, as pheromone production may be stimulated by JH in decapitated beetles (where there is no source of secondary brain hormones that JH could stimulate the release of). In contrast, aggregation pheromone production in male European fir engraver beetles *Pityokteines curvidens*, *P. spinidens* and *P. vorontzovi* (Harring, 1978), and the bark beetle *Ips paraconfusus* (Hughes and Renwick, 1977b) is controlled by feeding or JH. Interestingly, stimulation of pheromone production by JH is prevented by decapitation (indicating another brain factor, or neural impulses, is/are required) and production was recovered when the CC (with or without the CA) were implanted. Furthermore, the effect of JH stimulation could be mimicked by gut distention (by feeding or artificially by air injection), indicating that a component from the specific host was not required. Whether feeding stimulates JH production or acts through a separate mechanism (perhaps by bypassing JH and stimulating the release of a second brain factor) remains to be determined. Synthesis of ipsdienone, implicated precursors of the two terpenoid components of the *I. paraconfusus* aggregation pheromone blend, has been localized in the metathorax (Ivarsson *et al.*, 1998). Interestingly, the mRNA for ß-hydroxy-ß-methylglutaryl-CoA reductase (HMG-R), the rate limiting enzyme in terpene biosynthesis, also specifically accumulates in the thorax (Ivarsson *et al.*, 1998) and may be stimulated further by JH treatment (Tittiger *et al.*, 1999). Although progress in this area is promising, increased HMG-R mRNA has not yet been linked to increased HMG-R levels, nor has HMG-R been implicated in the biosynthetic pathway of *I. paraconfusus* aggregation pheromones.

Modulation of pheromone production by JH has been demonstrated in several non-beetle insect species as well. In moths, pheromone biosynthesis activating neuropeptide (PBAN) is the apparently ubiquitous regulator of sex pheromone biosynthesis and JH has only been implicated as a regulator in two noctuid moths: *Pseudaletia unipuncta* and *Agrotis ipsilon* (Raina, 1997; McNeil *et al.*, 1997). While PBAN still regulates pheromone biosynthesis in both *P. unipuncta* (Cusson and McNeil, 1989; Cusson *et al.*, 1994) and *A. ipsilon* (Gadenne, 1993; Picimbon *et al.*, 1995). PBAN biosynthesis is, in turn, regulated by JH. It is possible that this higher regulation of sex pheromone production serves some ecological purpose, as these moths are migratory and most others studied are not (McNeil *et al.*, 1997). The desert locust *Schistocerca gregaria* produces a four-component aggregation and maturation inducing pheromone blend (Tawfik *et al.*, 1997). When fifth instar nymphs or adults were exposed to JH by injection, topical application or by fumigation, onset of pheromone production was retarded and maximal production levels were lower than in untreated individuals (Tawfik *et al.*, 1997). Unfortunately, as the effect was greater in nymphs than adults, this decrease is likely due to the juvenizing effects of JH (retarding maturation) rather than direct control of pheromone biosynthesis. Females of the german cockroach, *Blatella germanica*, and the brown-banded cockroach, *Supella longipalpa*, produce their respective sex attractant pheromones upon maturation. The advent of pheromone production is completely prevented by CA removal, and may be rescued by re-implantation of the CA or topical treatment with JH (Schal *et al.*, 1997). Unfortunately, it is unknown whether JH acts directly on the sternal pit glands, which produce pheromone, or by stimulation of a secondary brain hormone as in *P. unipuncta* and *A. ipsilon*.

Although this review of the literature for JH regulation of pheromone biosynthesis is not exhaustive, it summarizes current knowledge in the best-studied systems. In addition to the

evolution of many different classes of pheromones (frass, volatile, contact, etc.), pheromones are used to communicate a wide diversity of messages (aggregation, sex attractant, copulation, copulation release, growth inducing, and alarm, to name a few). Taken together with the diverse biosynthetic origins of pheromone molecules, these factors present a diverse mixture of molecules and likely an almost as diverse collection of biosynthetic pathways, making it extremely unlikely that a single overlying mechanism exists to regulate biosynthesis of all coleopteran pheromones. Furthermore, no coleopteran sex attractant pheromones have been studied with which to draw parallels with 4-methylnonanol biosynthesis in the yellow mealworm.

1.2.0. RESEARCH PROJECT SYNOPSIS

The long-term goal of these studies is to elucidate the regulated steps of 4-methylnonanol biosynthesis at the metabolic level. *In vivo* studies have shown that the JHA methoprene is able to stimulate the last step of pheromone biosynthesis, the reduction of 4-methylnonanoic acid to pheromone in immature and decapitated females (which contain little or no pheromone by bioassay) (Islam, 1996). While it is more typical to regulate a pathway as early as possible to prevent accumulation of intermediates, regulation at the terminal step of pheromone production is not unprecedented. Regulated acyl-CoA reductions to alcohol pheromones are also present in two moth species, *Bombyx mori* (Ozawa *et al.*, 1993) and *Spodoptera littoralis* (Martinez *et al.*, 1990). It is possible that terminal regulation of these pathways serves some evolutionary advantage, as having a stockpile of pheromone precursor would dramatically speed pheromone production upon up-regulation. However, the drawback of *in vivo* studies such as those performed by Islam (1996) is that other potentially regulated processes involved in the intact animal cannot be resolved from biosynthesis. For example,

availability of cofactors, transport between tissues where different steps of the biosynthesis may occur, pheromone release from secretory tissue or organ and even pheromone degradation may be regulated by JH to affect pheromone levels in the beetle at any given time. *In vitro* experiments minimize the influence of these factors, as extracellular transport processes are abolished and cofactor availability may be carefully controlled. By comparing *in vivo* and *in vitro* data, extra-cellular events such as those listed above may be resolved from events involving transcription, translation or enzyme activity.

The overall goal of this project is to develop an *in vitro* assay for the reduction of 4-methylnonanoic acid (or derivative) to 4-methylnonanol in *T. molitor* and to confirm regulation by JH III. Reduction of fatty acids has been reviewed by Riendeau and Meighen (1985), and progress since then has not added considerably to the field. Fatty acids must be activated as the CoA derivative before they can be reduced to their corresponding alcohols, although many cell-free preparations will reduce the free acid if provided with CoA and ATP in addition to reducing cofactor. All known alcohol-generating acyl-CoA reductases are microsomally located and have a strong preference for NADPH (except *Euglena gracilis*, which uses NADH). In the algae, *Euglena gracilis* (Kolattukudy, 1970), jojoba seed (Pollard *et al.*, 1979), duck uropygial gland (Wang and Kollatukudy, 1995), and pea leaves (Vioque and Kollatukudy, 1997), the reduction of acyl-CoA to aldehyde to alcohol has been shown to be catalyzed by the same enzyme with only minute quantities of aldehyde intermediate released from the enzyme. In the bacteria *Acinetobacter calcoaceticus*, however, a gene involved in wax ester synthesis has been identified whose protein product catalyzes the reduction of fatty acyl-CoA to aldehyde, suggesting an aldehyde reductase is also involved in long chain alcohol formation (Reiser and Somerville, 1997). In insects, *in vitro* evidence for the presence of an acyl-CoA reductase in pheromone biosynthesis has been demonstrated in the orange tortrix moth (Wolf and Roelofs, 1983), *S.*

littoralis (Martinez *et al.*, 1990) and *B. mori* (Ozawa *et al.*, 1993; Matsumoto *et al.*, 1996). Unfortunately, the reduction has only been studied in any detail in the silkworm moth (Matsumoto *et al.*, 1996), where the reduction appears to require NADPH, although no evidence is given indicating NADPH is the preferred or only accepted reducing cofactor. The authors hypothesize that the reductase may also be inhibited by protein phosphorylation, though this remains to be substantiated. Therefore, in the yellow mealworm beetle, reduction of 4-methylnonanoic acid to 4-methylnonanol is likely catalyzed by a single microsomal enzyme that prefers NADPH as the reducing cofactor. Although 4-methylnonanoyl-CoA is likely the actual enzyme substrate, it is possible that the free acid may be used *in vitro*, as long as ATP and CoA are supplied.

1.2.1. *Project Objectives*

Development of an *in vitro* reduction assay will likely require high sensitivity, as mature female yellow mealworm beetles only contain about 30 nanograms of 4-methylnonanol (Tanaka *et al.*, 1986). This means that the enzyme(s) of interest may be expressed at low levels, or exhibit low activity. Secondly, although the literature suggests that the reduction from acid (or CoA derivative) to alcohol is likely catalyzed by one enzyme, this still remains to be substantiated. It is possible that one enzyme may catalyze the reduction of 4-methylnonanoic acid (or CoA derivative) to the aldehyde, 4-methylnonanal, and that a second enzyme (which need not be present in the same sub-cellular compartment) then reduces the aldehyde to 4-methylnonanol. Thus, the assay must also provide the chemical identity of any/all product(s) produced, especially if multiple reductase activities are discovered. A spectrophotometric assay would be convenient, as such assays offer moderate sensitivity and real-time monitoring of activity lends itself to convenient kinetic studies. Unfortunately, the UV/visible spectra of 4-

methylnonanoic acid. 4-methylnonanal and 4-methylnonanol are not sufficiently different to provide any information on product identity. For these reasons, it was decided that the best assay method would be to monitor the fate of radiolabelled 4-methylnonanoic acid (or its CoA derivative) *in vitro*. After incubation, unreacted substrate and any labeled products may be resolved from one another by a variety of chromatographic techniques and quantified by liquid scintillation counting. Product identification could be achieved by product resolution by a high-resolution chromatographic technique, such as HPLC, and by comparison of retention times to those of authentic standards. Unfortunately, the radiolabelled substrates required for this assay is are not commercially available. Thus, the project objectives were as follows: first, to synthesize the necessary substrates and any necessary standards; second, to develop and optimize the *in vitro* assay for reduction of 4-methylnonanoic acid (or CoA derivative); and third, to use the optimized assay to determine whether or not the reduction of 4-methylnonanoic acid (or CoA derivative) is a regulated step of 4-methylnonanol biosynthesis in the yellow mealworm beetle. The approach to each of these objectives is discussed in more detail below.

1.2.2. *Synthesis of Required Chemicals*

Several synthetic routes have been published for either racemic or enantiomerically enriched 4-methylnonanol (Carpita *et al.*, 1989; Tanaka *et al.*, 1989; Odonikov *et al.*, 1991; Odonikov *et al.*, 1993; Kitahara and Kang, 1994). Unfortunately, these syntheses are undesirable for our purposes for two reasons. First, the easiest route for the synthesis of radiolabelled 4-methylnonanoic acid would require a double bond close to the end of the synthesis for tritium addition by reduction with tritium gas, which none of the existing routes contain. Second, all of the published routes involve synthetically complex steps, or costly reagents, or both. The ideal synthetic route would be amenable to label incorporation, would not require a specialized

organic synthetic lab and would be practical for investigators with only moderate experience in organic synthesis. A suitable route was developed in our lab (summarized in Figure 3). However the overall yield was low, making it unsuitable for larger scale synthesis. Although only a few milligrams of radiolabelled substrate were required for the entire study, considerably more unlabelled 4-methylnonanol and 4-methylnonanoic acid were required for dilution of the radiolabelled substrate to an appropriate specific activity and for use as standards and cold carrier. Before any serious biochemical studies can be performed, a more practical and efficient synthesis for the acid and alcohol will be required.

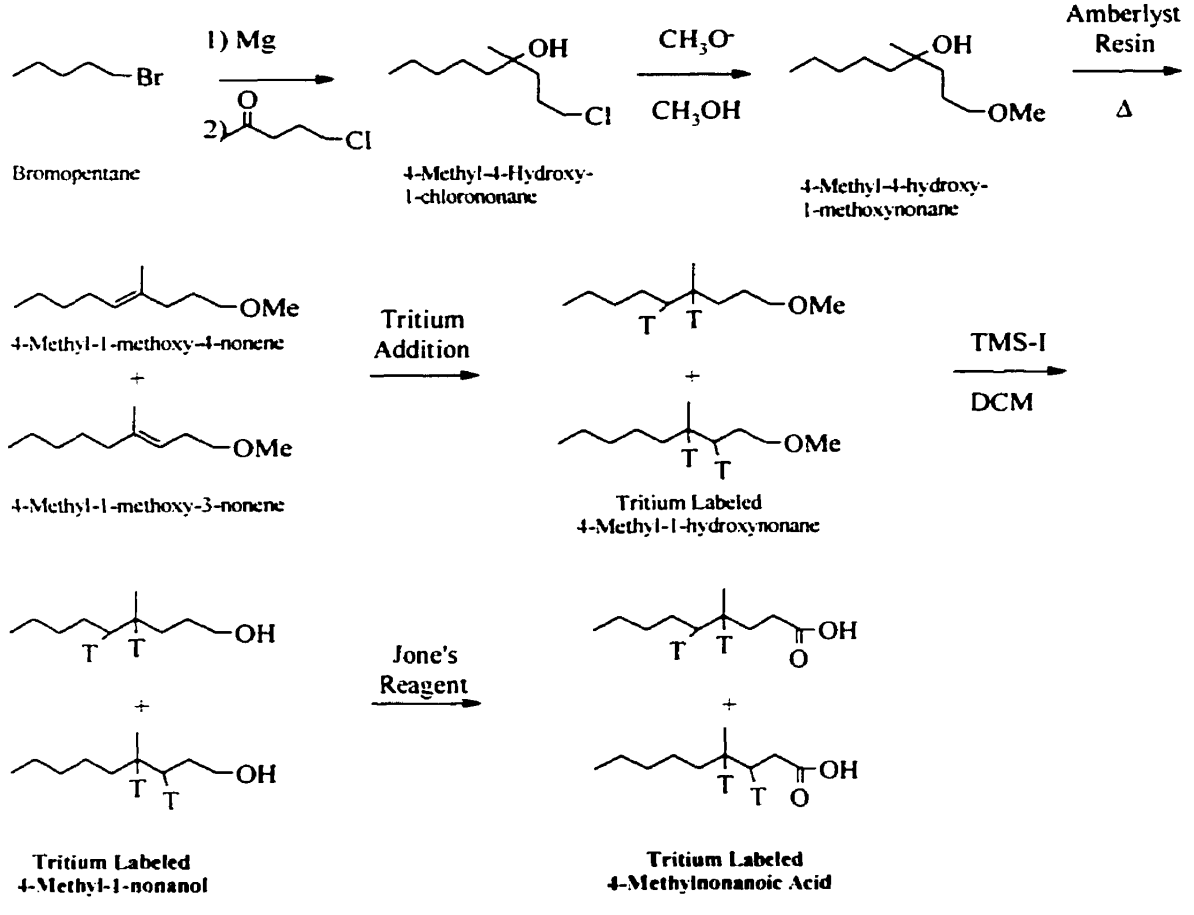

Figure 3: Synthetic route to tritium labeled 4-methyl-1-nonanol and 4-methylnonanoic acid.

As mentioned previously, the *in vitro* enzyme assay may require the use of 4-methylnonanoyl CoA as substrate. Although the free acid may function *in vitro* with crude protein preparations, the CoA derivative will be necessary to assay purified or partially purified enzyme preparations. In addition, assaying reduction of the CoA derivative directly may improve activity, as only one enzymatic conversion will have to be optimized instead of two (acyl-CoA synthesis and reduction). Several chemical methods have been published for the syntheses of acyl-CoAs. These involve chemically reacting CoA with the acid chloride of the fatty acid (Seubert, 1960; Bishop and Hajra, 1980), the anhydride of the fatty acid (Sánchez *et al.*, 1973; Stadtman, 1957) or the *N*-hydroxysuccinimide ester (Al-Arif and Blecher, 1969). The major setback of the chemical synthesis methods is that the product is invariably purified by crystallization, which is difficult when working at such a small scale that the crystalline product is not visible to the naked eye. Furthermore, all methods require chemical modification of the fatty acid before condensation. When synthesizing CoA derivatives with radiolabelled fatty acids, it is desirable to manipulate the fatty acid as little as possible during the process, as there is always some loss inherent with any chemical procedure and the fatty acid is by far the more costly reagent. Enzymatic syntheses of radiolabelled CoA derivatives are preferable, as the enzyme requires free fatty acid and thus no prior modification is necessary. There are several published syntheses that use partially purified acyl-CoA synthetase (Banis *et al.*, 1976; Galliard and Stumpf, 1968; Kornberg and Pricer Jr., 1953), however preparation of enzyme would be unnecessary as purified acyl-CoA synthetase is commercially available. The method of Banis *et al.* (1976) seemed the most promising to adapt for use in our laboratory because the authors used TLC for product purification instead of precipitation. Product purification by TLC is convenient because the entire incubation mixture may simply be applied to the plate, resolved and then extracted using a suitable solvent/buffer system.

1.2.3. *In vitro REDUCTION ASSAY DEVELOPMENT*

A crude *in vitro* assay for 4-methylnonanoic acid reduction has been established in our lab (Gameiro, 1996; Zolondek 1996; Khuu, 1996). Unfortunately the preliminary results have not been straightforward. While Khuu (1996) was able to observe 4-methylnonanol production by incubating free 4-methylnonanoic acid (+ATP, +CoA, +NADH, and +NADPH) with mature female homogenates, Gameiro (1996) and Zolondek (1996) were unable to duplicate the activity and required the acyl-CoA derivative to observe any conversion. Furthermore, all three investigators were only able to observe low conversion levels. The confounding substrate requirements and low activity must be resolved before the existing assay may be used for further investigations.

1.2.4. *Determination of JH Effects on 4-Methylnonanol Formation*

Once the assay is optimized, it may be used to study the regulation of 4-methylnonanoyl CoA reduction. Regulation of reductase activity will be investigated by comparing the ability of enzyme preparations from mature females to those from immature females and immature females pre-treated with methoprene. If the reduction is indeed regulated, immature females would be expected to be able to perform the conversion only after pre-treatment with hormone. It may also be interesting to compare methoprene pre-treated enzyme preparations to those of immature females where methoprene is included in the incubation. If JH is functioning as a transcriptional regulator, then only pre-treated preparations should demonstrate reductase activity. Stimulation by methoprene included in the assay mixture would be unexpected and would be suggestive of regulation at the protein level, either allosterically or by some signaling pathway.

A second interesting aspect of 4-methylnonanoyl CoA reduction, which deserves attention, is the fact that crude mature male homogenates are able to reduce 4-methylnonanoyl CoA, even though the male beetle does not produce pheromone (Gameiro, 1996). At low substrate concentrations, homogenates prepared from females exhibit more reductase activity, but when the substrate concentration is increased 4-fold, male homogenate activity becomes comparable (Gameiro, 1996). Although the results are interesting, these experiments were preliminary and will have to repeated using an optimized assay. A similar phenomenon is observed in the biosynthesis of muscalure, the female-produced sex pheromone of the housefly *Musca domestica* (Tillman-Wall *et al.*, 1992). In females, enzyme activity of the regulated biosynthetic step is linear at low substrate concentration, but demonstrates saturation as substrate levels increase. Male activity on the other hand, is much lower than female activity at lower (and presumably more physiological) substrate levels and increases linearly with substrate with no demonstrable saturation. It would be interesting to if this is also the case in *T. molitor*.

These studies will lay the groundwork for further study of pheromone biosynthesis in the yellow mealworm beetle. Once the regulated steps of 4-methylnonanol biosynthesis are determined and assays for their activity developed, study of regulation at the cellular and molecular levels may begin. A clear understanding of pheromone biosynthesis in the yellow mealworm will be directly applicable to related studies in other beetle species.

2. MATERIALS AND METHODS

2.1. PURCHASED CHEMICALS

2.1.1. *General*

All solvents were purchased from Mallinckrodt (Kentucky, USA) and were of spectrophotometric grade or better. All other reagents were obtained from BDH (Toronto, Ontario, Canada) or Mallinckrodt (Kentucky, USA), and were of ACS grade or better. Gases were obtained from CANOX (Mississauga, Ontario, Canada) and were 'extra dry' grade. For column chromatography, silica gel (Merck grade 60, 230-400 mesh, 60 Å) was obtained from Aldrich (Milwaukee, Wisconson, USA) and Florisil (100-200 mesh) was obtained from BDH (Toronto, Ontario, Canada). The liquid scintillation cocktails Scintisafe Plus 50% and Scintisafe Econo F were obtained from Fisher Scientific (Fairlawn, New Jersey, USA). Deuterated chloroform (containing 0.05% TMS) for NMR analysis was purchased from CDN Isotopes (Point Claire, Quebec, Canada). Specialty chemicals were obtained from the suppliers specified below and were used 'as is' without further purification, unless otherwise noted.

2.1.2. *Malonic Ester Synthetic Route*

Dimethyl malonate (97%), 2-bromoheptane (technical) and lithium aluminum hydride (95%) were obtained from Aldrich (Milwaukee, Wisconson, USA). Hydrobromic acid (48% w/v) and methyl iodide were purchased from Mallinckrodt (Kentucky, USA) and powdered potassium hydroxide from Fluka (CH-9471 Buchs, Switzerland).

2.1.3. *Claisen Orthoester Synthetic Route*

2-Bromopropene (99%), pentanal (97%), TMOA (99%) and palladium on charcoal (5% Pd) were all obtained from Aldrich (Milwaukee, Wisconsin, USA).

2.1.4. *Synthesis of Radiolabelled 4-Methylnonanoyl CoA*

The tritium labeled 4-methylnonanoic acid used in this synthesis consisted of a mixture of isomers labeled on carbon 4 and either carbon 3 or 5 (the synthetic route is summarized in Figure 3). Tris HCl and Tergitol 15-S-9 were purchased from Sigma (Oakville, Ontario, Canada). 5'-Adenosine triphosphate (dipotassium salt) and Coenzyme A (CoA, trilithium salt dihydrate) were purchased from Calbiochem (San Diego, California, USA). Magnesium chloride hexahydrate was supplied by BDH. Acyl CoA synthetase (from *Pseudomonas fragi*) was obtained from Boehringer-Mannheim (Laval, Québec, Canada). Silica gel TLC plates (60 mesh, 250 μm thickness) were obtained from EM Separations Technology (Gibbstown, New Jersey, USA).

2.1.5. *Biochemical Studies*

Mono- and di-basic potassium phosphates were purchased from Calbiochem. Horse heart cytochrome c, ascorbic acid (Sigmaultra grade), N,N,N,N-tetramethylphenylene diamine (TMPD), sodium orthovanadate, Fiske-Subbarow reducer, sodium azide (ACS grade), 1,4-Piperazinebis(ethanesulfonic acid) (PIPES, Sigmaultra grade), 4-(2-hydroxyethyl)-1-piperazineethanesulfonic acid (HEPES, min. 99.5%), ethylenebis(oxyethylenenitrolo)tetraacetic acid (EGTA, min. 97%) and mammalian protease inhibitor cocktail were supplied by Sigma

(Oakville, Ontario, Canada). TMPD was recrystallized from ethanol before use. Magnesium chloride hexahydrate and 2-propanol were obtained from BDH. NADH (disodium salt) and NADPH (tetrasodium salt) were obtained either from Sigma or Calbiochem.

2.2. SYNTHESIS OF REQUIRED CHEMICALS

Syntheses of target molecules were performed as outlined below. Purification by flash chromatography was performed using the method of Still *et al.* (1978). ^{1}H and proton decoupled ^{13}C NMR spectra were acquired on a Varian Gemini 200 spectrometer. Gas chromatographic analyses were conducted on a Hewlett Packard 5890 gas chromatograph equipped with a flame ionization detector and a 25 m x 0.2 mm Hewlett Packard FFAP fused silica capillary column with a 0.25 μm stationary phase thickness. Helium gas was used as carrier at a head pressure of 10 psi. The GC oven was held at 80 °C for 0.5 minute, then ramped at 20 °C/minute to 180 °C, where it was maintained until the end of the run. The GC injector and detector were held at 180 °C and 250 °C, respectively. Mass spectral analyses were conducted on a Hewlett Packard model 5890 GC, using helium gas as carrier, coupled to a Hewlett Packard 5989A mass spectrometer operating in the electron impact mode at 70 eV. The GC was equipped with a 30 m x 0.25 mm Supelco SPB-5 capillary column with a 0.25 μm stationary phase thickness, operating in the splitless injection mode under a 15 psi head pressure. The oven was maintained at 55 °C for the first three minutes, at which point the temperature was ramped at 10 °C/minute to 180 °C, where it was held until the end of the run. The temperatures of the injector port, GC/MS transfer line, source and quadrupole were 190 °C, 280 °C, 275 °C and 100 °C, respectively.

2.2.1. *Malonic Ester Route*

Dimethyl 2-heptylmalonate (1). Sodium methoxide was generated by dissolving freshly cleaned sodium metal (2.066 g, 90.8 mmol) in methanol (75 ml) under nitrogen atmosphere with magnetic stirring. Dimethyl malonate (9.943 g, 75.7 mmol) was added via pressure equalized dropping funnel and the resulting mixture was stirred at room temperature. After one hour, 2-bromoheptane (13.557 g, 75.7 mmol) was added drop-wise over a 10 minute period using a pressure equalized dropping funnel. The mixture was allowed to reflux for eighteen hours at which point it was poured into a separatory funnel containing water (250 ml). The mixture was then extracted with diethyl ether (3 x 50 ml). The pooled organic phases were washed with water (4 x 50 ml), then brine (3 x 30 ml). The extract was then dried over anhydrous magnesium sulfate for thirty minutes, filtered, and the solvent was removed by rotary evaporation under reduced pressure. The resulting oil was purified by distillation under reduced pressure (0.75 mm Hg, 88 °C), resulting in the colorless oil **1** (10.63 g, 45.1% yield): ^{1}H NMR (200 MHz, $CDCl_3$) δ 3.73 (s, 6H), 3.27 (d, *J*=7.9 Hz, 1H), 2.23 (m, 1H), 1.27 (m, 8H), 0.972 (d, *J*=6.8 Hz, 3H), 0.88 (t, *J*=6.56 Hz, 3H); ^{13}C NMR (50.3 MHz, $CDCl_3$) δ 169.45, 169.28, 57.56, 52.24, 34.28, 33.53, 31.78, 26.46, 22.56, 16.96, 14.03; MS *m/z* 41.05 (33%), 55.15 (23%), 69.15 (35%), 100.10 (44%), 101.15 (30%), 132.20 (100%), 133.20 (14%); MS-CI (methane) *m/z* 231.25 (34%), 229.25 (12%), 199.30 (100%), 132.15 (13%), 101.20 (15%).

Methyl 3-methyloctanoate (2). The diester **(1)** (7.957 g, 34.55 mmol) was dissolved in DMSO (50 ml), along with H_2O (0.623 g, 34.55 mmol), and lithium chloride (2.929 g, 69.1 mmol). The mixture was stirred magnetically and heated to reflux under nitrogen atmosphere. As the reaction progressed, the mixture slowly changed from a clear, light yellow solution to a turbid, yellow-brown solution. After one hour, the reaction mixture was allowed to cool under inert

atmosphere and then poured onto water (300 ml). After acidification with hydrochloric acid (5% v/v in water), the mixture was extracted with pentane (4 x 30 ml). The combined organic layers were washed with water (4 x 30 ml) and then brine (2 x 30 ml), then dried over anhydrous magnesium sulfate. Filtration and solvent removal by rotary evaporation under reduced pressure resulted in a yellow oil which was subsequently distilled under reduced pressure (0.75 mm Hg, 65 °C), to yield the colorless oil **2** (4.77 g, 80.0% yield): ^{1}H NMR (200 MHz, $CDCl_3$) δ 3.67 (s, 3H), 2.364-2.224 (m, 1H), 2.161-2.019 (m, 1H), 1.954 (m, 1H), 1.270 (m, 8H), 0.927 (d, *J*=6.51 Hz, 3H), 0.882 (t, *J*=6.87 Hz, 3H); ^{13}C NMR (50.3 MHz, $CDCl_3$) δ 173.835, 51.356, 51.293, 41.681, 36.674, 31.930, 30.503, 26.559, 22.614, 19.737, 14.047; MS *m/z* 98.25 (18%), 87.10 (61%), 69.15 (27%), 60.15 (82%), 57.15 (100%), 56.15 (30%), 55.15 (39%), 43.10 (65%), 41.05 (73%); MS-CI (methane) *m/z* 159.30 (100%), 141.35 (15%).

3-Methyl-1-octanol (3). A 250 ml three-neck round bottom flask, equipped with a magnetic stir bar and pressure equalized dropping funnel, was purged with nitrogen and flame dried. Once cool, anhydrous diethyl ether was added (100 ml) and cooled to 0 °C. The nitrogen atmosphere was broken briefly for the addition of lithium aluminum hydride (1.715 g, 45.20 mmol) via a funnel. The ester **2** (4.768 g, 30.13 mmol) was added drop-wise over a five minute period via pressure equalized dropping funnel. Once complete, diethyl ether (2 x 10 ml) was used to rinse any residual ester from the funnel into the reaction flask. Reaction progress was monitored by GC (1 drop reaction mixture added to 1 ml diethyl ether over 5% HCl, organic layer retained and dried with anhydrous sodium sulfate) for the disappearance of **2**, and the appearance of **3**. After 60 minutes, the reaction mixture was poured slowly onto ice water (200 ml). Concentrated hydrochloric acid was then added until the mixture was acidic to litmus paper. The ether layer was removed, and the aqueous was extracted with diethyl ether (2 x 30 ml). The combined organic layers were washed with water (3 x 30 ml), and brine (2 x 30 ml), then dried over

anhydrous magnesium sulfate. Solvent removal by reduced pressure rotary evaporation, yielded the colorless oil **3** (4.16 g, 90.8% yield): ^{1}H NMR (200 MHz, $CDCl_3$) δ 3.686 (d of t, *J*= 6.72 Hz, 2.4 Hz, 2H), 1.70-1.50 (m, 2H), 1.326-1.249 (m, 8H), 0.909 (d, *J*= 6.47 Hz, 3H), 0.885 (t, *J*= 6.96 Hz, 3H); ^{13}C NMR (50.3 MHz, $CDCl_3$) δ 61.772, 40.485, 37.576, 32.626, 29.978, 27.106, 23.180, 20.137, 14.589; MS *m/z* 98.30 (28%), 70.20 (85%), 69.20 (45%), 57.10 (74%), 56.10 (90%), 55.10 (100%), 43.10 (92%), 42.10 (32%), 41.10 (90%); MS-CI (methane) *m/z* 127.30 (10%), 125.30 (11%), 97.25 (10%), 85.25 (73%), 83.25 (26%), 71.20 (100%), 70.30 (13%), 69.15 (59%).

3-Methyl-1-bromooctane (4). The alcohol **3** (6.46 g, 44.78 mmol) was added to hydrobromic acid (37.75 g, 223.9 mmol) in a 100 ml round bottom flask with a condenser. The mixture was refluxed under nitrogen with magnetic stirring. The reaction progress was monitored by GC for the disappearance of **3** and the appearance of **4** (sample preparation: 1 drop reaction mixture in 1 ml ether over 5% sodium bicarbonate, organic layer retained and dried over anhydrous sodium sulfate before analysis). After sixteen hours the reaction mixture was allowed to cool, poured onto water (200 ml), then extracted with pentane (3 x 30 ml). The combined organic phases were then washed with 5% (w/v) sodium bicarbonate (2 x 30 ml), then water (2 x 30 ml), and finally brine (2 x 30 ml) before being dried over anhydrous magnesium sulfate. Filtration and solvent removal by reduced pressure rotary evaporation resulted in the amber oil **4** (8.29 g, 91.0 % yield) which was used in the next step without further purification. For **4**: ^{1}H NMR (200 MHz, $CDCl_3$) δ 3.532 (m, 2H), 1.967-1.767 (m, 1H), 1.268 (m, 8H), 0.887 (t, *J*=6.60 Hz, 3H), 0.885 (d, *J*=6.35 Hz, 3H); ^{13}C NMR (50.3 MHz, $CDCl_3$) δ 40.069, 36.447, 32.268, 32.080, 31.663, 26.477, 22.672, 18.976, 14.101.

4-Methylnonanoic acid (5). A 250 ml 3-neck flask with a condenser and pressure equalized dropping funnel was assembled and flame dried under positive nitrogen pressure. Once cool, anhydrous diethyl ether (30 ml) was added, followed by freshly cleaned and dried magnesium (0.599 g, 24.65 mmol). The bromide **4** was dissolved in 30 ml diethyl ether and loaded into the pressure equalized dropping funnel. After addition of several drops of bromide, it was necessary to heat the ether to reflux before the reaction initiated (as indicated by gas evolution from the magnesium turnings). The bromide solution was added drop-wise over a 2.5 hour period, while the reaction mixture was maintained at reflux and stirred magnetically. One half hour after bromide addition was complete, carbon dioxide was introduced to the mixture at a slow bubble. After thirty minutes, the reaction mixture was poured over water (100 ml), and acidified with 5% hydrochloric acid. The ether layer was removed and the aqueous phase extracted with diethyl ether (2 x 30 ml). The combined ether extracts were washed with water (3 x 20 ml), and brine (2 x 20 ml), then dried with anhydrous magnesium sulfate. After solvent removal by reduced pressure rotary evaporation, the resulting oil was dissolved in pentane (20 ml) and extracted with 5% (w/v) sodium hydroxide. The aqueous extracts were combined, acidified with concentrated hydrochloric acid, and extracted with diethyl ether (4 x 20 ml). The ether extracts were pooled and washed with water (2 x 20 ml), and brine (2 x 20 ml), then dried over anhydrous magnesium sulfate. Solvent removal, by rotary evaporation under reduced pressure, resulted in the slightly yellow oil **5** (1.86 g, 39.6% yield). The product was purified by flash chromatography (silica gel, 99% diethyl ether: 1% acetic acid) in smaller batches as needed. For **5**: ^{1}H NMR (200 MHz, $CDCl_3$) δ 11.119 (s, 1H), 2.378 (d of d, J=6.55 Hz, 3.63 Hz, 1H), 2.334 (d of d, J=6.65 Hz, 2.83 Hz, 1H), 1.798-1.549 (m, 1H), 1.549-1.387 (m, 2H), 1.387-1.008 (m, 8H), 0.885 (t, J=6.53 Hz, 0.882 (d, J=6.18 Hz, 3H); ^{13}C NMR (50.3 MHz, $CDCl_3$) δ 180.612, 36.579, 32.327, 32.129, 31.878, 31.616, 26.567, 22.675, 19.252, 14.100; MS (as methyl ester) *m/z* 98.25 (18%), 87.10 (61%), 69.15 (27%), 60.15 (82%), 57.15 (100%), 56.15 (30%), 55.15 (39%), 45.10 (20%), 43.10

(65%), 42.10 (24%), 41.05 (73%); MS-CI (methane) *m/z* 188.25 (12%), 187.25 (100%), 185.25 (11%), 153.20 (13%).

4-Methylnonanol (6). A 250 ml three-neck flask equipped with a condenser and pressure equalized dropping funnel was dried at 110 °C overnight then assembled hot and allowed to cool under nitrogen atmosphere. Diethyl ether (20 ml) was added and cooled to 0 °C on ice. Lithium aluminum hydride (0.264 g, 6.97 mmol) was added to the ether with magnetic stirring. The acid **5**, dissolved in ether (20 ml), was added drop-wise to the three-neck flask via the pressure equalized dropping funnel over thirty minutes. Once addition was complete, any remaining acid was rinsed into the reaction flask with ether (2 x 5 ml). Reaction progress was monitored by GC (sample preparation: 1 drop reaction mixture added to 1 ml ether over 5% (w/v) hydrochloric acid, organic layer retained, dried with anhydrous sodium sulfate and methylated with diazomethane before analysis). After two hours, the reaction had halted at 53% complete and more lithium aluminum hydride was added (0.025 g, 0.66 mmol). After twenty five hours, the reaction had again halted at 75% complete, necessitating the addition of more lithium aluminum hydride (0.025 g, 0.66 mmol). Once the reaction was complete (26 hours), the reaction mixture was poured onto ice water (100 ml). The resulting mixture was acidified with 5% (w/v) hydrochloric acid (100 ml) and the ether layer removed. The aqueous phase was extracted with pentane (3 x 30 ml). The combined organic layers were washed with water (2 x 30 ml), and brine (2 x 30 ml), then dried over anhydrous magnesium sulfate. Solvent was removed by rotary evaporation under reduced pressure, followed by swirling under high vacuum for fifteen minutes. The product was the colorless oil **6** (0.87 g, 85.2% yield), which was purified by flash chromatography (silica gel, 70% pentane: 30% diethyl ether) in small batches as required. For **6**: ^{1}H NMR (200 MHz, $CDCl_3$) δ 3.631 (t, *J*=6.80 Hz, 2H), 1.696-1.457 (m, 2H), 1.414-1.117 (m, 10H), 0.885 (t, *J*=6.15 Hz, 3H), 0.869 (d, *J*=6.23 Hz, 3H); ^{13}C NMR (50.3 MHz, $CDCl_3$) δ

63.473, 36.959, 32.964, 32.647, 32.236, 30.374, 26.720, 22.727, 19.654, 14.136; MS *m/z* 112.20 (10%), 97.20 (12%), 84.20 (22%), 70.10 (29%), 69.10 (80%), 57.15 (100%), 56.15 (81%), 55.15 (41%), 43.05 (51%), 42.05 (22%), 41.05 (92%); MS-CI (methane) *m/z* 158.25 (1%), 157.25 (9%), 141.30 (11%), 99.25 (27%), 97.25 (30%), 85.25 (100%), 83.25 (62%), 71.30 (75%), 69.15 (45%).

Methyl 4-methylnonyl ether (7). 4-Methylnonanol, **6**, (0.25 g, 1.60 mmol) was added to dimethylsulfoxide (3 ml) under nitrogen atmosphere and with magnetic stirring. After five minutes, powdered potassium hydroxide (0.39 g, 6.9 mmol) was added and the reaction flask was cooled in an ice bath for ten minutes. Once cold, the flask was removed from the ice bath and methyl iodide (0.49 g, 3.50 mmol) was added drop-wise. Sixty minutes later, the reaction mixture had changed from a light yellow with white precipitate, to a colorless solution with white precipitate. The reaction mixture was then poured onto water (40 ml), and extracted with pentane (4 x 5 ml). The combined organic extracts were washed with water (2 x 5 ml), then 5% (w/v) copper sulfate (2 x 5 ml) and dried over anhydrous magnesium sulfate. The product was purified by flash chromatography (silica gel, 90% hexane: 10% diethyl ether) to yield the colorless oil **7** (0.169 g, 56.2% yield): ^{1}H NMR (200 MHz, $CDCl_3$) δ 3.354 (t, *J*=6.65 Hz, 2 H), 3.333 (s, 3H), 1.643-1.453 (m, 3H), 1.452-1.034 (m, 10H), 0.877 (t, *J*=6.80 Hz, 3H), 0.846 (d, *J*=6.41 Hz, 3H); ^{13}C NMR (50.3 MHz, $CDCl_3$) δ 73.364, 36.923, 33.326, 32.676, 32.220, 27.212, 26.690, 22.704, 19.615, 14.109; MS *m/z* 112.25 (22%), 97.15 (25%), 84.15 (36%), 70.20 (34%), 69.05 (61%), 57.05 (81%), 56.05 (97%), 55.05 (41%), 45.10 (100%), 43.10 (35%), 41.10 (55%); MS-CI (methane) *m/z* 173.30 (7%), 172.30 (2%), 171.30 (12%), 141.35 (34%), 139.35 (23%), 99.30 (27%), 97.30 (47%), 85.20 (84%), 83.20 (100%), 71.20 (71%), 69.20 (54%).

2.2.2. *Claisen Orthoester Rearrangement Route*

2-Methyl-1-hepten-3-ol (8). All glassware for this reaction was assembled, flame dried under nitrogen atmosphere, and allowed to cool before use. Freshly cleaned magnesium (0.201 g, 8.27 mmol) was added to tetrahydrofuran (freshly distilled over potassium under nitrogen atmosphere, 5 ml) and heated to reflux. 2-Bromopropene (1.00 g, 8.27 mmol), dissolved in tetrahydrofuran (10 ml), was loaded into a pressure equalized dropping funnel and several drops were added to the magnesium turnings. Within fifteen minutes, the reaction mixture starting to go turbid, indicating the reaction was proceeding. The remainder of the 2-bromopropene solution was added drop-wise over a 60 minute period, and the mixture left to react for a further fifteen minutes. Pentanal (0.785 g, 9.09 mmol) was added to the reaction flask all at once, resulting in a very exothermic reaction. The reaction was allowed to proceed a further 30 minutes before cooling to room temperature and pouring onto water (100 ml). After acidification with concentrated hydrochloric acid, the mixture was extracted with diethyl ether (3 x 20 ml). The organic extracts were pooled, washed with water (2 x 20 ml), then brine (2 x 20 ml), and dried over anhydrous magnesium sulfate. Solvent was removed by rotary evaporation under reduced pressure, followed by high vacuum for 10 minutes resulted in the colorless oil **8** (0.93 g, 79.2% yield). The product was purified by flash chromatography (silica gel, 70% pentane: 30% diethyl ether) as necessary. ^{1}H NMR (200 MHz, $CDCl_3$) δ 4.934 (t, J=<1 Hz, 1H), 4.830 (t, J=1.49 Hz, 1H), 1.724 (broad singlet, 3H), 1.610-1.495 (m, 2H), 1.400-1.200 (m, 2H), 0.907 (t, J=6.69 Hz, 3H); ^{13}C NMR (50.3 MHz, $CDCl_3$) δ 147.691, 110.916, 76.014, 34.638, 27.758, 22.627, 17.450, 14.033; MS *m/z* 86.10 (19%), 72.10 (10%), 71.10 (100%), 58.15 (16%), 57.15 (15%), 43.05 (62%), 41.05 (45%); MS-CI (methane) *m/z* 129.25 (7%), 128.25 (1%), 127.25 (6%), 111.25 (92%), 109.25 (12%), 85.20 (12%), 71.20 (37%), 69.20 (100%).

Methyl 4-methylnon-4-enoate (9). Toluene (20 ml), TMOA (6.97 g, 58.0 mmol), propanoic acid (0.179 g, 2.42 mmol), and the alcohol **8** (0.93 g, 7.25 mmol) were combined in a 50 ml round bottom flask. The reaction flask was provided with a nitrogen atmosphere and heated to reflux. Reaction progress was monitored by GC (sample preparation: 1 drop reaction mixture added to 1 ml hexane over 1 ml water, organic phase retained and dried over anhydrous sodium sulfate before analysis). At completion (30 hours), the reaction flask was outfitted with distillation apparatus and distillate was collected until the vapor temperature reached 100 °C (18 ml distillate collected), in order to remove most of the toluene. The still leavings were cooled, shaken with water (30 ml), and the organic layer removed. The aqueous phase was then extracted with hexane (2 x 10 ml). The combined organic extracts were then washed with water (3 x 10 ml), then brine (2 x 10 ml), then dried over anhydrous magnesium sulfate. Solvent removal by rotary evaporation under reduced pressure, followed by high vacuum for 10 minutes resulted in the colorless oil **9** (1.05 g, 78% yield, >95% pure by GC). The product was purified by flash column chromatography (silica gel, 90% hexane: 10% diethyl ether) in small batches as required. For **9**: ^{1}H NMR (200 MHz, $CDCl_3$) δ 5.128 (trip of quart, J_1=7.17 Hz, J_2=1.28 Hz, 1H), 3.632 (s, 3H), 2.420-2.205 (m, 4H), 1.943 (m, 2 H), 1.576 (s, 3H), 1.311-1.221 (m, 4H), 0.856 (t, J=6.74 Hz, 3H); ^{13}C NMR (50.3 MHz, $CDCl_3$) δ 173.946, 133.015, 125.674, 51.442, 34.715, 33.082, 31.899, 27.560, 22.280, 15.829, 13.982.

Methyl 4-methylnonanoate (10). Palladium on charcoal (5% w/w, 10 mg) was added to the ester **9** (1.05 g, 5.70 mmol), dissolved in 95% ethanol (15 ml). Hydrogen atmosphere was introduced (1 atm) and the mixture was stirred magnetically at room temperature. Reaction progress was monitored by GC (sample preparation: 1 drop reaction mixture added to 1 ml hexane over 1 ml water, organic phase retained and dried over anhydrous sodium sulfate before analysis). At completion (8.5 hours), the reaction mixture was filtered and added to water (150

ml) and extracted with hexane (3 x 20 ml). The pooled organic extracts were washed with water (3 x 20 ml), then brine (2 x 20 ml), and dried with anhydrous magnesium sulfate. Purification by flash column chromatography (silica gel, 80% hexane: 20% diethyl ether) resulted in the colorless oil **10** (0.509 g, 43.2% yield): ^{1}H NMR (200 MHz, $CDCl_3$) δ 3.667 (s, 3H), 2.334 (d of d, J_1=7.02 Hz, J_2=3.01 Hz, 1H), 2.289 (d of d, J_1=6.68 Hz, J_2=2.65 Hz, 1H), 1.665-1.480 (m, 2H), 1.480-1.285 (m, 2H), 1.275-1.195 (m, 8H), ^{13}C NMR (50.3 MHz, $CDCl_3$) δ 174.592, 51.443, 36.600, 32.401, 32.125, 31.912, 26.573, 22.665, 19.268, 14.084; MS *m/z* 98.25 (18%), 87.10 (61%), 69.15 (27%), 60.15 (82%), 57.15 (100%), 56.15 (30%), 55.15 (39%), 45.10 (20%), 43.10 (65%), 42.10 (24%), 41.05 (73%); MS-Cl (methane) *m/z* 188.25 (12%), 187.25 (100%), 185.25 (11%), 153.20 (13%).

4-Methylnonanol (6). All glassware was flame-dried and allowed to cool under nitrogen gas before use. Lithium aluminum hydride (40 mg, 1.073 mmol) was added to anhydrous diethyl ether (20 ml) and stirred magnetically under nitrogen atmosphere. The mixture was cooled on an ice bath and methyl 4-methylnonanoate (100 mg, 0.537 mmol), dissolved in anhydrous diethyl ether (10 ml), was introduced drop-wise via pressure-equalized dropping funnel over a ten minute period. Any remaining ester was rinsed into the reaction flask with anhydrous diethyl ether (2 x 1 ml). The ice bath was removed and the reaction allowed to proceed, during which time progress was monitored by GC [sample preparation: 1 drop reaction mixture added to 1 ml diethyl ether over 5% (w/w) hydrochloric acid, organic layer retained and dried with anhydrous sodium sulfate before analysis]. At completion (one hour), the reaction mixture was added to ice cold 5% (w/w) hydrochloric acid. The mixture was shaken and the organic layer removed. The aqueous phase was further extracted with diethyl ether (2 x 20 ml). The combined organic extracts were then washed with saturated sodium chloride (2 x 20 ml) and dried over anhydrous magnesium sulfate. Solvent was removed by rotary evaporation under reduced pressure

followed by a gentle nitrogen stream (45 minutes) to produce the colorless oil **6** (71.0 mg, 83.6% yield). The product was used without purification, as the NMR spectra were indistinguishable from those of purified 4-methylnonanol from the previous route (**6**). For **6**: ^{1}H NMR (200 MHz, $CDCl_3$) δ 3.631 (t, *J*=6.80 Hz, 2H), 1.696-1.457 (m, 2H), 1.414-1.117 (m, 10H), 0.885 (t, *J*=6.15 Hz, 3H), 0.869 (d, *J*=6.23 Hz, 3H); ^{13}C NMR (50.3 MHz, $CDCl_3$) δ 63.473, 36.959, 32.964, 32.647, 32.236, 30.374, 26.720, 22.727, 19.654, 14.136; MS *m/z* 112.20 (10%), 97.20 (12%), 84.20 (22%), 70.10 (29%), 69.10 (80%), 57.15 (100%), 56.15 (81%), 55.15 (41%), 43.05 (51%), 42.05 (22%), 41.05 (92%); MS-CI (methane) *m/z* 158.25 (1%), 157.25 (9%), 141.30 (11%), 99.25 (27%), 97.25 (30%), 85.25 (100%), 83.25 (62%), 71.30 (75%), 69.15 (45%).

2.2.3. *Tritium Labeled 4-Methylnonanoyl CoA*

The incubation mixture consisted of Tris buffer (pH 8.00, 500 mM), with 3% (v/v) Tergitol 15-S-9, 60 mM $MgCl_2$, 40 mM ATP, 20 mM CoAS-H and [^{3}H]-4-methylnonanoic acid (between 0.176 mCi and 1.85 mCi) in a total volume of 0.1 ml. The reaction was initiated by the addition of 1-5 units of Acyl Coenzyme A synthetase and allowed to continue for 4 hours at 30 °C, at which point it was terminated by the addition of 25 µl of concentrated hydrochloric acid. The reaction mixture was spotted as a line across a thin layer chromatography plate (silica gel 60, 250 µm thickness) and the plate was allowed to dry. The TLC plate was developed with 5:2:3 butanol: acetic acid: water (4-5 hours), removed from the developing chamber and allowed to dry for two hours at room temperature. The TLC plate was scraped in bands and the silica gel transferred to pre-weighed test tubes (so that radioactivity could later be normalized to the silica gel mass for easier comparison, since all bands were not necessarily the same size). Each fraction was extracted with methanol (3 x 1 ml) and a 1 µl aliquot quantified by scintillation counting in 3 ml Scintisafe Plus 50%. The bulk of the radioactivity was localized in a band

ahead of the unreacted co-enzyme A ($R_f \approx 0.75$). These extracts were pooled and buffered with 1 mM acetate buffer, pH 5, such that the resulting solution was 80% methanol. Typically, the fractions containing acyl-CoA were extracted a second time with methanol (3 x 1 ml). To recover any unreacted [^{3}H]-4-methylnonanoic acid, the solution was extracted with pentane (5 x 1 ml). To ensure no pentane remained, the sample was cooled on ice and a gentle stream of N_2 was passed over it for fifteen minutes. The activity of the product was determined and it was kept frozen in liquid nitrogen until needed. Sample degradation (hydrolysis) was monitored regularly by spotting 1-2 µl of solution on a 1.5 cm x 8 cm TLC plate and developing with 50:50:1 ether: hexane: acetic acid. The plate was then cut horizontally into 0.5 cm strips and the radioactivity of each strip was quantified using a Beckman model 6500 liquid scintillation counter using 3 ml Scintisafe Plus 50%. While unreacted fatty acid would migrate with the solvent front, acyl-CoA would remain at the origin. Any free acid was then extracted with pentane as above, and the activity of the remaining acyl-CoA solution was re-determined.

2.3. REARING OF INSECTS

T. molitor larvae were obtained from Northwest Scientific Supply Ltd.(Victoria, Brittish Columbia, Canada). Larvae were fed on 4:2:1 (v/v) wheat bran/rolled oats/wheat germ and were provided moisture from moistened paper towels, which were spread over the colonies. Colonies were maintained at 28-30 °C on a photoperiod (12 hours dark: 12 hours light). Pupae were collected from the colonies and sexed using the method of Battacharya *et al.*, 1970. Males and females were segregated at the pupal stage. Mature beetles (between 7 and 11 days post-eclosion) were used for experimentation.

2.4. BIOCHEMICAL STUDIES

2.4.1. *Buffers*

For the preliminary activity assays, the buffer systems used by previous investigators in our lab (Gameiro, 1996; Khuu, 1996; Zolondek, 1996) were used. Low sucrose buffer (LSB), which was used for all crude protein assays, consisted of 0.1 M potassium phosphate buffer, pH 7.2, with magnesium chloride (2 mM), dithiothreitol (1 mM) and sucrose (0.25 mM). For initial investigations of sub-cellular fraction activity, high sucrose buffer (HSB) was used, which was a 0.1 M potassium phosphate buffer, pH 7.2, containing magnesium chloride (2 mM), dithiothreitol (1 mM) and sucrose (25 mM). Later in the project, the buffer system was changed to one that was more amenable to the isolation of intact mitochondria (Rickwood *et al.*, 1987). The new buffer (referred to as 'MITO buffer' for convenience) consisted of 5 mM HEPES and 5 mM potassium dihydrogen phosphate, pH 7.4, with 300 mM sucrose, 1 mM EGTA, 1 mM DTT and 2 mM magnesium chloride. All buffers used for enzyme preparation were supplemented with mammalian protease inhibitor cocktail (1 ml per 20 g of wet tissue, as suggested by the manufacturer), with the assumption that each beetle possessed 100 mg of non-cuticular tissue.

2.4.2. *Preparation of Crude Protein for Assays*

Beetles were cold immobilized by chilling in a petri dish over ice. The number of beetles used varied from 2-5 per assay tube and was limited by availability. Generally, as many beetles were used as possible to ensure adequate protein yield. The beetles were wrapped in cheesecloth, then crushed using an ice-cold mortar and pestle in 3 ml buffer (containing protease inhibitors). After removing the homogenate to an ice-cold homogenizing tube, the remains were

re-extracted twice more in a similar fashion, using a more vigorous grinding action each time. Protein extract was then homogenized in an ice-cold size 23 Duall glass homogenizer using 10 full up and down strokes with a twisting motion. The crude homogenate was centrifuged at 1000 x g for 10 minutes in a Beckman Model L3-50 Ultracentrifuge thermostatted to 4 °C, using either a Beckman SW 28 swinging bucket or a TI45 fixed angle rotor. The pellet (containing unlysed cells, nuclei, cuticle bits, etc.) was discarded and the supernatant used directly for experimentation. Protein concentration was determined using the method of Bradford (1976) using BSA as a standard.

2.4.3. *Effect of Protease Inhibitor Cocktail on Reductase Activity*

Each of the five treatments (NADH + protease inhibitors, NADPH + protease inhibitors, NADH – protease inhibitors, NADPH – protease inhibitors, and no protein control) was performed in triplicate. Each assay tube contained final concentrations of the appropriate reducing cofactor and 300 000 DPM of [^{3}H]-4-methylnonanoyl CoA in a total volume of 1 ml. Each assay was started with the addition of 27 mg crude protein (3.3 beetle equivalents), or buffer for the no protein control, and incubated for sixty minutes in a 30 °C shaking water bath (60 strokes/minute). The reaction was terminated by the addition of 0.5 M ethanolic potassium hydroxide (1.0 ml). Tubes were left overnight at ambient temperature to allow any remaining acyl-CoA to hydrolyze. Prior to extraction, tubes were acidified with the addition of 0.6 M hydrochloric acid (1 ml).

2.4.4. *Preference for NADH or NADPH as Reducing Cofactor*

The activity of crude female homogenates in the presence of NADH or NADPH was compared to a no protein control in triplicate. Each assay tube contained 300 000 DPM [^{3}H]-4-methylnonanoyl CoA and 1 mM of either NADH or NADPH with a final volume of 1 ml. The reaction was initiated was initiated with the addition of 11.5 mg protein (4 beetle equivalents), or buffer for the no protein controls and the incubation was carried out, terminated and prepared for work-up as in the previous experiment (see Section 2.4.3.).

2.4.5. *Crude Assay: Comparison of Males and Females*

The five treatment groups [females + NADH, females + NADPH, males + NADH, males + NADPH and no protein control (+ NADH and NADPH)] were run in triplicate. Each assay tube contained 300 000 DPM [^{3}H]-4-methylnonanoyl CoA and 1 mM of either NADH or NADPH in a total volume of 1 ml. Each assay tube was initiated by the addition of 3.3 beetle equivalents of protein (or buffer for the no protein controls), then incubated, killed and treated as described in Section 2.4.3.

2.4.6. *Sub-cellular Localization of Activity: Males vs. Females*

Crude enzyme preparations were prepared from 50 female and 50 male beetles (as described in Section 2.4.3) using HSB. In an attempt to obtain a mitochondrially enriched fraction, the 1000 x g supernatant was centrifuged at 25 000 x g for 10 minutes at 4 °C. The 25 000 x g supernatant was subsequently centrifuged at 100 000 x g for 90 minutes to obtain a

microsomal fraction. The final supernatant was retained as the 'soluble' fraction. Both pellets were kept on ice until needed, at which point they were re-suspended in LSB (6 ml for the 'mitochondrial' pellets and 3 ml for the 'microsomal' pellets) using a #19 Potter-Elvehjem homogenizer. Each of the sub-cellular fractions were assayed in triplicate and compared to a no protein control. The reaction was initiated by the addition of protein [6.7 beetle equivalents mitochondrial (16.2 mg male, 15.5 mg female), 13.3 beetle equivalents microsomal (10 mg male, 24.7 mg female), or 4 beetle equivalents soluble (10.1 mg male, 20.4 mg female)] to yield a 1 ml incubation mixture with 1 mM NADH and 300 000 dpm [^{3}H]-4-methylnonanoyl CoA. Otherwise, assay tubes were incubated and terminated as described previously (Section 2.4.3).

2.4.7. *Marker Enzyme Analysis*

Cytochrome c oxidase was assayed as a mitochondrial marker using the procedure of Rafael (1983). Mitochondrial (25 000 x g), microsomal (100 000 x g) and soluble (100 000 x g supernatant) sub-cellular fractions were obtained from 20 mature beetles as previously described. Duplicate analyses were performed on each sub-cellular fraction from two separate preparations. Dilutions of active fractions were assayed to ensure the observed activity was linear with enzyme concentration.

Alcohol dehydrogenase (soluble marker) was assayed by monitoring the NAD^+ dependant oxidation of 2-propanol based on the method of Elliott and Knopp (1981). The assay medium consisted of 0.1 M glycine buffer, pH 9.3, with 1.68 mM NAD^+ and 0.218 M 2-propanol. Each assay was initiated by protein addition, providing a total assay volume of 2.0 ml. Absorbance at 340 nm was monitored at three minute intervals over a thirty minute assay period and compared to a no-2-propanol control. The analysis was carried out on sub-cellular fractions

from three discrete protein preparations. To maximize activity in less active fractions, as much protein was used as possible while avoiding excessive turbidity. In the case of active fractions, several protein addition levels were assayed to ensure the observed activity was linear with protein load.

As a plasma membrane (microsomal) marker, sodium/potassium ATPase activity was assayed following the method of Bowman and Bowman (1988). Mitochondrial (25 000 x g), microsomal and soluble sub-cellular fractions were obtained from 25 mature beetles as described previously with the exception that a phosphate free buffer was used in the isolation (10 mM PIPES, pH 7.2, with 5 mM magnesium chloride, 1 mM dithiothreitol and 150 mM ammonium chloride). The 25 000 x g pellet was re-suspended in 3.0 ml of buffer and had a total of 48.06 mg protein. The microsomal pellet was re-suspended in 1.5 ml buffer and contained 3.27 mg protein. The remaining soluble fraction had a volume of 4.2 ml and contained 36.05 mg protein. To ensure that a suitable protein concentration was supplied to the assay, either 10 µl, 100 µl or 500 µl of each fraction was assay. The assay was carried out as prescribed (Bowman and Bowman, 1988) except that the assay was terminated with the addition of 1.0 ml 20% TCA (for a final volume of 2.0 ml). TCA-precipitated samples were centrifuged and a 1.5 ml aliquot of each assay tube was used for phosphate determination using the method of Fiske and Subbarow (1925).

2.4.8. *Refinement of Sub-Cellular Location*

Crude enzyme extracts (prepared as described in Section 2.4.3) were prepared from 25 mature females using MITO buffer, and further centrifuged to produce a 3 000 x g pellet, a 10 000 x g pellet, a 100 000 x g 'microsomal' pellet and the 100 000 x g supernatant, or 'soluble'

fraction. Pellets were re-suspended in MITO buffer just prior to assay (6 ml for the 3 000 x g pellet, and 3 ml for the 10 000 x g and microsomal pellets) using a #19 Potter-Elvehjem homogenizer. Protein concentration of each fraction was determined using the method of Bradford (1976) using BSA as a standard. Reductase activity in each fraction was assayed in the presence of 1 mM NADH and 300 000 dpm [^{3}H]-4-methylnonanoyl CoA (1 ml final assay volume) in triplicate and compared to a no protein control. The assay was initiated with the addition of 700 µl protein (12.1 mg 3000 x g, 1.7 mg 10 000 x g, 9.5 mg microsomal and 12.6 mg soluble) and was executed as described in Section 2.4.3, with the exception that the incubation was terminated with the addition of 20% trichloroacetic acid. Tubes were also extracted within one hour of termination (as opposed to being left on the bench overnight).

2.4.9. *Determination of Protein Curve*

For this experiment, only a 10 000 x g pellet was obtained by using the method from the previous experiment (see Section 2.4.8) and omitting the 3 000 x g spin. The 10 000 x g pellet was re-suspended in 5 ml MITO buffer using a #19 Potter-Elvehjem homogenizer and protein concentration was determined as in the previous experiments. The assay was carried out in triplicate with each assay tube having a final volume of 1 ml, and consisting of 1 mM NADH, 300 000 dpm [^{3}H]-4-methylnonanoyl CoA and 10 mg, 7.5 mg, 5 mg, 2.5 mg, 1 mg, 0.5 mg, 0.1 mg or 0 mg protein. Each reaction was initiated by the addition of protein and incubated as in previous experiments, except only for 15 minutes. Reaction was terminated by the addition of 20% trichloroacetic acid (1 ml). Tubes were extracted within one hour of termination.

2.4.10. *Determination of Time Curve*

A 10 000 x g enzyme preparation was prepared as in the previous experiment (see Section 2.4.9). All assay tubes contained 1 mM NADH, 300 000 dpm [^{3}H]-4-methylnonanoyl CoA and 0.1 mg protein from the 10 000 x g pellet in a total volume of 1 ml. All assays were initiated by the addition of protein and allowed to incubate as previously described for 0, 1, 5, 10, 15, 20, 25 or 30 minutes before termination with 20% trichloroacetic acid (1 ml). Tubes were extracted within one hour of termination.

2.4.11. *Determination of NADH and NADPH Substrate Curves*

Protein from the 10 000 x g pellet was prepared as for the protein and time curves. All assay tubes contained 300 000 dpm [^{3}H]-4-methylnonanoyl CoA and a variable amount of NADH or NADPH. The reaction was initiated by addition of 0.1 mg protein from the 10 000 x g pellet, producing a final assay volume of 1.0 ml. Tubes were incubated for ten minutes in a shaking water bath at 30 °C before the reaction was terminated with the addition of 20% trichloroacetic acid (1 ml). Products were extracted within one hour of termination.

2.4.12. *Extraction and Resolution of Products From Assay Mixtures*

Assay tubes, either after overnight hydrolysis and acidification for KOH/ethanol terminated assays or immediately after trichloroacetic acid termination, were extracted with pentane (5 x 1 ml). For each assay tube, the combined extracts were washed with 10% aqueous sodium sulfate (3 x 1 ml) and dried over anhydrous magnesium sulfate. Samples not immediately subjected to column chromatography were stored in the refrigerator.

The organic products were resolved by mini-column chromatography on florisil. The mini-columns were packed with a 7 cm bed of florisil and wetted with pentane prior to sample loading. During sample loading, all pentane was collected as a single fraction in a 20 ml scintillation vial. The column was first eluted with 80:20 pentane/diethyl ether and seven 3 ml fractions were collected in 7 ml scintillation vials. The column was next eluted with 99:1 diethyl ether/acetic acid until a total of seven 3 ml fractions had been collected. All column fractions were mixed with an equal volume of either Scintisafe Econo F or Scintisafe Plus 50% cocktails and radioactivity was quantified by scintillation counting. Results were compared to the elution profiles of standard [^{3}H]-4-methylnonanoic acid and [^{3}H]-4-methylnonanol.

2.4.13. *Statistical Analysis*

Statistical comparison of means was carried out with the application of a Student-Neuman-Keuls test. Means were deemed significantly different if $p<0.05$.

3.0. DATA AND RESULTS

3.1. SYNTHESIS OF REQUIRED CHEMICALS

3.1.1. *Malonic Ester Synthetic Route*

4-Methyl-1-methoxynonane, 4-methylnonanoic acid and 4-methylnonanol were successfully synthesized (Figure 4) in overall yields of 11.8%, 10.1% and 5.7%, respectively. The carbanion of dimethyl malonate was created using sodium methoxide and subsequently

reacted with 2-bromoheptane to form the diester **1**. Dealkoxycarbonylation using the method of Krapcho (1982a, b) produced 3-methyl-1-octanol **(3)**, which was then brominated to form 3-methyl-1-bromooctane **(4)**. The Grignard-derivative of **4** was generated and coupled with carbon dioxide to form the first product, 4-methylnonanoic acid **(5)**. Routine reduction of **5** with lithium aluminum hydride formed the second product, 4-methylnonanol **(6)**. 4-Methyl-1-methoxynonane **(7)** was synthesized by methylation of **6** with methyl iodide. The yields reported in Figure 4 are corrected for product purity, which was determined by GC. The reported purity and thus the yield for each step are likely higher than reported, as samples were generally over-injected on the GC to emphasize the baseline. Detector saturation during the elution of the product peak would result in the resulting signal being artificially low relative to the other peaks detected, thereby reducing the apparent product purity and corrected yield. In any case, the prevalence of any particular species never exceeded 0.5% of the total area, unless noted.

3.1.2. *Claisen Orthoester Rearrangement Route*

4-Methylnonanol was successfully synthesized with 21.2% overall yield (Figure 5). Pentanal was coupled with the Grignard derivative of 2-bromopropene to form 2-methyl-1-hepten-3-ol **(8)**. The Claisen orthoester rearrangement of **8** produced methyl 4-methylnon-4-enoate **(9)**. Palladium-catalyzed hydrogen reduction yielded methyl 4-methylnonanoate **(10)** and subsequent reduction with lithium aluminum hydride produced the target molecule 4-methylnonanol **(6)** in 21.2% overall yield.

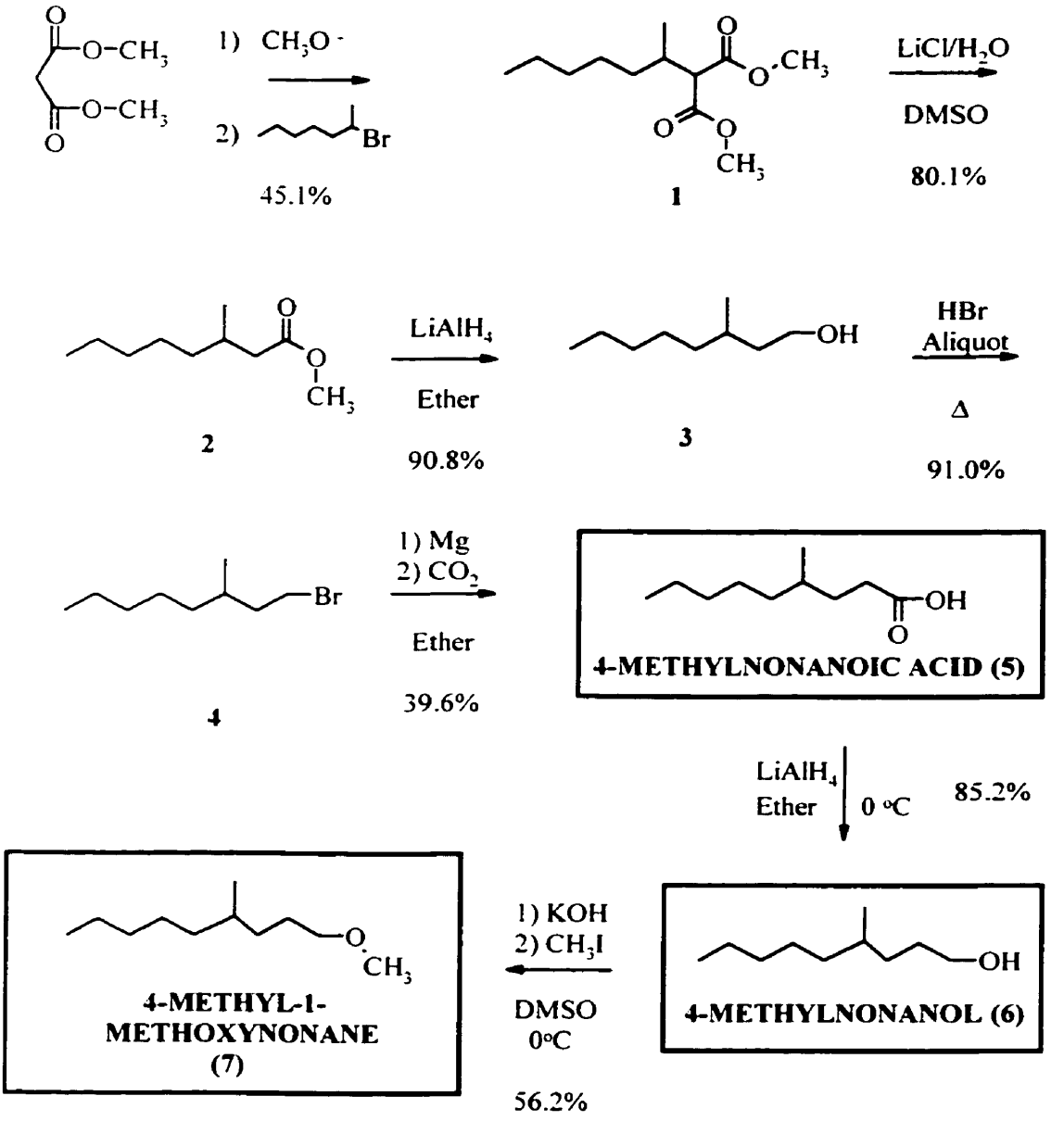

Figure 4: Malonic ester based synthetic route to racemic 4-methylnonanoic acid, 4-methylnonanol and 4-methyl-1-methoxynonane.

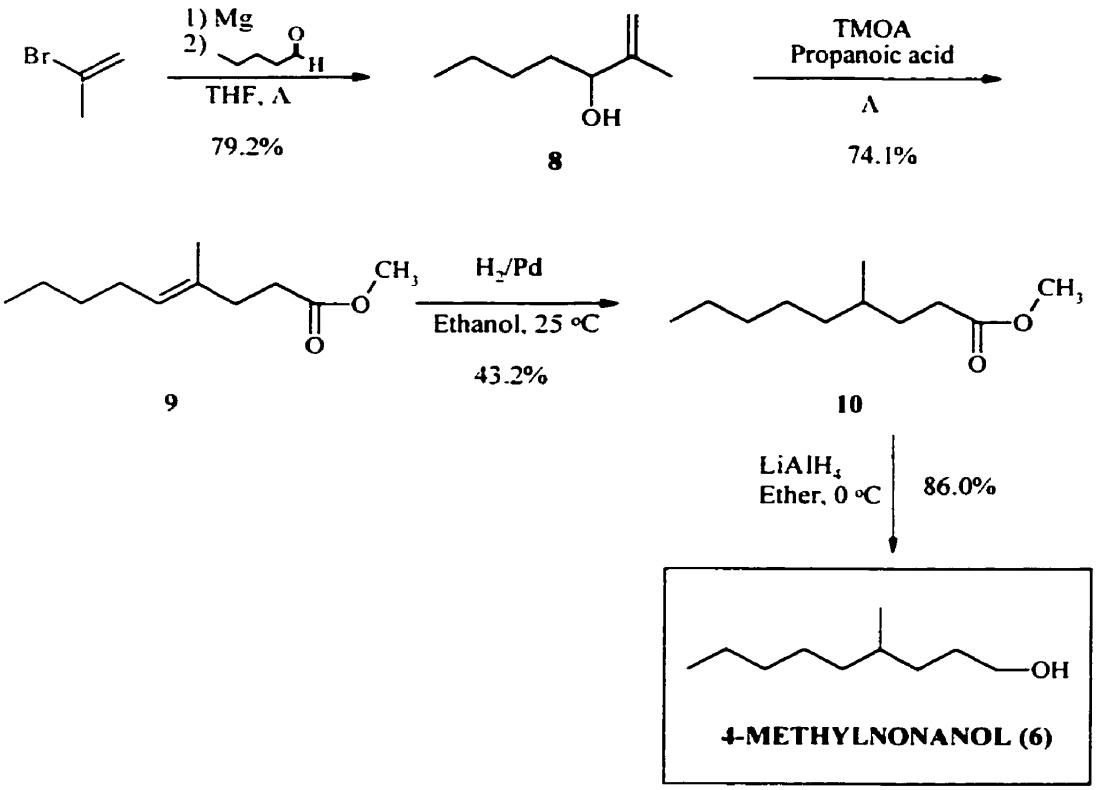

Figure 5: Claisen Orthoester Rearrangement route to racemic 4-methylnonanol.

3.1.3. *Synthesis of Tritium Labeled 4-Methylnonanoyl-CoA*

[^{3}H]-4-Methylnonanoyl CoA was successfully synthesized from available [^{3}H]-4-methylnonanoic acid with yields ranging from 10% to 20%. Recovery of unreacted [^{3}H]-4-methylnoanoic acid was consistently very poor (<10%) when extracted either from the reaction mixture after termination or from the TLC plate after purification.

3.2. BIOCHEMICAL STUDIES

3.2.1. *Effect of Protease Inhibitor Cocktail on Reductase Activity*

The benefit of isolating protein in the presence of protease inhibitors was investigated. Abnormal chromatographic profiles resulted in the elimination of one sample from each of the NADH + protease inhibitors and NADH – protease inhibitors treatments, resulting in duplicate data sets for these treatments. In both cases, there was an abnormal amount of radioactivity in F1 (where only hydrocarbons should elute) and in the pre- diethyl ether/acetic acid fractions. This 'streaking' is consistent with the loss of chromatographic resolution observed when samples are wet with a polar solvent such as water (improperly dried) or ethanol (likely introduced during reaction termination). The mean 4-methylnonanol production and standard error were calculated for each treatment using the remaining samples. Results are represented graphically in Figure 6. Enzyme isolation in the presence of protease inhibitors resulted in a 2-fold increase in reductase activity in the presence of NADH and a 1.6-fold increase in the presence of NADPH. Activity in the absence of protease inhibitors was not significantly different from the no protein control. In the presence of protease inhibitors, activity was increased 1.5-fold in the presence of NADH than NADPH.

3.2.2. *Preference for NADH or NADPH as Reducing Cofactor*

Reductase activity was assayed using crude protein in the presence of either NADH or NADPH in order to establish whether a reducing cofactor preference exists. Mean reductase activity and standard error for each treatment (n=3) are shown graphically in Figure 7. Slightly lower activity was observed in the presence of NADH than in the last experiment, even though slightly more protein was used (4 beetle equivalents as opposed to 3.3 in the previous experiment). Like the previous experiment, reduction in the presence of NADPH was not significantly different from the no protein control.

3.2.3. *Comparison of Males and Females*

The ability of males and females to reduce [^{3}H]-4-methylnonanoyl CoA in the presence of NADH was assessed. A single experiment was conducted (n=3 for each treatment). One trial from each of the no protein control and males treatments was discarded (resulting in n=2 for the no protein control and male treatments, n=3 for female treatments) due to abnormal chromatographic behavior, as described previously. Crude protein derived from male beetles was unable to catalyze the reduction of [^{3}H]-4-methylnonanoyl CoA in the presence of NADH under these conditions (Figure 8). Conversely, crude protein from females demonstrated activity consistent with that in the previous experiments.

3.2.4. *Sub-Cellular Localization of Activity in Males and Females*

Reductase activity was assayed in sub-cellular fractions generated from mature male and female beetles in a single experiment (for each treatment, n=3). Microsomal and soluble fraction protein were unable to catalyze the reduction of 4-methylnonanoyl-CoA, however, both male and female mitochondrial (25 000 x g pellet) protein showed activity (Figure 9). The conversion by female mitochondrial protein matched the magnitude observed in the previous experiments, even though substantially more protein was used (6.7 beetle equivalents compared to 3.3 or 4 beetle equivalents). Contrary to observations from the previous experiment, males were able to perform the reduction, although not as well as females at equal beetle equivalents of protein. Although the mitochondrial protein concentrations were comparable between males and females for the mitochondrial fraction, females possessed substantially more microsomal and soluble protein. This is to be expected, as females are actively engaged in oogenesis.

3.4.5. *Marker Enzyme Analysis*

The 25 000 x g sub-cellular fraction (Figure 10A) contained 96.9% of the total cytochrome C oxidase activity. The two sub-cellular preps analyzed yielded similar cytochrome C oxidase activities, 12.42 mkat/beetle and 15.42 mkat/beetle, respectively (1 kat = 1 mole e^- transferred to oxygen per second).

The majority of alcohol dehydrogenase activity was localized in the soluble sub-cellular fraction (Figure 10B) as expected (Elliott and Knopp, 1981). Alcohol dehydrogenase activity obtained from the three protein preparations tested was slightly more variable than that of

cytochrome C oxidase, with the yield averaging 1.0 ± 0.2 EU/beetle (1 EU = 1 μmol NADH formed/minute).

Results obtained from the analysis of the plasma membrane Na^+/K^+-ATPase were not straightforward (Figure 10C). Although the highest activity was observed in the mitochondrial fraction at the lowest protein level and drops off dramatically as more protein is supplied to the assay. Activity in the microsomal fraction, however, was consistently low. Activity in the soluble fraction was substantial at the 10 μl protein level, but minimal at higher concentrations.

3.2.6. *Refinement of Sub-Cellular Localization in Females*

The sub-cellular distribution of female reductase activity was assayed using pellets obtained at 3 000 x g, 10 000 x g and 100 000 x g (microsomal fraction), as well as the post-100 000 x g supernatant (soluble fraction). A single experiment was conducted with each treatment assayed in triplicate. This was the first assay in which MITO buffer was utilized in protein isolation and the assay itself. The most important observation is the 11-fold increase in activity compared to the previous buffer system. Although activity was detected in the 3 000 x g and microsomal pellets, the bulk of the activity was localized in the 10 000 x g pellet (Figure 11B). This resulted in a substantial purification of the reductase activity, as the 3000 x g pellet contained substantial amounts of protein (104 mg, 29% of the total isolated protein) while the 10 000 x g pellet contained a total of 6.55 mg protein (1.8% of the total isolated protein). The high activity present in the small 10 000 x g pellet is readily apparent when the activity is normalized to protein content for each sub-cellular fraction (Figure 11C). Specific activities could not be determined, as it was not known whether the activity in each fraction was linear with time.

Substantial amounts of free 4-methylnonanoic acid were recovered from incubations with all sub-cellular fractions (Figure 11A). In contrast, almost no free acid was isolated from the no protein control. In previous experiments, assays were terminated with the addition of ethanolic potassium hydroxide with the intention of hydrolyzing and unreacted 4-methylnonanoyl CoA. The use of trichloroacetic acid in the termination procedure preserved unreacted acyl-CoA and led to the discovery of substantial hydrolysis that occurred in the presence of protein, especially from the soluble fraction.

3.2.7. *Determination of Protein Curve*

A protein-activity curve was generated using 10 000 x g pellet protein in order to gain an idea of the amount of enzyme required to observe activity in a convenient assay time (15 minutes). Enzyme activity was determined by subtracting the mean no protein control activity from the mean activity observed at each protein concentration assayed. Enzyme activity in the 15 minute assay was approximately linear at protein concentrations less than 0.1 mg and reached a maximum between 0.25 and 0.5 mg protein (Figure 12). Since the 10 000 x g pellet yielded 1.1 mg protein per beetle used, only 0.5 beetle equivalents of protein was required to obtain maximal activity in a 15 minute time frame. Based on these findings, a protein concentration of 0.1 mg/ml was chosen for further characterization of reductase activity in female beetles.

3.2.8. *Determination of Time Curve*

Using 0.1 mg of 10 000 x g pellet protein, a time curve for the reduction of 4-methylnonanoyl CoA was obtained (Figure 13). Mean activity at each time interval was control-

subtracted. Activity was approximately linear until nearly the 10 minute mark, at which point it began demonstrating saturation.

3.2.9. *Determination of NADH and NADPH Substrate Curves*

Substrate activity curves were derived for both NADH (Figure 14A, B) and for NADPH (Figure 14A). A hyperbolic activity curve could not be obtained for NADH using 10 000 x g protein. In fact, similar activity was obtained regardless of whether NADH was supplied to the preparation or not (Figure 14B). The NADPH curve derived in Figure 14A may be demonstrating some dependence on concentration as activity is much lower with 1 μM NADPH than the rest of the curve.

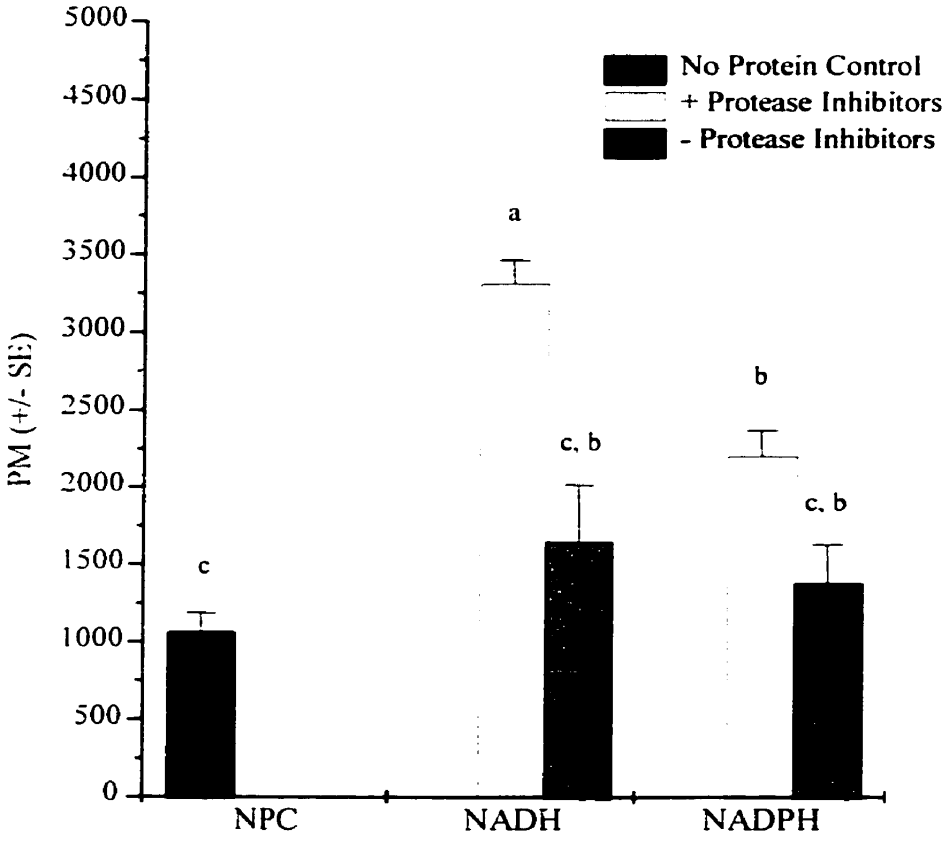

Figure 6: Effect of protease inhibitor cocktail use during enzyme isolation on the reduction of [^{3}H]-4-methylnonanoyl CoA (in the presence of NADH or NADPH) by crude homogenates of mature female *T. molitor*. Means not labeled with the same letter are statistically different ($p<0.05$).

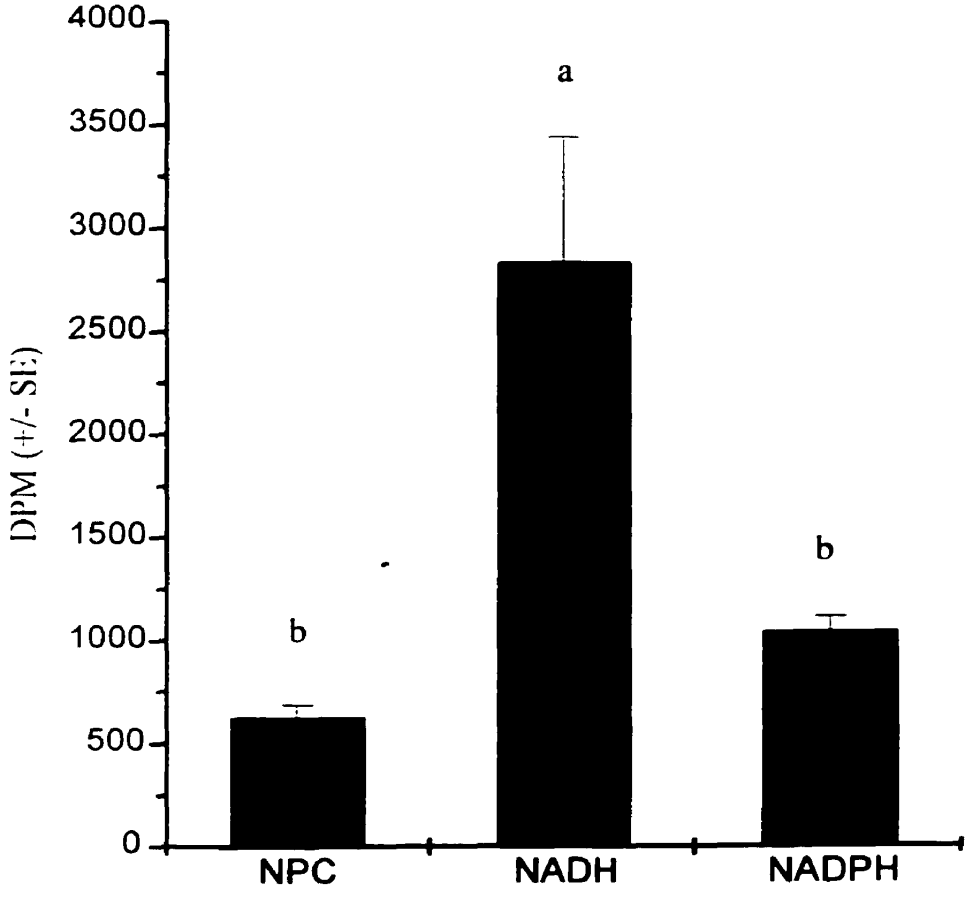

Figure 7: Reducing cofactor preference in the reduction of [^{3}H]-4-methylnonanoyl CoA by crude homogenates of mature female *T. molitor* (isolated in the presence of protease inhibitors). Means labeled with a different letter are significantly different ($p<0.05$).

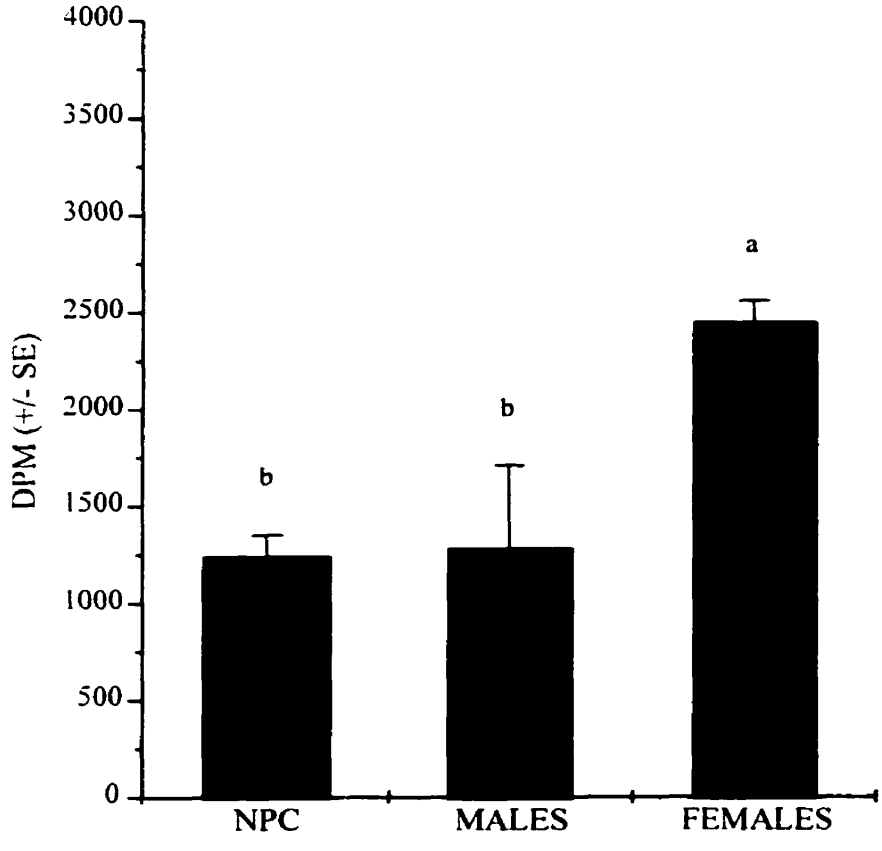

Figure 8: Reduction of [^{3}H]-4-methylnonanoyl CoA (in the presence of NADH) by crude homogenates of mature male or female *T. molitor* beetles isolated in the presence of protease inhibitors. Differentially labeled means are significantly different ($p<0.05$).

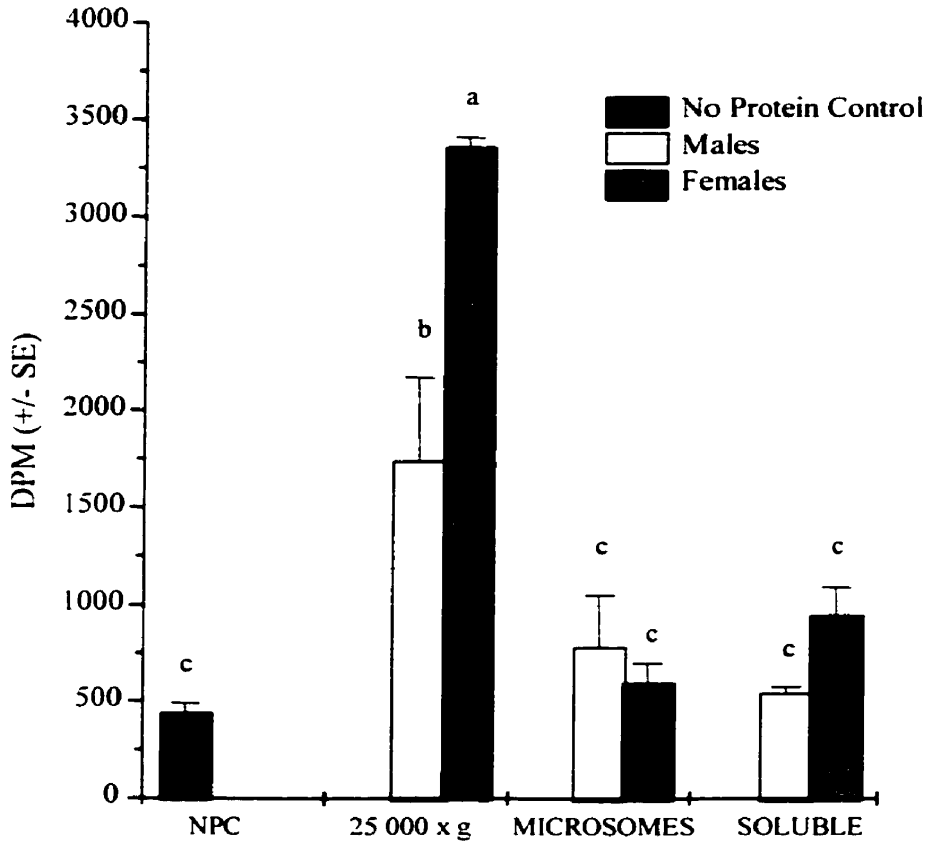

Figure 9: Sub-cellular localization of [^{3}H]-4-methylnonanoyl CoA reductase activity in mature male and female *T. molitor* (in the presence of NADH). Enzyme preparations from both sources were obtained in the presence of protease inhibitors. Differentially labeled means are significantly different ($p<0.05$).

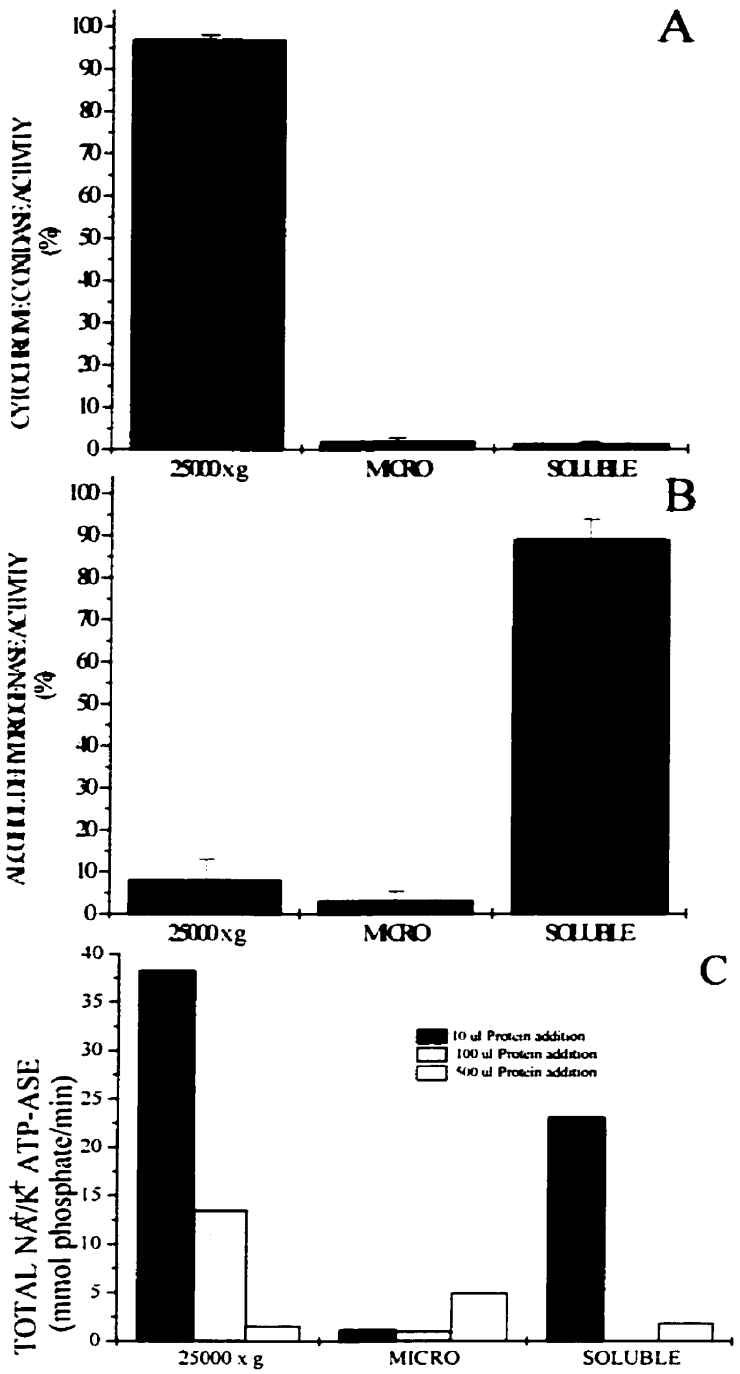

Figure 10: Sub-cellular distribution of marker enzyme activities. **A:** Cytochrome C oxidase (mitochondrial marker). For each treatment, n=2. **B:** Alcohol dehydrogenase (soluble marker). For each treatment, n=3. **C:** Sodium/potassium ATP-ase (plasma membrane marker). Activity was assayed using 10µl, 100µl or 500µl of protein from the respective sub-cellular fraction. Activity was normalized to sub-cellular fraction volume for comparison.

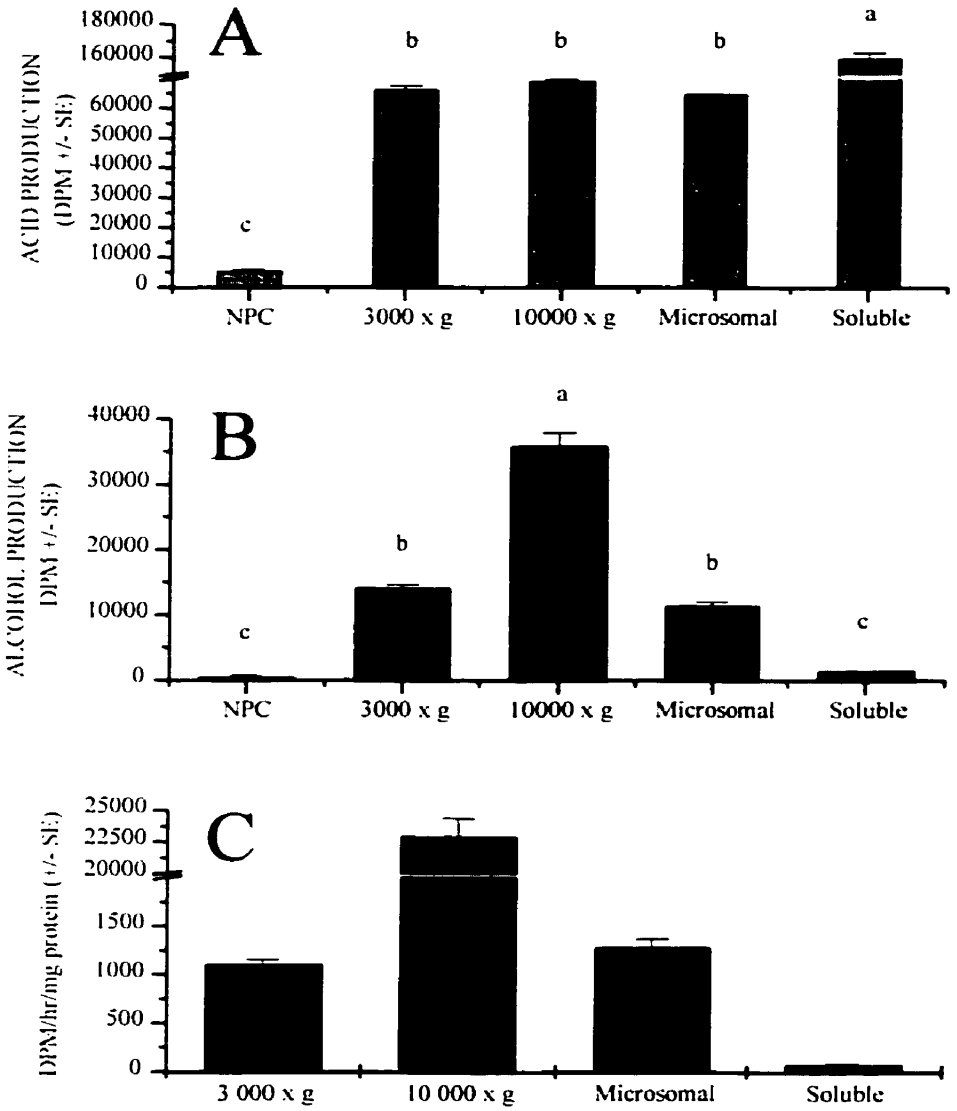

Figure 11: Refinement of sub-cellular localization of 4-methylnonanoyl CoA reductase activity. Acid and alcohol production in the presence of NADH by sub-cellular fractions of mature female *T. molitor* beetles using enzyme isolated in the presence of protease inhibitors. Differentially labeled means are significantly different ($p<0.05$). **A:** 4-Methylnonanoic acid production from [^{3}H]-4-methylnonanoy CoA. **B:** 4-Methylnonanol production from [^{3}H]-4-methylnonanoyl CoA. **C:** Total sub-cellular reductase activity normalized to protein content.

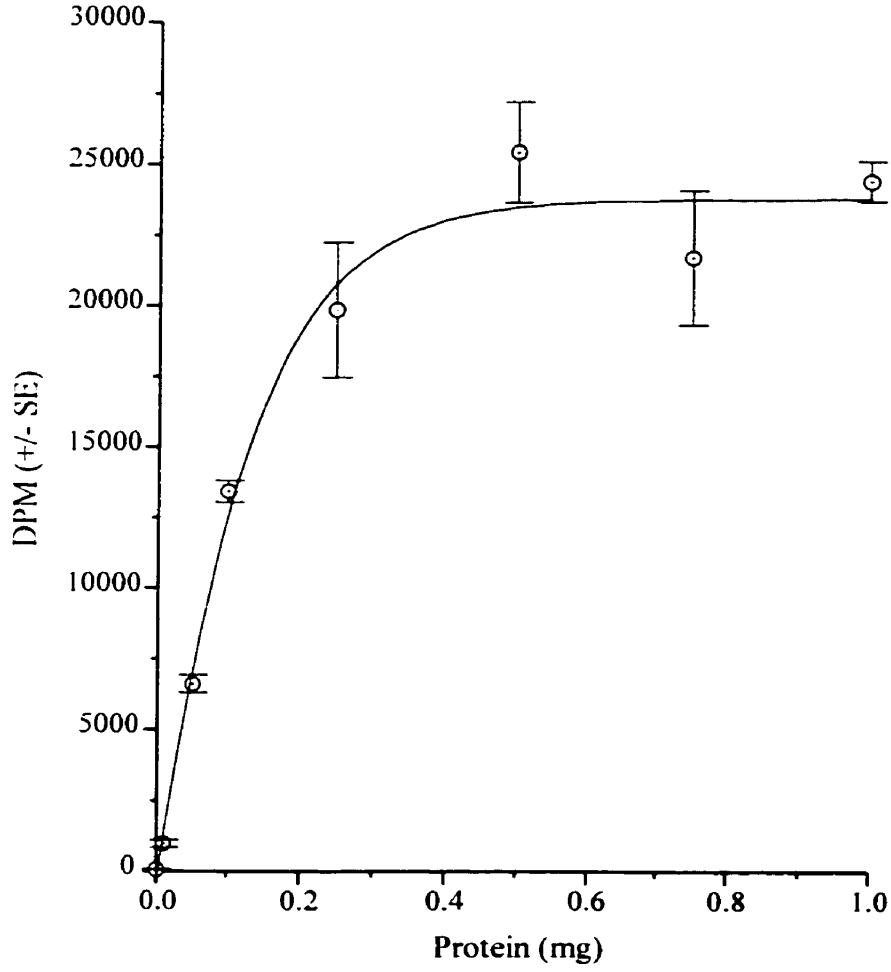

Figure 12: Dependence of reductase activity on 10 000 x g pellet protein obtained from mature female *T. molitor* beetles in the presence of protease inhibitors. Activity was assayed in the presence of NADH and [^{3}H]-4-methylnonanoyl CoA using a 15 minute assay. n=3 for each protein concentration.

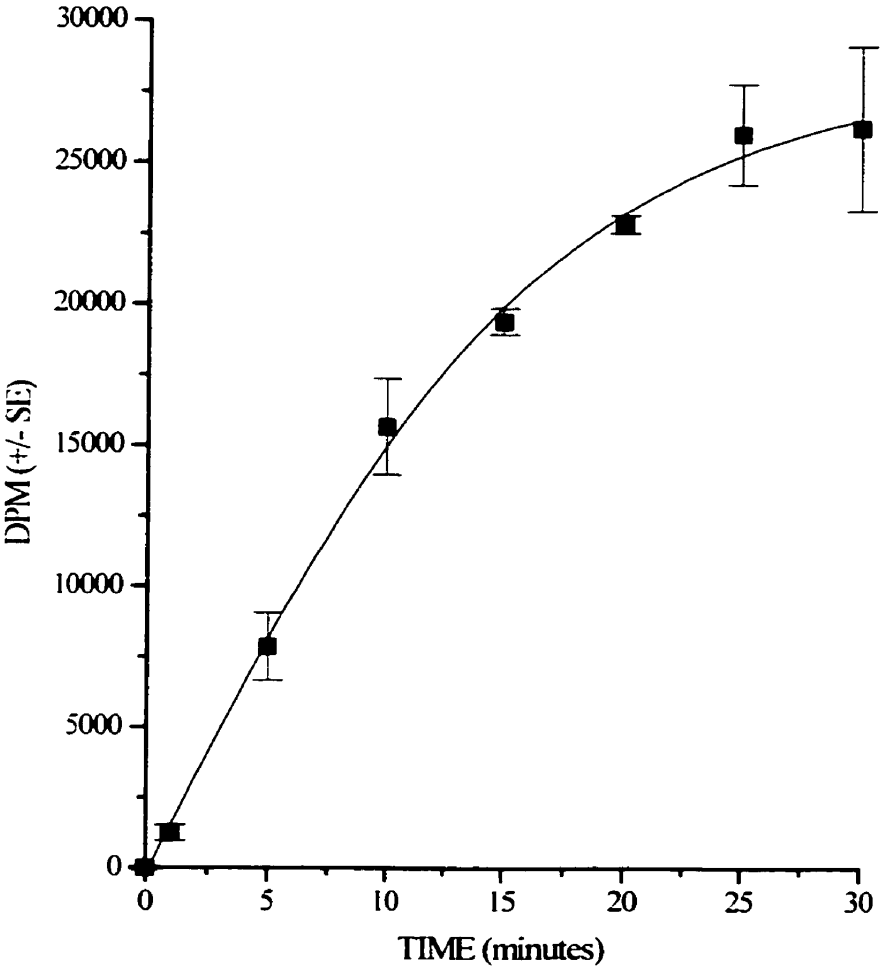

Figure 13: Time curve for the reduction of [^{3}H]-4-methylnonanoyl CoA in the presence of NADH using 10 000 x g pellet protein obtained from mature female *T. molitor* beetles (isolated in the presence of protease inhibitors). n=3 for each time point.

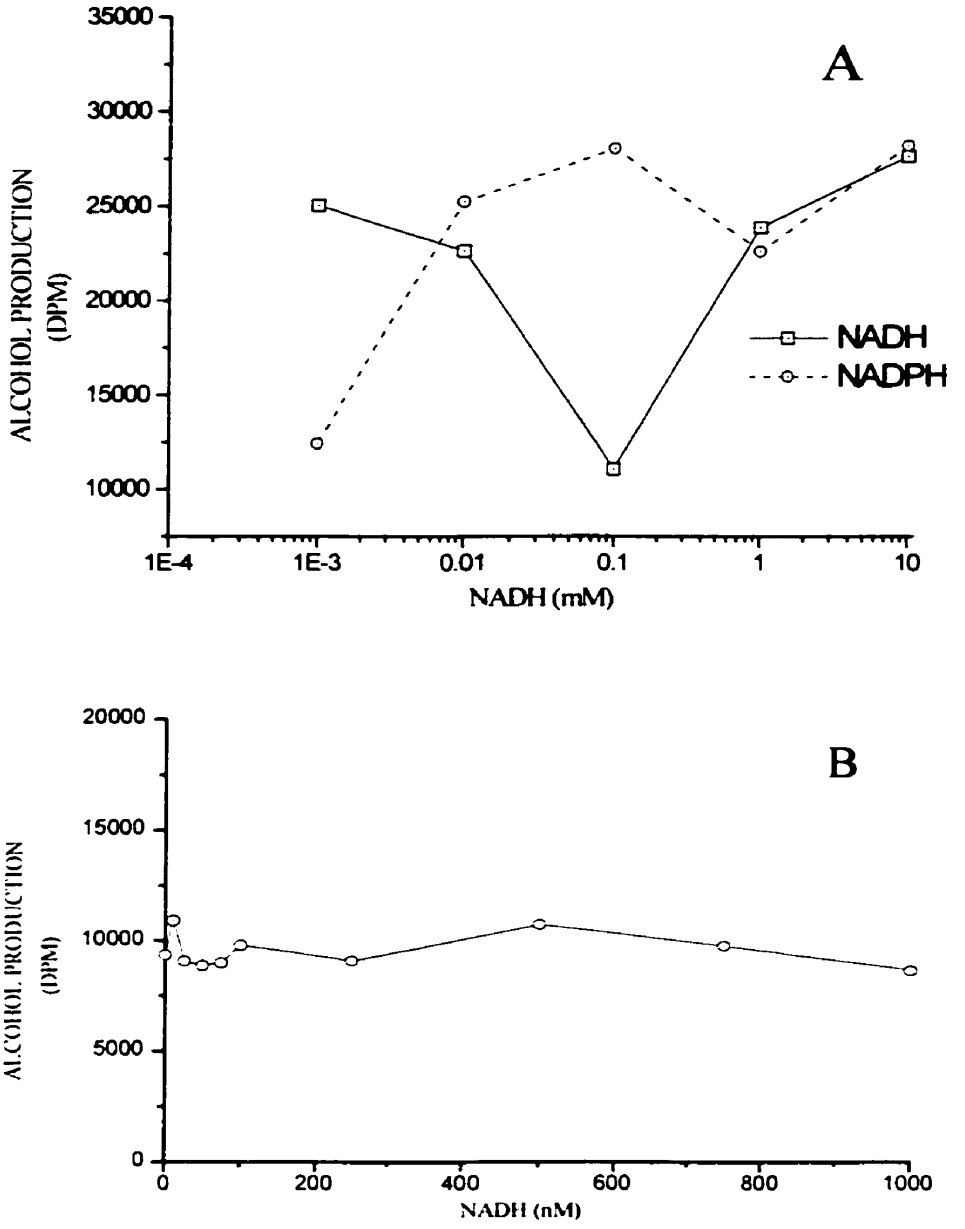

Figure 14: Dependence of reducing cofactor on reduction of [^{3}H]-4-methylnonanoyl CoA in the presence of 10 000 x g pellet protein obtained from mature female *T. molitor* beetles. **A:** Activity curves for 1 μM to 10 mM NADH and NADPH (n=1 for each concentration point). **B:** NADH activity curve for 10 nM to 1 μM added cofactor (n=1 for each concentration).

4.0. DISCUSSION

4.1. SYNTHESIS OF REQUIRED CHEMICALS

The synthesis of 4-methylnonanoic acid 4-methylnonanol using the malonic ester-based route was achieved with overall yields of 11.8% and 10.2%, respectively (the product yield at each step is summarized in Figure 4). The first step of the synthesis, the addition of 2-bromoheptane to the carbanion of dimethyl malonate, was the least successful, with a yield of only 45.1%. While the reaction itself ran smoothly, product isolation was not straightforward. Solvent extraction was unable to remove more than 60% of the product from the reaction mixture, with the reported protocol being the most successful. The use of diethyl ether instead of pentane increased recovery, while using more or less water in the work-up and acidification prior to extraction had no significant effect. With the hypothesis that the presence of methanol was solubilizing the product in the aqueous phase, a distillation step was added prior to extraction in order to remove as much methanol as possible. Unfortunately, this was unsuccessful in improving product recovery. The difficulty in isolating the product from the reaction mixture was unforeseen, as reactions such as this have been used extensively over the last century from micro- to industrial-scale, typically in high yield. It is entirely possible that recovery could be enhanced dramatically through further optimization of the extraction protocol.

The second step of the pathway, dealkoxycarbonylation via the Krapcho reaction (Krapcho, 1982a, b), proceeded essentially quantitatively with no side products detectable by GC or NMR. Unfortunately, the product **(2)** possessed an acrid odor, likely from thermal decomposition products arising from the DMSO used as solvent. These odorous contaminants were successfully removed by distillation, although this did reduce the yield to 80.1% (Figure 4).

Attempts to oxidize and remove the contaminants (by increasing their water solubility) by washing the product with a 0.5% bleach solution initially seemed successful, as it eliminated the odor. However, the odor reappeared later in the synthesis (after reduction with lithium aluminum hydride) indicating the contaminants had been oxidized but not removed by the bleach washes. This was unfortunate, as the yield would have been increased significantly if the distillation could have been avoided.

After routine reduction by lithium aluminum hydride, the alcohol **(3)** was brominated to form 3-bromooctane **(4)** by refluxing with hydrobromic acid. Hydrobromic acid was initially selected as a brominating agent based on its simplicity, both during the reaction and product isolation. Serendipitously, the reaction worked well enough that it was unnecessary to develop an alternative.

Chain elongation by carbonylation of the Grignard derivative of 3-bromooctane to form 4-methylnonanoic acid **(5)** proved to be the lowest yield step (39.6%) in the route. The generation of the Grignard derivative of 3-bromooctane, magnesium 3-bromooctyl bromide, proved to be the most complicated step, as is the case with Grignard reagents produced from many aliphatic halides. Care must be taken to add enough 3-bromooctane to initiate reaction with the magnesium but not so much as to have excess bromide in solution (which may react with freshly generated Grignard reagent and dimerize). It is possible that the addition of carbon dioxide to the Grignard reagent was incomplete when the reaction was worked up, however, it is unlikely as Grignard reagents are quite reactive (especially with carbon dioxide) and a generous reaction time was allowed in the procedure. In the future, the progress of this reaction could be monitored using GC to verify that complete reaction was indeed achieved. Most likely, the sluggish reactions of magnesium with 3-bromooctane, coupled with hasty bromide addition were

responsible for the low yield obtained. In the future, the yield of this step may be improved by using 3-iodooctane rather than 3-bromooctane, as iodides react more readily than bromides. Alternatively, tetrahydrofuran (THF) may be used as the solvent for the reaction. THF has a higher boiling point than diethyl ether thereby providing more energy to aid the reaction of alkyl halide with magnesium. However, it is more difficult to remove THF from the product than diethyl ether.

Formation of 4-methylnonanol **(6)** by reduction of 4-methylnonanoic acid **(5)** with lithium aluminum hydride proceeded nearly quantitatively and in high yield. The yield and purity listed in Figure 4 are that of the crude product, as it was not purified after extraction. The purity of the crude product was 90% by GC and in fact was likely greater due to sample over-injection during analysis (as explained in the Data and Results section) and the absence of any other species of significant abundance. Samples were analyzed in this manner because it was deemed more important to gain qualitative information about the species present in the sample than the GC purity. As a precautionary measure, the product was purified by column chromatography in small batches as needed to guard against sample decomposition or contamination during storage.

The Claisen orthoester rearrangement route (Figure 5) was slightly more successful than the malonic ester route, providing 4-methylnonanol in 21.2% overall yield. Although the first step of this route involved a Grignard reaction, which proved to be the major setback of the previous route, the bromide used was allylic rather than aliphatic. Allylic halides differ from aliphatic halides in that they are much less reactive with magnesium, requiring higher boiling solvents (March, 1992). Indeed, the generation of the Grignard reagent of 2-bromopropene did not proceed in diethyl ether at all and in THF only under reflux. In addition, allylic Grignard

reagents are much poorer nucleophiles due to the presence of the π electron cloud from the double bond (March, 1992). This proved to be a substantial advantage, as any generated reagent would not react readily with unreacted 2-bromopropene in solution. Furthermore, when pentanal was added, the reaction proceeded so exothermically it nearly boiled out of the flask. The 88% yield obtained is excellent and the product purity was exceptional, as no substantial side reactions occurred and any unreacted starting materials had a low enough boiling point that they were removed with the solvent during rotary evaporation.

The Claisen orthoester rearrangement of 2-methyl-1-hepten-3-ol **(8)** to form methyl 4-methylnon-4-enaote **(9)** likewise proceeded in high yield and excellent purity (>95% before purification). The only undesirable factor was the prolonged (30 hour) reaction time. The palladium-catalyzed addition of hydrogen across the double bond of **9** to produce methyl 4-methylnonanote **(10)** proceeded poorly, resulting in a low 48% yield. Unfortunately, the cause for the low yield was incorrectly set GC parameters, which resulted in the reaction being deemed complete prematurely. It was not discovered until the product was purified that substantial unreacted starting material remained. The long (8.5 hour) reaction time is likely due to the double bond being tertiary (containing three alkyl substituents), as reaction rates decrease with increasing substitution of the double bond (March, 1992). In the future, using an elevated temperature or using a hydrogen atmosphere of greater than 1 atmosphere (although special apparatus would be required for this) could be used to decrease reaction times. To complete the synthesis, methyl 4-methylnonanoate was reduced with lithium aluminum hydride to form 4-methylnonanol although a simple hydrolysis of the ester would also form 4-methylnonanoic acid in high yield.

Although only completed on a small 'test' scale, the Claisen orthoester route shows promise as a replacement for both the malonic ester route to unlabelled alcohol and acid as well as the existing synthesis for radiolabelled substrate. In the synthesis of radiolabelled 4-methylnonanol and 4-methylnonanoic acid, the presence of a double bond in a defined position on **9** (Figure 5) makes it a better candidate for tritium addition than the mixed alkene product obtained in the existing synthesis (summarized in Figure 3). In addition, the required radiolabelled molecule, 4-methylnonanoic acid, is produced in a single step by a routine hydrolysis rather than two steps in the existing pathway. In general, the less product manipulation required after radiolabelling the better, to minimize both loss and the potential for a major accident (e.g. spillage), especially when working with large amounts of radioactivity. Finally, in the existing synthesis (Figure 3), 4-methylnonanol is produced by the cleavage of methyl 4-methylnonyl ether, which is then oxidized to the acid. The problem arises with the use of the acid as a substrate in the *in vitro* reduction assay, as care must be taken to ensure that no residual alcohol remains. Contaminating radiolabelled 4-methylnonanol would increase the background 'activity' detected in the assay, thereby reducing the sensitivity of the assay and could even be mistaken for actual enzymatic reduction. These problems would be avoided by using substrate produced using the Claisen orthoester synthesis, as 4-methylnonanoic acid is produced directly.

The enzymatic synthesis of acyl-CoA from [^{3}H]-4-methylnonanoic acid was successful, although the yield was low (10%-20%). The low yield is likely a product of both incomplete CoA derivatization as well as product hydrolysis during the work-up procedure. When reaction progress was monitored using TLC, maximal acyl-CoA production (42%) was achieved within one hour (data not shown). The actual conversion determined is likely an underestimate, however, as the free fatty acid would be counted more accurately than acyl-CoA in TLC plate

scrapings by LSC. This discrepancy arises from the fact that the free fatty acid has a lower affinity for silica gel than the acyl-CoA and produces a much more homogeneous (and more accurately counted) LSC sample. Since the yield of the reaction ranged from 10%-20% after purification, this would suggest that more than half of the product degraded during the isolation and purification procedure. Although much better than acid precipitation, the preparatory TLC product purification is only an improvement, not a solution. Silica gel is well known to catalyze the hydrolysis of a wide variety of esters, even in the absence of water. The TLC purification method uses a mobile phase which is 50% water, increasing the potential for hydrolysis. To make matters worse, the TLC plate requires 4-6 hours to develop plus a further 2-3 hours to dry before the product may be extracted from it. The prolonged exposure of product to wet silica gel poses a serious threat to product stability, which seems to be validated by the loss in yield observed during product isolation.

In addition to the low yield of the acyl-CoA synthesis, problems were also encountered recovering synthesized acyl-CoA from the TLC plate. The failure to efficiently extract synthesized [^{3}H]-4-methylnonanoyl CoA from the TLC plate scrapings is likely due to the short carbon chain length of the acyl portion of the molecule. The water solubility of acyl-CoA molecules is derived from the highly polar CoA portion of the molecule, while the carbon chain length of the acyl group linked to the CoA reduces this polarity, due to its hydrophobic character. The longer the acyl moiety is, the less polar the acyl-CoA is, and the easier it is to extract from a polar TLC plate. Conversely, the shorter the acyl group is, the more polar the resulting acyl-CoA becomes, and the higher affinity it has for a polar stationary phase such as silica gel. To offset the increased polarity of 4-methylnonaoyl CoA, relative to palmitoyl-CoA which is seven carbons longer or oleoyl-CoA which is nine carbons longer, a more polar solvent (methanol) was selected than that used by Banis *et. al* (1976). Unfortunately, methanol still proved not to be

polar enough to efficiently extract the product from the plate, as demonstrated by the persistent radioactivity in successive extractions of the acyl-CoA containing TLC fractions. Attempts to extract the acyl-CoA with acetate buffer were unsuccessful as the silica gel became sludgy and the extract could not be completely removed from the gel. Isolating the product in a water-based medium would have been preferable, as the extract could be readily lyophilized in order to increase the concentration of the resulting acyl-CoA solution. Methanol is much more troublesome to remove *in vacuo* as it does not remain frozen like water does and the risk of solvolysis increases dramatically.

Although the yield of [^{3}H]-4-methylnonanoyl CoA was low, sufficient quantities were generated for experimental use, and the synthesis would not be wasteful if the unreacted fatty acid could be recovered. Unfortunately, attempts to recover the unreacted 4methylnonanol were unsuccessful. Again, the likely reason for the failure in recovery is the TLC purification stage. The problem with working with shorter chain fatty acids is they possess substantial vapor pressures, making them quite volatile compared to long chain fatty acids, which are generally not very volatile. It is likely that the combination of the long TLC development time, the minute quantities of fatty acid being used as well as the extremely high surface area of the TLC plate resulted in the evaporation of the majority of the unreacted fatty acid. Attempts to extract the reaction mixture with pentane before TLC purification were also unsuccessful due to the small volumes involved and resulted in a loss of reaction mixture on the side of the vial. The failure to reclaim unreacted fatty acid was disappointing, as the synthesis of radiolabelled 4-methylnonanoic acid was not only time consuming but costly as well.

The problems of acyl-CoA isolation and unreacted fatty acid recovery may be solved using reverse phase HPLC instead of TLC for product purification. As HPLC possesses much

higher resolution than TLC, product dilution would be kept to a minimum, as it would elute in a much tighter band. Also, there is no chance for evaporation from an HPLC column, so loss of unreacted fatty acid would be minimal. Most importantly, the entire reaction mixture could be purified in one or two thirty minute HPLC runs, as opposed to the protracted TLC process. The synthesis was successful overall, as sufficient acyl-CoA was generated for several weeks of experimentation. Although the synthesis itself could probably be optimized to provide a higher yield by varying the cofactor concentrations and reaction times, it is probably not worth while until the purification step is optimized or replaced. The low yield could easily be reconciled by the recovery of unreacted fatty acid, as the synthesis could then be repeated.

4.2. BIOCHEMICAL STUDIES

In vitro reduction of radiolabelled 4-methylnonanoyl CoA by homogenates of mature female yellow mealworm beetles was observed. However, the assay has not been completely optimized. The first step in the assay development was to test the effect of protease inhibitors on reductase activity. Enzyme samples isolated in the presence of protease inhibitors should be 'healthier' than those unprotected from endogenous proteases. However this does not always translate to an increase in activity. Although the mechanism of fatty acyl reduction has not been elucidated, it likely proceeds through a tetrahedral intermediate, as does peptide hydrolysis (Figure 15). As most competitive protease inhibitors are stable mimics of these intermediates, they may also behave as competitive inhibitors towards various reductases as well. Although protease inhibitors have a high affinity for their peptide-based active sites and the substrate binding site of an acyl-CoA reductase should be quite different from that of a protease, it is still possible that one or more protease inhibitors may have sufficient affinity to reduce the activity of the enzyme of interest. The cocktail selected was designed for use in mammalian systems and

contained 4-(2-aminoethyl)benzenesulfonyl fluoride, pepstatin A, trans-epoxysuccinyl-L-leucylamido(4-guanidino)butane, bestatin, leupeptin and aprotinin. When used in protein isolation at concentrations recommended by the manufacturer, reductase activity was increased 2-fold and 1.5-fold when using NADH or NADPH as a reducing co-factor, respectively (Figure 6). Although activity could possibly have been increased further by evaluation of other inhibitor combinations and concentrations, it was not deemed necessary in light of the activity levels observed in later experiments (Figures 11-14).

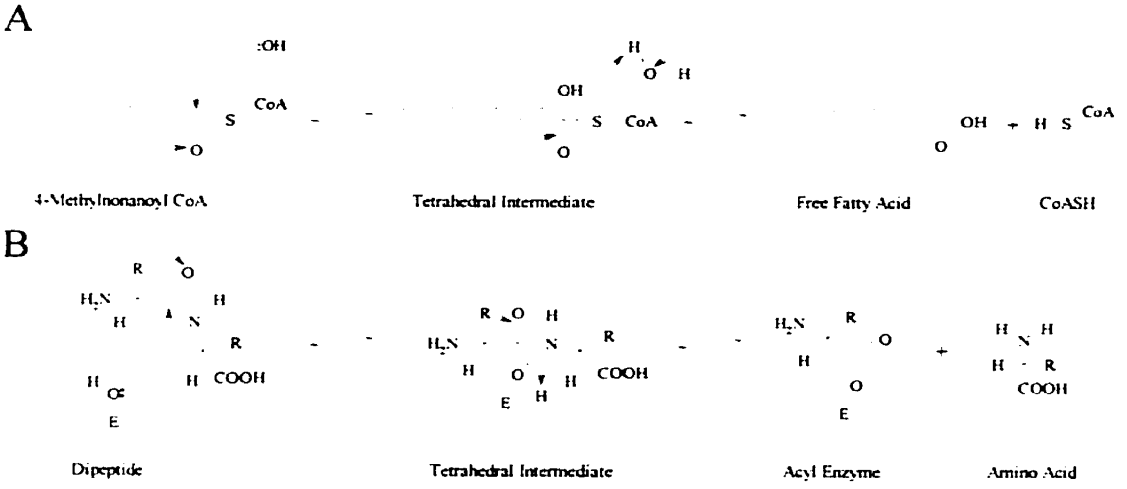

Figure 15: Thioester and peptide hydrolysis showing common tetrahedral intermediate. **A.** The nucleophilic hydroxyl group (either hydroxide ion or active site serine/threonine) attacks the thioester, forming a tetrahedral intermediate, which decomposes to yield a fatty acid and CoAS-H. **B.** Nucleophilic attack from the enzyme active site hydroxyl group (serine, for example) forms a tetrahedral intermediate. The intermediate decomposes, forming a free amino acid (or peptide) and anacylenzyme conjugate, which undergoes further hydrolysis.

Attempts to remove extraneous protein from the assay by differential centrifugation yielded unexpected results. Although all eukaryotic acyl-CoA reductases studied are microsomally localized (Riendeau and Meighen, 1985; Wang and Kollatukudy, 1995; Vioque

and Kollatukudy, 1997), 81.4% of the reductase activity was found in the 25000 x g pellet and only 4.5% in the microsomal pellet (Figure 9). Although the 25 000 x g pellet used in the assay was not purely mitochondria, it did contain 97% of the total cytochrome C oxidase activity (Figure 10A), suggesting that virtually all of the cellular mitochondria were in this pellet.

Based on the potential and unexpected mitochondrial localization of reductase activity, the development of other enzyme assays was undertaken in order to establish the composition of the 25 000 x g, microsomal and soluble sub-cellular fractions. Classical eukaryotic marker enzymes were selected, with an effort made to select enzymes that had been used in other insect systems. Alcohol dehydrogenase (a soluble marker) was selected because it has been used in other insect systems including *Drosophila melanogaster* (Leal and Barbancho, 1993; Elliott and Knopp, 1981), *Acheta domesticus* and *Periplaneta americana* (Borgeson and Blomquist, 1993). Although no cytosolic contamination of the 25 000 x g or microsomal pellets was expected, alcohol dehydrogenase was selected as a control to form a complete set of marker enzymes. Alcohol dehydrogenase activity was segregated to the soluble fractions as expected (Figure 10B). The sodium/potassium ATPase was selected as a plasma membrane marker based on its use in both *A. domesticus* and *P. americana* (Borgeson and Blomquist, 1993). The assay measures phosphate liberated from ATP both in the presence and absence of orthovanadate, a specific inhibitor of the plasma membrane ATPase. The activity lost in the presence of vanadate when compared to activity in the absence of vanadate is equal to the sodium/potassium ATPase. The activity observed from this assay was erratic and confusing (Figure 10C). The only inference that may be drawn from these results is that the plasma membrane likely did not sediment with the microsomes, but with the 25 000 x g pellet instead. This assay will have to be repeated before any solid conclusions may be draw, however. The major problem with the assay was that it was performed as a stopped-time assay, which made it nearly impossible to be sure

activity was linear with protein load or time. Furthermore, the observation of activity only at the end of the assay led to the results being dependent on a single data point. In the future, much more information could be gained by assaying at different time intervals in order to construct activity-time curves (this would also provide multiple data points per assay, allowing for the recognition and deletion of outliers). p-Nitroanisole demethylase was selected as a marker for the mixed-function oxidase system of the endoplasmic reticulum using the method of Hansen and Hodgson (1971), however the assay failed to produce any substantial amounts of activity. p-Nitroanisole demethylase has been used studied extensively in insects, mainly in the field of pesticide resistance, so failure to observe meaningful activity was unexpected. The development of a complement of marker enzyme assays was put aside at this point, as it was drawing an enormous amount of time from the project objective (the development of an *in vitro* reductase assay to determine whether reduction to 4-methylnonanol was a regulated step of pheromone biosynthesis).

To further investigate the co-localization of cellular mitochondria with the reductase activity, the literature was reviewed for a more suitable speed at which to isolate mitochondria. Van den Bergh (1965) detailed the isolation of intact mitochondria from several insect species at 3000 x g, while in a review, Rickwood *et al.* (1987) reported a value of 10 000 x g, irrespective of the tissue or source. When activity in each of these pellets was compared to that of the microsomal and soluble fractions, 59% of the activity was found in the 10 000 x g pellet (Figure 11B). Even more surprisingly, the 10 000 x g pellet contained only 1.8% of the total protein isolated. The substantial purification of reductase activity is readily apparent when the individual sub-cellular fractions are normalized to protein content (Figure 11C). Unfortunately, specific activities could not be calculated as it was not known if the activities were linear with time. The 3 000 x g pellet contained 22% of the total activity, but 29% of the total isolated

protein. Substantial activity was observed in the microsomal pellet, though this was disregarded as residual activity that failed to sediment at the lower speeds, especially since this microsomal activity was absent in the previous experiment (Figure 9). Further studies will be required to determine the mitochondrial distribution on these centifugal fractions and whether or not the 4-methylnonanoyl CoA reductase activity is located in the mitochondria. As the current project involved the development of an assay for the *in vitro* reduction of 4-methylnonanoyl CoA, the sedimentation at 3 000 x g was eliminated and a single 10 000 x g pellet encompassing the total reductase activity was used for subsequent analyses.

The possibility of the reduction of 4-methylnonanoyl CoA occurring in the mitochondria led to a re-evaluation of the buffer system used both for enzyme isolation and in the assay. The phosphate buffer initially used for the preliminary studies (Sections 2.4.3 through 2.4.6), which yielded only low amounts of activity, was replaced by the MITO buffer (see section 2.4.1) suggested by Rickwood *et al.* (1987) for the isolation of intact mitochondria. Use of the new buffer system led to a ten-fold increase in activity (Figure 11B). The low reductase activity observed in the early experiments was likely at least partially due to the extreme ionic strength of the phosphate buffer used. As many proteins are not stable at high salt concentrations, a wide range of enzymes was likely inactivated during isolation. If the reduction did indeed occur in the mitochondria, activity could be limited further by an intact mitochondrial membrane separating substrate and enzyme. Unfortunately, attempts at lysis using ultrasound, osmotic shock and freeze-thawing following the procedure of Robinson *et al.* (1987) did not lead to any increase in reductase activity (data not shown). While ultrasonic lysis runs the risk of inactivating the enzyme of interest, freeze-thawing and osmotic shock are usually more gentle (Robinson *et al.*, 1987). Failure of all three of these methods to increase activity, coupled with the fact that insect mitochondria are significantly less stable than those from other animal sources (Van den Bergh,

1965), suggests that after enzyme isolation there is no longer, if there ever was, an intact membrane barrier.

Preliminary experiments showed that the reduction of 4-methylnonanoyl CoA seemed to prefer NADH over NADPH as reducing co-factor in some cases (Figures 6 and 7). However in some cases there was no difference (data not shown). The preference for NADH over NADPH as reducing co-factor is an interesting prospect, as all known eukaryotic acyl-CoA reductases have a strong preference for NADPH (Riendeau and Meighen, 1985; Wang and Kollatukudy, 1995; Vioque and Kollatukudy, 1997). Drawing any conclusions about co-factor preference from these early experiments would be premature, however, as the assays used crude protein and were not optimized. In many cases, enzymes will have a substantially higher affinity for one reducing co-factor over the other, but will accept the other when it is present at extremely high concentration. Since the NADH and NADPH concentrations were high (1 mM) for the early experiments, it is plausible that preference for NADH could be seen in some experiments but not others. The results of these crude assays could not be compared to each other, however, as the amount of protein used in each experiment varied. Since low activity was observed in the crude protein experiments (Figures 6-9), as much protein was used as possible in each experiment in case the enzyme in question was present only at low levels or had low activity. Subsequent experimentation showed this was not the case and the assay buffer was responsible for the low activity.

Based on the crude experiments (Figures 6 and 7), NADH was selected as the reducing co-factor of choice for optimization of the reduction assay since it produced the same or better activity than NADPH. The next factor optimized was the protein levels used in the assay. When a protein curve was constructed using protein from the 10 000 x g pellet, it was found that

activity was linear with protein below 0.15 mg protein, in a 15 minute assay (Figure 12). This was considerably less protein than was used in the crude experiments earlier, where 10-30 mg crude protein was used. Although using the 10 000 x g pellet enriched the target enzyme considerably, the protein levels used in the crude assays were obviously much greater than required (especially with the 60 minute incubation time). Using 10 000 x g protein, 0.1 mg/ml protein was selected as the optimal protein concentration for future assays, as it was on the linear portion of the protein curve (Figure 12). Using the conditions established thus far (0.1 mg/ml 10 000 x g protein and 1 mM NADH), a time curve was derived (Figure 13). Observing normal kinetic behavior, activity was linear until approximately 10 minutes, at which point saturation occurred. Based on these results, the assay time was shortened to 10 minutes for the future. Attempts to produce NADH and NADPH concentration curves to resolve the reducing co-factor uncertainty resulted in failure. Activity in the presence of NADH was insensitive to co-factor concentration, with equal activity observed even when no endogenous reducing co-factor was added (Figure 14A, B). In the presence of NADPH, it is possible that some dependence on co-factor concentration was being demonstrated (Figure 14A), although the "trend" depends on a single data point. The experiment would have to be repeated at lower NADPH concentrations to substantiate the observed trend. These results led to the realization that the crude comparisons between NADH and NADPH (Figures 6 and 7) were fundamentally flawed in that they lacked a 'no reducing co-factor' treatment. Regardless, the crude experiments still did demonstrate a difference in activity between NADH and NADPH, which was not seen in the most recent experiments. It is too early to draw any conclusions from this data and the matter will require future study. Since the 10 000 x g pellet likely contains all the mitochondria, there is a good chance that high levels of NADH are present in the protein isolate, as NADH is abundant in mitochondria while NADPH is not (Van den Bergh, 1965). Since the radiolabelled substrate is present at low micromolar concentrations, it is possible that enough NADH is present to produce

the activity seen. A more disturbing possibility is that a competing enzymatic process is occurring whose product co-elutes with 4-methylnonanol under the column chromatography conditions currently employed, although this is not likely, as there are no other plausible products that could form under the current assay conditions. Attempts to resolve the enzyme products by HPLC in order to effect positive identification were not successful, as the sample could not be solubilized in the available mobile phases. Future work will be necessary to resolve the identity of the product(s) generated by the assay and to resolve the preferred reducing co-factor before the assay may be use to investigate any aspects of regulation of the reduction of 4-methylnonanoyl CoA in *T. molitor*.

4.3. SUMMARY

Two synthetic routes were developed for the synthesis of 4-methylnonanoic acid and 4-methylnonanol, the Claisen orthoester rearrangement route being the more promising of the two. Although the overall product yield was low (21.2% for 4-methylnonanol), it is expected to increase dramatically with continued development. In addition, it is also suitable for future production of radiolabelled compounds. An enzymatic synthesis for 4-methylnoanoyl CoA was also developed. The yield for this reaction was also low (10-20%) but expected to increase with further development, most notably with the move to an HPLC based product recovery.

An *in vitro* assay for the reduction of 4-methylnonanoic acid was developed, but not fully optimized. Adequate activity was detected with the assay with the use of protease inhibitors in initial enzyme isolation and the improved buffer system. However, the product(s) of the assay were not identified with complete certainty. Although there are no other conceivable labeled products that may form from [^{3}H]-4-methylnonanoic acid (or the CoA

derivative) under the current assay conditions, it still remains to verify product identity by a high-resolution method such as HPLC or mass spectrometry. The issue of reducing cofactor preference still remains to be resolved. In the presence of crude protein, there was preference for NADH over NADPH. When using protein from the 10 000 x g pellet, however, maximal activity was detected in the absence of exogenous cofactor. The problem likely lies with endogenous mitochondrial NADH present in the assay. This problem remains to be overcome so that proper concentration curves may be constructed (for NADH and NADPH) and the preferred cofactor and concentration may be determined. The presence of an extremely active thioesterase activity plagued activity in crude experiments by dramatically reducing available substrate. This problem was largely overcome by differential centrifugation, as the reductase activity resided in the 10 000 x g pellet and the thioesterase activity was mostly in the soluble fraction. With the reductase activity being localization in the 10 000 x g pellet, it is possible that the reductase may be mitochondrially localized. Coupled with a potential preference for NADH over NADPH, this prospect is both significant and intriguing, as all other eukaryotic acyl-CoA reductase characterized to date are microsomally localized and prefer NADPH. Further study will be required to resolve the sub-cellular localization of the reductase responsible for the reduction of 4-methylnonanoyl CoA and its reducing cofactor preference.

REFERENCES

Al-Arif, A. and M. Blecher. 1969. Synthesis of Fatty Acyl CoA and Other Thiol Esters Using *N*-Hydroxysuccinimide Esters of Fatty Acids. *Journal of Lipid Research* **10:** 344-345

Banis, R. J., C. S. Roberts, G. B. Stokes and S. B. Tove. 1976. Procedure for Enzymatic Synthesis and Isolation of Radioactive Long Chain Acyl-CoA Esters. *Analytical Biochemistry* **73:** 1-8

Bhattacharya, A. K., J. J. Ameel and G. P. Waldbauer. 1970. A Method for Sexing Living Pupal and Adult Yellow Mealworms. *Annals of the Entomological Society of America* **63:** 1783

Bishop, J. E. and A. K. Hajra. 1980. A Method for the Chemical Synthesis of ^{14}C-Labelled Fatty Acyl Coenzyme A's of High Specific Activity. *Analytical Biochemistry* **106:** 144-350

Borgeson, C. E. and G. J. Blomquist. 1993. Subcellular Location of the Δ^{12} Desaturase Rules Out Bacteriocyte Contribution to Lineolate Biosynthesis in the House Cricket and the American Cockroach. *Insect Biochemistry and Molecular Biology* **23:** 297-302

Bowman, E. J. and B. J. Bowman. 1988. Purification of Vacuolar Membranes, Mitochondria and Plasma Membranes from *Neurospora crassa* and Modes of Discriminating Among the Different H^+-ATPases. *Methods of Enzymology* **157:** 562-573

Bradford, M. M. 1976. A Rapid and Sensitive Method for the Quantitation of Microgram Quantities of Protein Utilizing the Principle of Protein-Dye Binding. *Analytical Biochemistry* **72:** 248-254

Carpita A., E. De Magistris and R. Rossi. 1989. The Racemic Form and the Two Enantiomers of 4-Methyl-1-nonanol, A Sex Attractant of the Yellow Mealworm, *Tenebrio molitor* L. *Gazzetta Chemica Italiana* **119:** 99-105

Cusson, M. and J. N. McNeil. 1989. Involvement of Juvenile Hormone in the Regulation of Pheromone Release Activities in a Moth. *Science* **243:** 210-212

Cusson, M., S. S. Tobe and J. N. McNeil. 1994. Juvenile Hormones: Their Role in the Regulation of the Pheromone Communication System of the Armyworm Moth, *Pseudaletia unipuncta*. *Journal of Insect Physiology* **25:** 329-345

Dickens, J. C., W. L. McGovern and G. Wiygul. 1988. Effects of Antennectomy and a Juvenile Hormone Analog on Pheromone Production in the Boll Weevil (Coleoptera: Curculionidae). *Journal of Entomological Science* **23:** 52-58

Elliott, J. I., J. A. Knopp. 1981. Alcohol Dehydrogenase from *Drosophila melanogaster*. *Methods of Enzymology* **41:** 374-379

Fiske, C. H. and Y. Subbarow. 1925. The Colorimetric Determination of Phosphorous. *Journal of Biological Chemistry* **66:** 377-254

Gadenne, C. 1993. Effects of Fenoxycarb, Juvenile Hormone Mimetic, on Female Sexual Behaviour of the Black Cutworm, *Agrotis ipsilon* (Lepidoptera: Noctuidae). *Journal of Insect Physiology* **39:** 25-29

Galliard, T. and P. K. Stumpf. 1968. Radioactive Long-Chain *S*-Acyl Coenzyme A (Enzymatic Preparation). *Biochemical Preparations* **12:** 66-69

Gameiro, B. 1996. Regulation of Pheromone Biosynthesis in Mature Female *Tenebrio molitor.* Undergraduate thesis submitted to the Department of Chemistry, University of Winnipeg. Winnipeg, Manitoba

Gerber, G. H. 1973. Reproductive Behavior and Physiology of *Tenebrio molitor* (Coleoptera: Tenebrionidae). I. Initiation of Mating in Young Adults and the Effects of Adult Density. *Canadian Entomologist* **105:** 807-811

Hansen, L. G. and E. Hodgson. 1971. Biochemical Characteristics of Insect Microsomes. N- and O- Demethylation. *Biochemical Pharmacology* **20:** 1569-1578

Happ, G. H. 1970. Maturation of the Response of Male *Tenebrio molitor* to the Female Sex Pheromone. *Annals of the Entomological Society of America* **63:** 1782

Happ, G. H. and J. Wheeler. 1969. Bioassay, Preliminary Purification, and Effect of Age, Crowding and Mating on the Release of Sex Pheromone by Female *Tenebrio molitor. Annals of the Entomological Society of America* **62:** 846-851

Harring, C. M. 1978. Aggregation Pheromones of the European Fir Engraver Beetles *Pityokteines curvidens, P. spinidens* and *P. vorontzovi* and the Role of Juvenile Hormone in Pheromone Biosynthesis. *Zeitschrift Angew Entomologie* **85:** 281-317

Hedin, P. A., O. H. Lindig and G. Wiygul. 1982. Enhancement of Boll Weevil *Anthonomus grandis* Boh. (Coleoptera: Curculionidae) Pheromone Biosynthesis with JHIII. *Experientia* **38:** 375-376

Hughes, P. R. and J. A. A. Renwick. 1977a. Hormonal and Host Factors Stimulating Pheromone Synthesis in Female Western Pine Beetles, *Dendroctonus brevicomus. Physiological Entomology* **2:** 289-292

Hughes, P. R. and J. A. A. Renwick. 1977b. Neural and Hormonal Control of Pheromone Biosynthesis in the Bark Beetle, *Ips paraconfusus. Physiological Entomology* **2:** 117-123

Islam, N. 1996. Pheromone Biosynthesis and Regulation in the Yellow Mealworm Beetle, *Tenebrio molitor.* Master of Science thesis submitted to the Department of Biochemistry and Molecular Biology, University of Manitoba, Winnipeg, Manitoba.

Islam, N., R. Bacala, A. Moore and D. Vanderwel. 1999. Biosynthesis of 4-Methyl-1-nonanol: Female-Produced Sex Pheromone of the Yellow Mealworm Beetle, *Tenebrio molitor* (Coleoptera: Tenebrionidae). *Journal of Insect Biochemistry and Molecular Biology* **29:** 201-208

Ivarsson, P., C. Tittiger, C. Blomquist, C. E. Borgeson, S. J. Seybold and G. J. Seybold. 1998. Pheromone Precursor Synthesis is Localized in the Metathorax of *Ips paraconfusus* Lanier (Coleoptera: Scolytidae). *Naturwissenschaften* **85:** 507-511

Judy, K. J., D. A Scooley, R. G. Troetscler, R. C. Jennings, B. J. Bergot and M. S. Hall. 1975. Juvenile Hormone Production by Corpora Allata of *Tenebrio molitor in vitro. Life Sciences* **16:** 1123-1139

Jones, G. 1995. Molecular Mechanisms of Action of Juvenile Hormone. *Annual Reviews of Entomology* **40:** 147-169

Khuu, Y. 1996. Exploration of the Substrate Specificity of the Enzyme Catalyzing the Reduction of 4-Methyl-1-nonanol in the Yellow Mealworm, *Tenebrio molitor.* Undergraduate thesis submitted to the Department of Chemistry, University of Winnipeg, Winnipeg, Manitoba.

Kitahara, T. and S. Kamg. 1994. Synthesis of Both Enantiomers of 4-Metyl-1-nonanol, the Sex Pheromone of the Yellow Mealworm. *Proceedings of the Japan Academy of Sciences, Series B* **70:** 181-184

Kollatukudy, P.E. 1970. Reduction of Fatty Acids to Alcohols by Cell-Free Preparations of *Euglena gracilis. Biochemistry* **9:** 1090-1102

Kornberg, A. and W. E. Pricer Jr. 1953. Enzymatic Synthesis of the Coenzyme A Derivatives of Long Chain Fatty Acids. *Journal of Biological Chemistry* **204:** 329-343

Krapcho, A. P. 1982a. Synthetic Applications of Dealkoxycarbonylations of Malonate Esters, β-Keto Esters, α-Cyano Esters and Related Compounds in Dipolar Aprotic Media - Part 1. *Synthesis* 805-822

Krapcho, A. P. 1982a. Synthetic Applications of Dealkoxycarbonylations of Malonate Esters, β-Keto Esters, α-Cyano Esters and Related Compounds in Dipolar Aprotic Media - Part 2. *Synthesis* 893-914

Laufer, H. and D. W. Borst. 1983. Juvenile Hormone and Its Mechanism of Action. pp 203-216. in *Endocrinology of Insects* (Laufer, H. and D. W. Borst, eds.). Alan R. Liss Inc., New York

Leal, J. F. M. and M. Barbarancho. 1993. Aldehyde Dehydrogenase (ALDH) Activity in *Drosophila melanogaster* Adults: Evidence for Cytosolic Localization. *Insect Biochemistry and Molecular Biology* **23:** 543-547

March, 1992. Advanced Organic Chemistry: Mechanisms and Structure, 4th ed. John Wiley and Sons, New York

Martinez, T., G. Fabriás and F. Camps. 1990. Sex Pheromone Biosynthetic Pathway in *Spodoptera littoralis* and Its Activation by a Neurohormone. *Journal of Biological Chemistry* **265:** 1381-1387

Matsumoto, S., R. Ozawa, K. Uchiumi and M. Kurihara. 1996. Cell-Free Production of the Silkworm Sex Pheromone Bombykol. *Bioscience, Biotechnology and Biochemistry* **60:** 369-373

McNeil, J. N., J. Deslisle and M. Cusson. 1997. Regulation of Pheromone Production in Lepidoptera: The Need for an Ecological Perspective, pp 31-41 in *Insect Pheromone Research New Directions* (Cardé, R. T. and A. K. Minks, eds.). ITP, New York.

Menon, M. 1970. Hormone-Pheromone Relationships in the Beetle, *Tenebrio molitor*. *Journal of Insect Physiology* **16:** 1123-1139

Menon, M., and K. Nair. 1976. Age-Dependent Effects of Synthetic Juvenile Hormone on Pheromone Synthesis in Adult Females of *Tenebrio molitor*. *Annals of the Entomological Society of America* **69:** 457-458

Nijhout, H. F. 1994. *Insect Hormones*. Princeton University Press, Princeton, New Jersey.

Odonikov, V. N., G. Yu. Ishmuratov, M. P. Yakovleva, R. L. Safiullin, V. D. Komissarov and G. A. Tolstikov. 1993. Optically Pure Acyclic Bifunctional Compounds From (-)-Menthone. Synthesis of *R*-4-Methyl-1-nonanol, the Sex Pheromone of the Larger Flour Beetle (*Tenebrio molitor* L.). *Russian Chemical Bulletin* **42:** 1244-1245

Odonikov, V. N., G. Yu. Ishmuratov, M. P. Yakovlea, O. V. Sokol'skaya, R. Ya. Kharisov, É. P. Serebryakov and G. A. Tolstikov. 1991. Insect Pheromones and their Analogues XLIII. Chiral Pheromones from (S)-(+)-3,7-Dimethylocta-1,6-diene. 3. Synthesis of (4R)-4-Methylnonan-1-ol – Sex Pheromone of *Tenebrio molitor* and its Racemic Analogue [In Russian]. *Khimiya Prirodnykh Soedinenii* **6:** 711-711

Ozawa, R., T. Ando, H. Nagasawa, H. Kataoka and A. Suzuki. 1993. Reduction of the Acyl Group: The Critical Step in Bombykol Biosynthesis That Is Regulated by the Neuropeptide Hormone in the Pheromone Gland of *Bombyx mori*. *Biosciences, Biotechnology and Biochemistry* **57:** 2144-2147

Picimbon, J. F., J. M. Becard, L. Sreng, J. L. Clement and C. Gadenne. 1995. Juvenile hormone stimulates release of pheromonotropic brain factor in the female black cutworm, *Agrotis ipsilon*. *Journal of Insect Physiology* **41:** 377-382

Pierce, A. M., H. D. Pierce Jr., J. H. Borden and A. C. Oehlschlager. 1986. Enhanced Production of Aggregation Pheromones in For Stored-Product Coleopterans Feeding on Methoprene-Treated Oats. *Experientia* **42:** 164-165

Pollard, M., T. McKeon, L. Gupta and P. Stumpf. 1979. Studies on Biosynthesis of Waxes by Developing Jojoba Seed. II. The Demonstration of Wax Biosynthesis by Cell-Free Homogenates. *Lipids* **14:** 651-662

Rafael, J. 1983. Cytochrome C Oxidase, pp 266-273 in *Methods of Enzymatic Analysis, 3rd edition* (H. U. Bergmeyer, ed.). Verlag Chemie, Germany.

Raina, A. K. 1997. Control of Pheromone Production in Moths, pp 21-30 in *Insect Pheromone Research New Directions* (Cardé, R. T. and A. K. Minks, eds.). ITP, New York

Reiser, S. and C. Sommerville. 1997. Isolation of Mutants of *Acinetobacter calcoaceticus* Deficient in Wax Ester Synthesis and Complementation of One Mutation with a Gene Encoding a Fatty Acyl Coenzyme A Reductase. *Journal of Bacteriology* **179:** 2969-2975

Rickwood, D., M. T. Wilson and V. M. Darley-Usmar. 1987. Isolation and Characteristics of Intact Mitochondria, pp1-16 in *Mitochondria a Practical Approach* (Darley-Usmar, V. M., D. Rickwood and M. T. Wilson, eds). IRL Press Limited, England.

Riendeau, D. and E. Meighen. 1985. Enzymatic Reduction of Fatty Acids and Acyl-CoAs to Long Chain Aldehydes and Alcohols. *Experientia* **41:** 707-712

Robinson, J. B. Jr., L. G. Brent, B. Sumegi and P. A. Srere. 1987. An Enzymatic Approach to the Study of the Krebs Tricarboxylic Acid Cycle, pp153-170 in *Mitochondria a Practical Approach* (Darley-Usmar, V. M., D. Rickwood and M. T. Wilson, eds). IRL Press Limited, England.

Sánchez, M., D. G. Nicholls and D. N. Brindley. 1973. The Relationship Between Palmitoyl-Coenzyme A Synthetase Activity and Esterification of *sn*-Glycerol 3-Phosphate in Rat Liver Mitochondria. *Biochemical Journal* **132:** 697-706

Schal, C., D. Liang and G. J. Blomquist. 1997. Neural and Endocrine Control of Pheromone Production and Release in Cockroaches, pp 1-20 in *Insect Pheromone Research New Directions* (Cardé, R. T. and A. K. Minks, eds.). ITP, New York

Seubert, W. 1960. S-Palmityl Coenzyme A. *Biochemical Preparations* **7:** 80-83

Stadtman, E. R. 1957. Preparation and Assay of Acyl Coenzyme A and Other Thiol Esters; Use of Hydroxylamine. *Methods in Enzymology* **3:** 931-941

Still, C. W., M. Kahn, A. Mitra. 1978. Rapid Chromatographic Technique for Preparative Separations with Moderate Resolution. *Journal of Organic Chemistry* **14:** 2923-2925

Tanaka, Y., H. Honda, K. Ohsawa and I. Yamamoto. 1986. A Sex Attractant of the Yellow Mealworm, *Tenebrio molitor* L., and its Role in the Mating Behavior. *Journal of Pesticide Science* **11:** 49-55

Tanaka, Y., H. Honda, K. Ohsawa and I. Yamamoto. 1989. Absolute Configuration of a Sex Attractant of the Yellow Mealworm, *Tenebrio molitor* L. *Journal of Pesticide Science* **14:** 197-202

Tawfik, A. I., E. O. Osir, A. Hassanali and S. H. Ismail. 1997. Effects of Juvenile Hormone on Phase Changes and Pheromone Production in the Desert Locust, *Schistocerca gregaria* (Forskal) (Orthoptera: Acrididae). *Journal of Insect Physiology* **43:** 1177-1182

Tillman-Wall, J. A., D. Vanderwel, M. E. Kuenzli, R. C. Reitz and G. J. Blomquist. 1992. Regulation of Sex Pheromone Biosynthesis in the Housefly, *Musca domestica*: Relative Contribution of the Elongation and Reduction Steps. *Archives of Biochemistry and Biophysics* **299:** 92-99

Tittiger, C., G. J. Blomquist, P. Ivarsson, C. E. Borgeson and S. J. Seybold. 1999. Juvenile Hormone Regulation of HMG-R Gene Expression in the Bark Beetle *Ips paraconfusus* (Coleoptera: Scolytidae): Implications for Male Aggregation Pheromone Biosynthesis. *Cellular and Molecular Life Sciences* **55:** 121-127

Tschinkel, W. C. Wilson and H. Bern. 1967. Sex Pheromone of the Yellow Mealworm (*Tenebrio molitor*). *Journal of Experimental Zoology* **164:** 81-86

Van den Bergh, S. G. 1965. Insect Mitochondria. *Methods in Enzymology* **12:** 117-122

Vanderwel, D. 1991. Pheromone Biosynthesis in Selected Species of Grain and Bark Beetles. PhD thesis submitted to the Department of Chemistry, Simon Fraser University, Burnaby, Brittish Columbia, Canada.

Vanderwel, D. 1994. Factors Affecting Pheromone Production in Beetles. *Archives of Insect Biochemistry and Physiology* **25:** 347-362

Vanderwel, D., B. Johnston and A. C. Oehlschlager. 1992. Cucujolide Biosynthesis in the Merchant and Rusty Grain Beetles. *Insect Biochemistry and Molecular Biology* **22:** 875-883

Vanderwel, D. and A. C. Oehlschlager. 1987. Biosynthesis of Pheromones and Endocrine Regulation of Pheromone Production in Coleoptera, pp175-216 in *Pheromone Biochemistry* (Prestwich, G. D. and G. J. Blomquist, eds.), Academic Press, Orlando, Florida.

Vioque, J. and P. E. Kollatukudy. 1997. Resolution of an Aldehyde-Generating and Alcohol-Generating Fatty Acyl-CoA Reductase from Pea Leaves (*Pisum savitum* L.). *Archives of Biochemistry and Biophysics* **340:** 64-72

Wang, X. and P. E. Kollatukudy. 1995. Solubilization, Purification and Characterization of Fatty Acyl-CoA Reductase from Duck Uropygial Gland. *Biochemical and Biophysical Research Communications* **208:** 210-215

Wiygul, G., J. C. Dickens and J. W. Smith. 1990. Effect of Juvenile Hormone III and Beta-Bisabolol on Pheromone Production in Fat Bodies From Male Boll Weevils, *Anthonomis grandis* Boheman (Coleoptera: Curculionidae). *Comparative Biochemistry and Physiology B* **95:** 489-491

Wolf, W. A. and W. L. Roelofs. 1983. A Chain Shortening Reaction in Orange Tortrix Moth Sex Pheromone Biosynthesis. *Insect Biochemistry* **13:** 375-379

Zolondek, S. 1996. Female *Tenebrio molitor* Pheromone Biosynthetic Pathway: Reduction of 4-Methylnonanoic Acid to 4-Methylnonanol. Undergraduate thesis submitted to the Department of Chemistry, University of Winnipeg, Winnipeg, Manitoba.

APPENDICES

LIST OF APPENDICES

APPENDIX 1 A: Dimethyl 2-heptylmalonate ^{1}H NMR spectrum

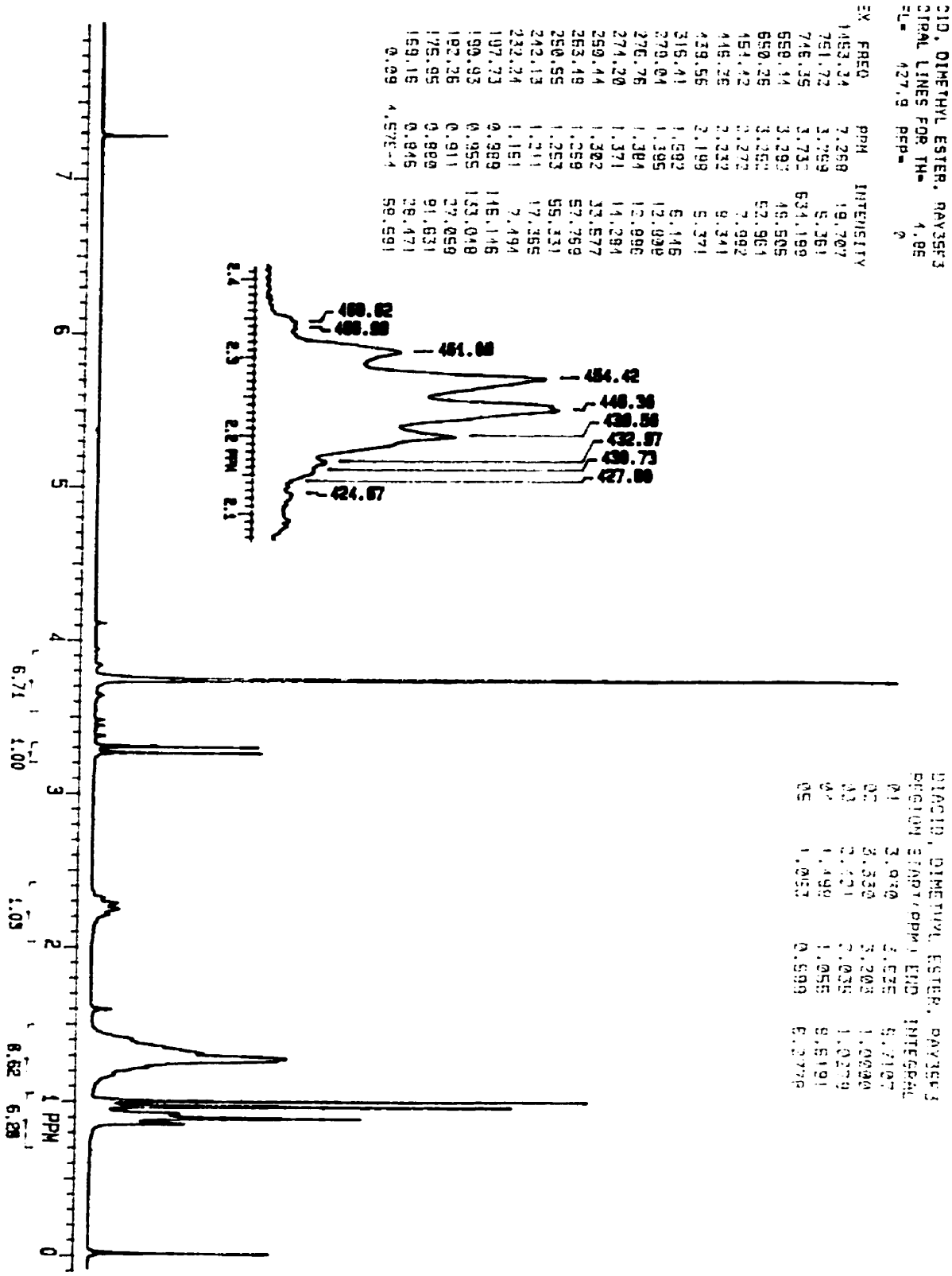

APPENDIX 1 B: Dimethyl 2-heptylmalonate ^{13}C NMR spectrum

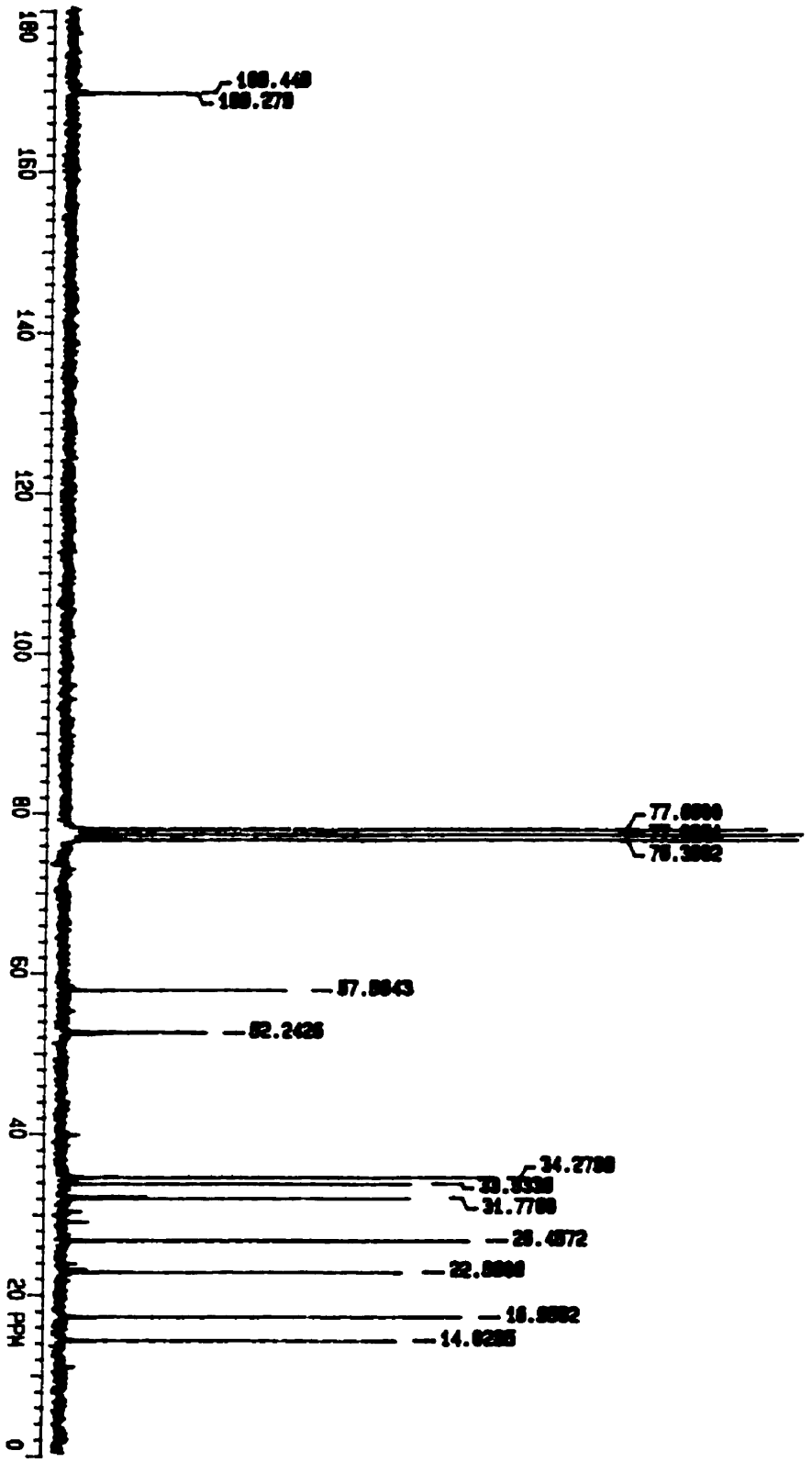

APPENDIX 1 C: Dimethyl 2-heptylmalonate mass spectrum (EI)

```
File        : C:\HPCHEM\1\DATA\JL14S1A.D
Operator    : Ray Bacala
Acquired    : 14 Jul 98  11:17 am using AcqMethod RAY10JL
Instrument :    5989B-MS
Sample Name: Sample 1
Misc Info   : 1 ul injection(54.3 ng/ul) range:40-250
Vial Number: 1
```

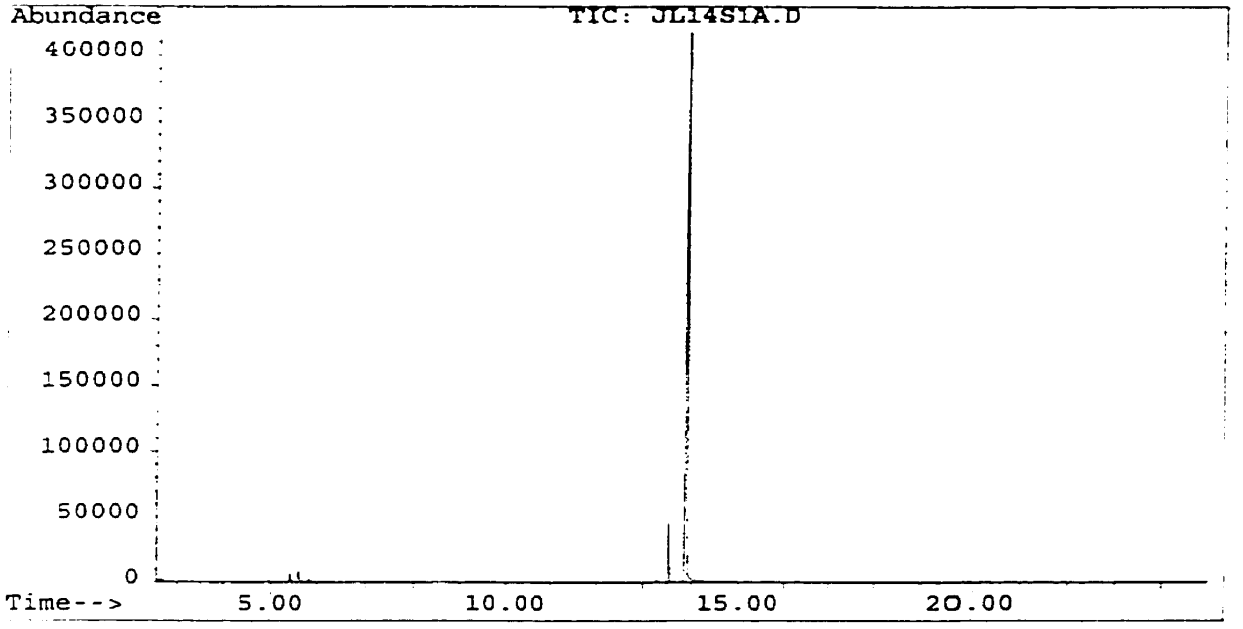

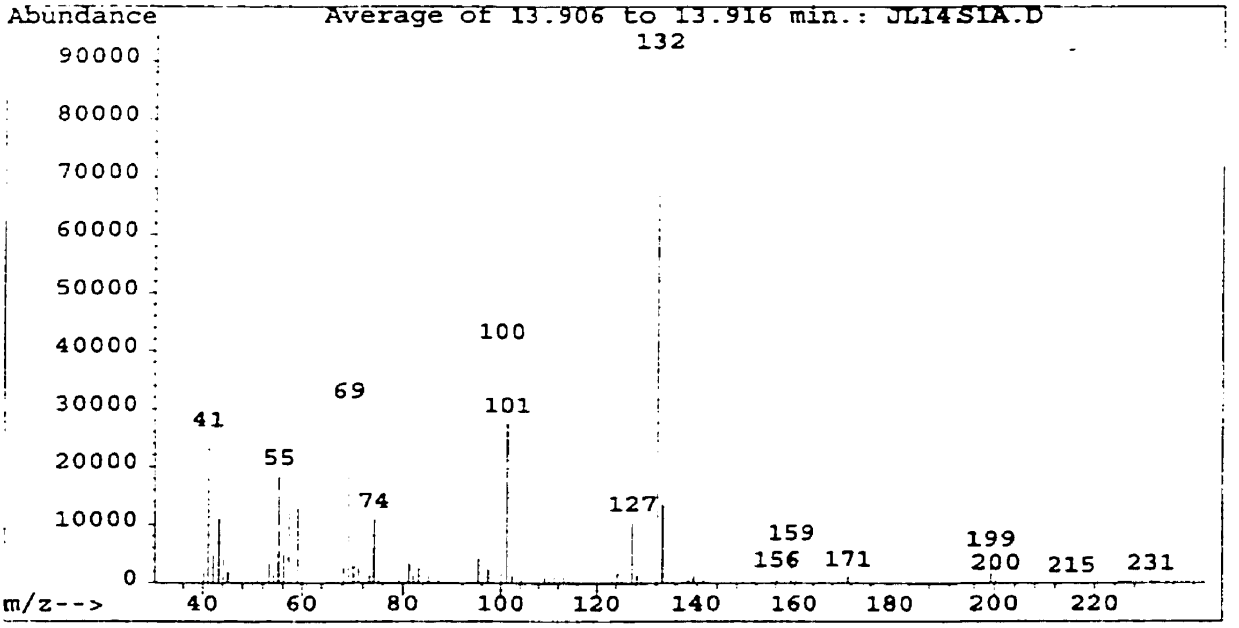

APPENDIX 1 C: Dimethyl 2-heptylmalonate mass spectrum (EI)

Average of 13.906 to 13.916 min.: JL14S1A.D
Modified:scaled

m/z	abund.	m/z	abund.	m/z	abund.	M/z	abund.
40.15	2	51.1	0	63.15	0	74.15	12
41.05	27	52.15	0	64.15	0	75.15	1
42.05	5	53.15	4	65.15	1	76.15	0
43.15	12	54.15	2	66.15	0	77.15	0
44.05	5	55.15	20	67.15	3	78.25	0
45.05	2	56.15	5	68.15	3	79.15	1
46.05	0	57.15	13	69.15	32	80.25	0
47.1	0	59.15	14	70.15	3	81.15	4
48.15	0	60.15	0	71.15	3	82.1	2
49.1	0	61.15	0	72.15	0	83.1	3
50.05	0	62.15	0	73.25	1	84.25	0

Average of 13.906 to 13.916 min.: JL14S1A.D

m/z	abund.	m/z	abund.	m/z	abund.	M/z	abund.
85.1	2	97.25	3	109.2	1	121.2	0
86.15	0	98.25	1	110.2	1	122.2	0
87.1	1	100.1	43	111.2	1	123.2	1
88.25	0	101.15	29	112.25	0	124.2	2
89.1	0	102.25	2	113.2	2	125.2	0
91.1	0	103.25	0	114.2	3	127.2	11
92.1	0	104.2	1	115.2	1	128.2	1
93.25	0	105.2	0	116.2	0	129.2	0
94.25	0	106.15	0	117.2	0	132.2	100
95.25	5	107.2	0	119.25	0	133.2	14
96.25	3	108.2	0	120.2	0	134.2	1

Average of 13.906 to 13.916 min.: JL14S1A.D

m/z	abund.	m/z	abund.	m/z	abund.	M/z	abund.
135.2	0	147.2	0	160.3	1	173.25	0
136.25	0	148.45	0	161.2	0	174.25	0
137.2	0	149.25	0	164.15	0	179.25	0
138.3	1	150.15	0	165.3	0	180.25	0
139.3	1	151.3	0	166.3	0	181.3	0
140.3	0	152.3	0	167.3	0	183.25	0
141.25	1	153.3	0	168.3	0	184.25	0
142.25	0	155.3	0	169.3	0	187.25	0
143.25	0	156.3	1	170.3	1	188.35	0
144.3	0	157.3	0	171.3	1	197.35	0
145.25	0	159.3	6	172.25	0	199.25	5

Average of 13.906 to 13.916 min.: JL14S1A.D

m/z	abund.
200.25	1
201.25	0
215.3	0
231.35	0
232.35	0

APPENDIX 1 D: Dimethyl 2-heptylmalonate mass spectrum (PCI)

```
File        : C:\HPCHEM\1\DATA\RAYPCI1.D
Operator    : Ray Bacala
Acquired    :  6 Oct 98  12:16 pm using AcqMethod RAYPCI
Instrument  :    5989B-MS
Sample Name: Sample 1
Misc Info   : 1 ul inj. (50 ng/ul), mass 60-250
Vial Number: 1
```

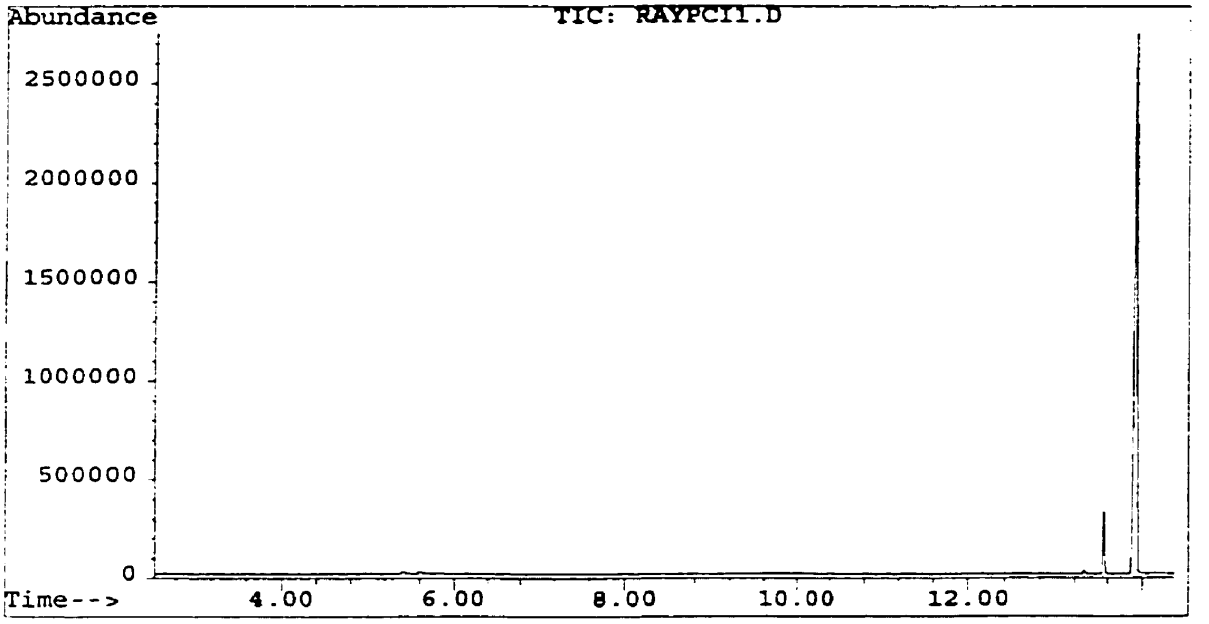

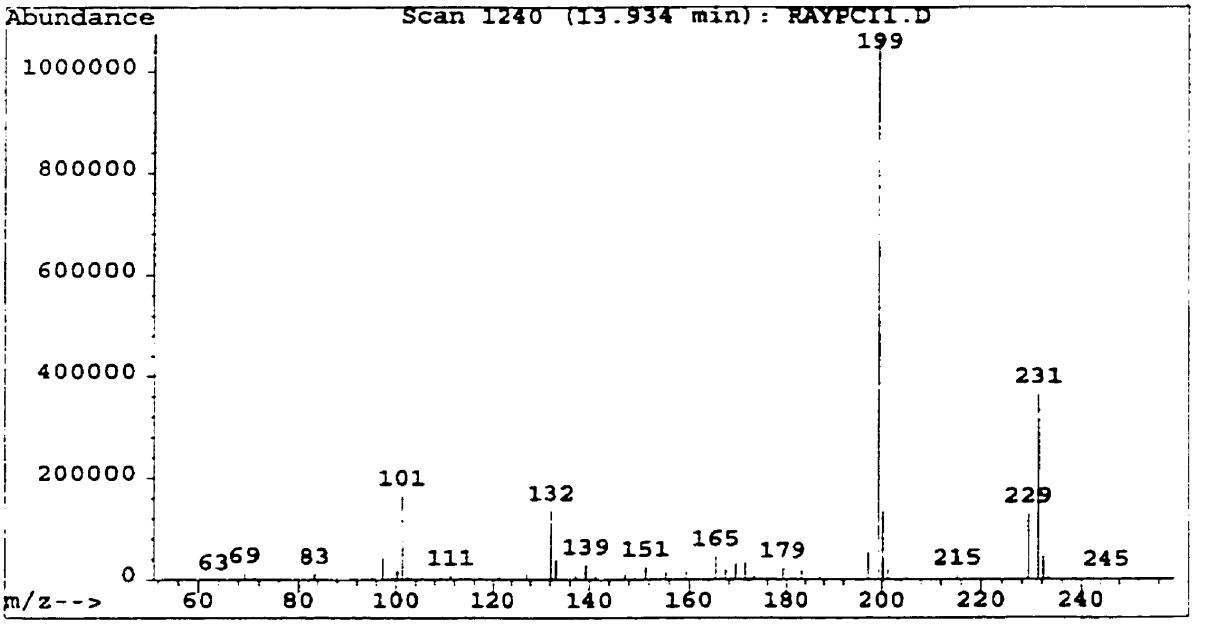

APPENDIX 1 D: Dimethyl 2-heptylmalonate mass spectrum (PCI)

Scan 1240 (13.934 min): RAYPCI1.D
Modified:scaled

m/z	abund.	m/z	abund.	m/z	abund.	M/z	abund.
61.15	0	72.3	0	82.25	0	93.25	0
62.15	0	73.25	0	83.25	1	94.1	0
63.05	0	74.15	0	84.25	0	95.25	0
64.3	0	75.15	0	85.25	0	97.25	4
65.05	0	75.9	0	86.25	0	98.25	0
65.3	0	77.15	0	87.25	0	99.25	1
67.15	0	78	0	88.1	0	100.25	2
68.3	0	78.25	0	89.25	0	101.2	15
69.15	1	79.25	0	89.85	0	102.2	1
70.15	0	80.25	0	91.25	0	103.2	0
71.15	0	81.25	0	92	0	105.2	0

Scan 1240 (13.934 min): RAYPCI1.D

m/z	abund.	m/z	abund.	m/z	abund.	m/z	abund.
106.35	0	117.2	0	129.2	0	141.3	1
107.2	0	118.3	0	130.15	0	142.3	0
108.2	0	119.3	0	132.15	13	143.3	0
109.2	1	120.3	0	133.15	4	144.25	0
110.2	0	121.3	1	134.15	0	145.15	0
111.2	1	122.3	0	135.3	0	147.15	1
112.35	0	123.2	0	136.05	0	148.25	0
113.2	0	124.3	0	137.15	1	149.25	1
114.2	0	125.2	0	138.3	0	151.25	2
115.2	0	127.2	1	139.3	3	152.25	0
116.3	0	128.3	0	140.3	0	153.25	0

Scan 1240 (13.934 min): RAYPCI1.D

m/z	abund.	m/z	abund.	m/z	abund.	m/z	abund.
153.9	0	165.25	4	176.2	0	189.95	0
155.25	1	166.25	0	177.6	0	190.2	0
156.25	0	167.25	2	179.2	2	191.05	0
157.25	0	168.25	0	180.2	0	191.8	0
159.25	2	169.25	3	181.2	0	193.2	0
160.1	0	170.25	1	183.2	2	194.05	0
161.25	0	171.25	3	184.2	0	194.95	0
162	0	172.2	0	185.2	0	197.2	5
162.25	0	173.2	1	187.2	1	199.3	100
162.6	0	174.2	0	188.2	0	200.15	12
163.35	0	175.2	0	189.2	0	201.15	2

Scan 1240 (13.934 min): RAYPCI1.D

m/z	abund.	m/z	abund.	m/z	abund.	m/z	abund.
209.3	0	217.25	0	223.25	0	229.25	12
209.9	0	218.5	0	224	0	231.25	34
211.3	0	219.25	0	224.4	0	232.25	4
212.15	0	220.4	0	224.75	0	233.25	1
213.3	0	221.25	0	225.25	0		
215.25	1	221.9	0	226	0		
216.25	0	222.65	0	227.25	0		

APPENDIX 2 A: Methyl 3-methyloctanoate ^{1}H NMR spectrum

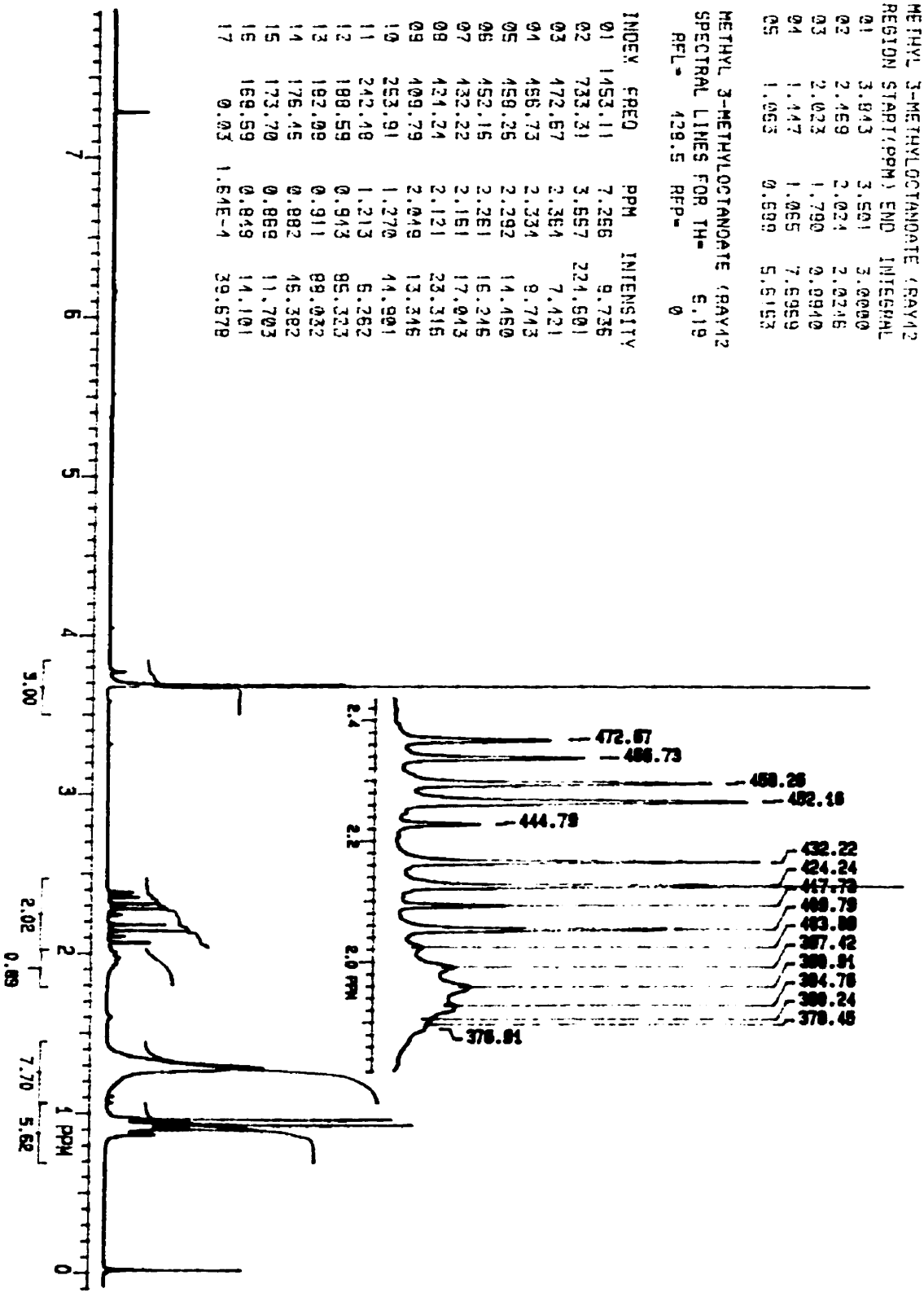

APPENDIX 2 B: Methyl 3-methyloctanoate ^{13}C NMR spectrum

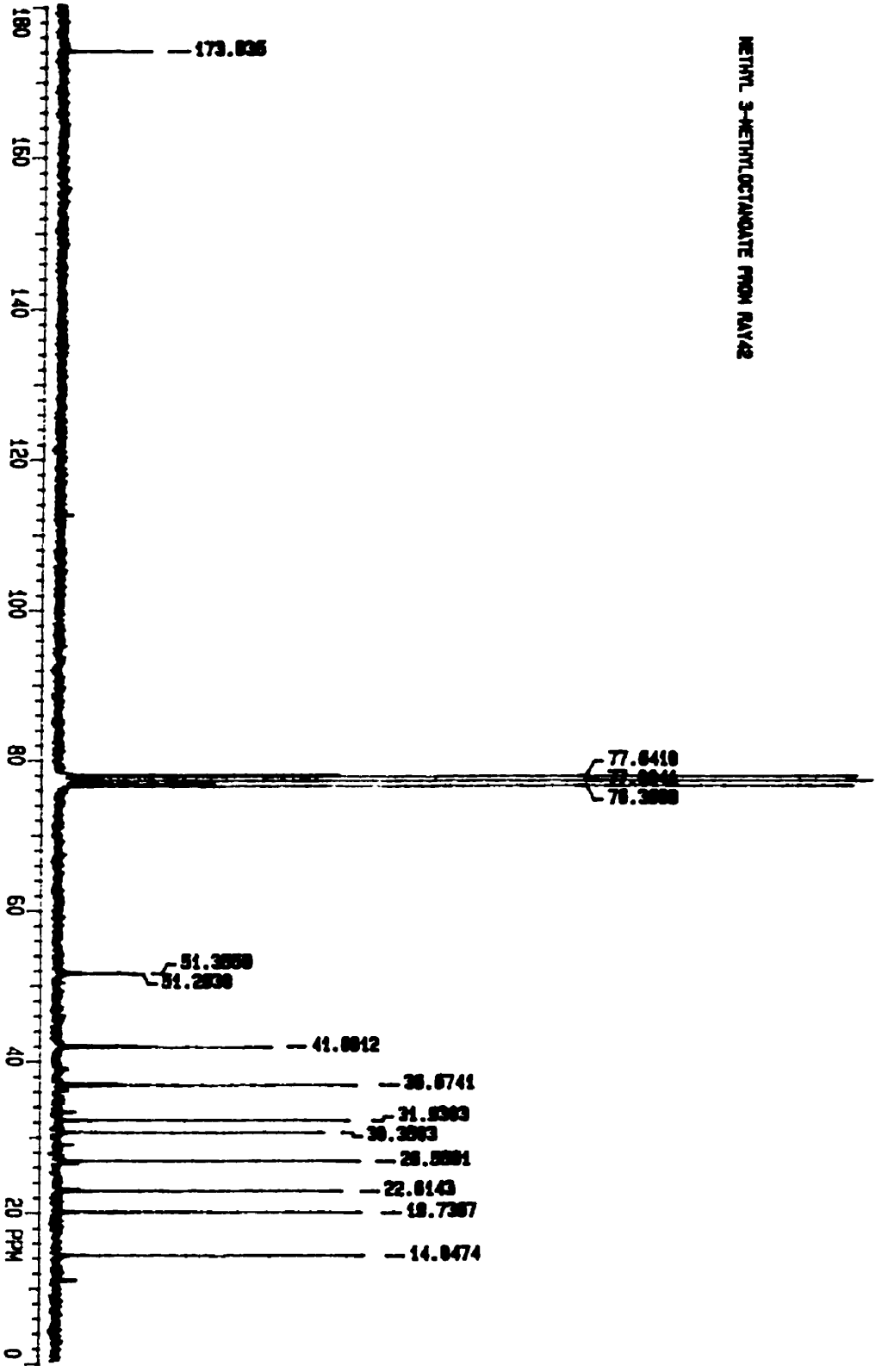

APPENDIX 2 C: Methyl 3-methyloctanoate mass spectrum (EI)

```
File        : C:\HPCHEM\1\DATA\JL14S2A.D
Operator    : Ray Bacala
Acquired    : 14 Jul 98  11:47 am using AcqMethod RAY10JL
Instrument  :    5989B-MS
Sample Name: Sample 2
Misc Info   : 1 ul inj(54.3 ng/ul) ran:40-250, fw=172.27
Vial Number: 1
```

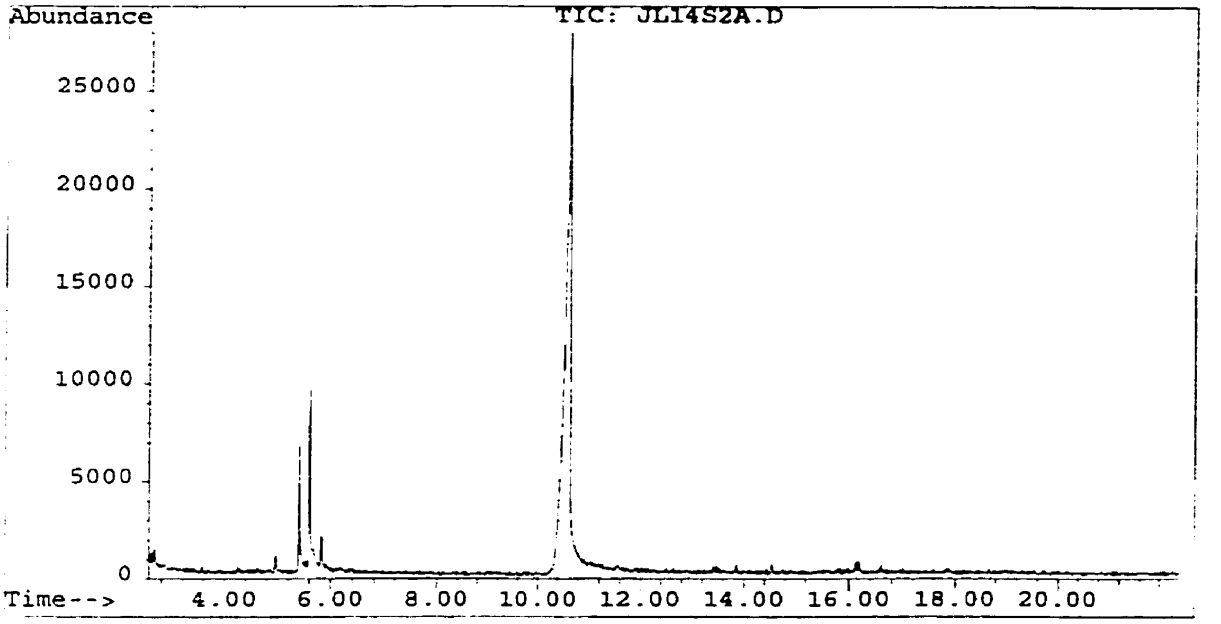

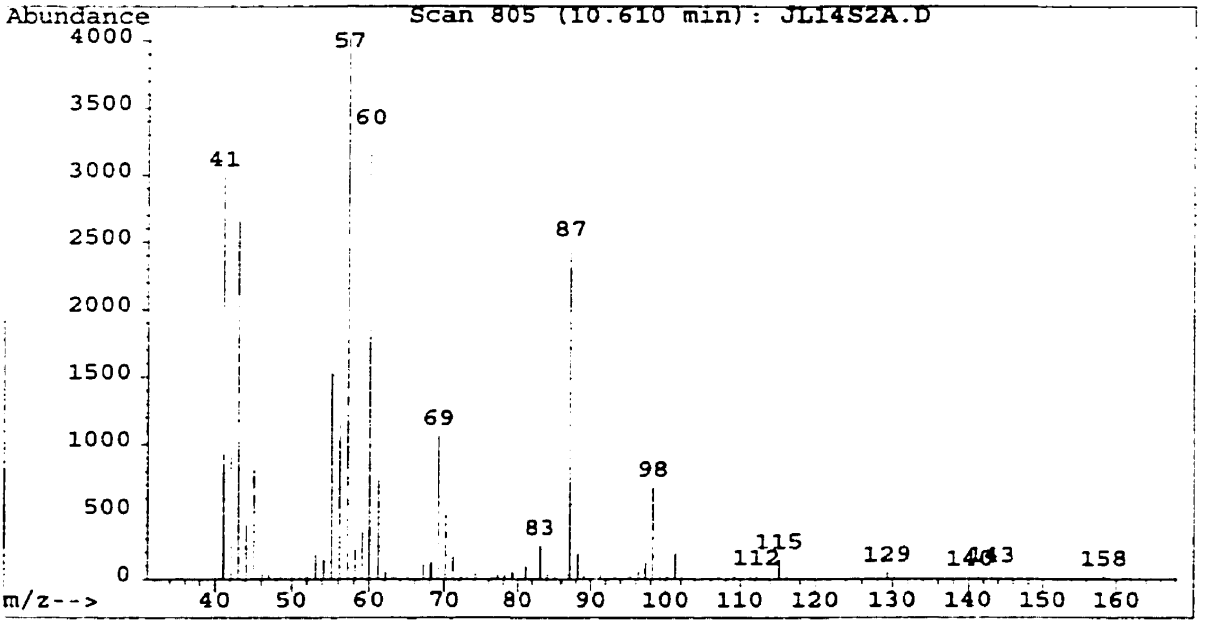

APPENDIX 2 C: Methyl 3-methyloctanoate mass spectrum (EI)

Scan 804 (10.600 min): JL14S2A.D
Sample 2 (Methyl 3-methyloctanoate)
Modified:scaled

m/z	abund.	m/z	abund.	m/z	abund.	m/z	abund.
41.05	72	54.15	3	66.15	1	80.15	1
42.05	24	55.15	37	67.15	2	81.15	2
43.05	64	56.15	29	68.25	3	82.1	2
44.05	11	57.15	100	69.15	26	83.25	6
45.05	20	58.15	6	70.15	15	84.25	1
46.05	1	59.15	11	71.15	4	85.1	1
47.05	1	60.15	85	72.15	1	87.1	63
50.05	1	61.15	20	73.15	16	88.1	4
51.05	2	62.15	1	74.15	1	89.25	1
52.3	1	63.15	1	77	1	91.25	1
53.15	5	65.15	1	79.15	1	93.35	1

Scan 804 (10.600 min): JL14S2A.D

m/z	abund.	m/z	abund.
94	1	115.2	4
95.25	1	116.2	1
96.25	2	120.45	1
97.25	3	122.45	1
98.25	18	125.35	1
99.25	4	129.2	1
100.35	1	143.3	2
101.25	4		
102.25	1		
111.35	1		
112.2	1		

APPENDIX 2 D: Methyl 3-methyloctanoate mass spectrum (PCI)

```
File        : C:\HPCHEM\1\DATA\RAYPCI2.D
Operator    : Ray Bacala
Acquired    :  6 Oct 98  12:38 pm using AcqMethod RAYPCI
Instrument :    5989B-MS
Sample Name: Sample 2 (Methyl
Misc Info   : 1 ul inj. (50 ng/ul), mass 60-200, fw=172.27
Vial Number: 1
```

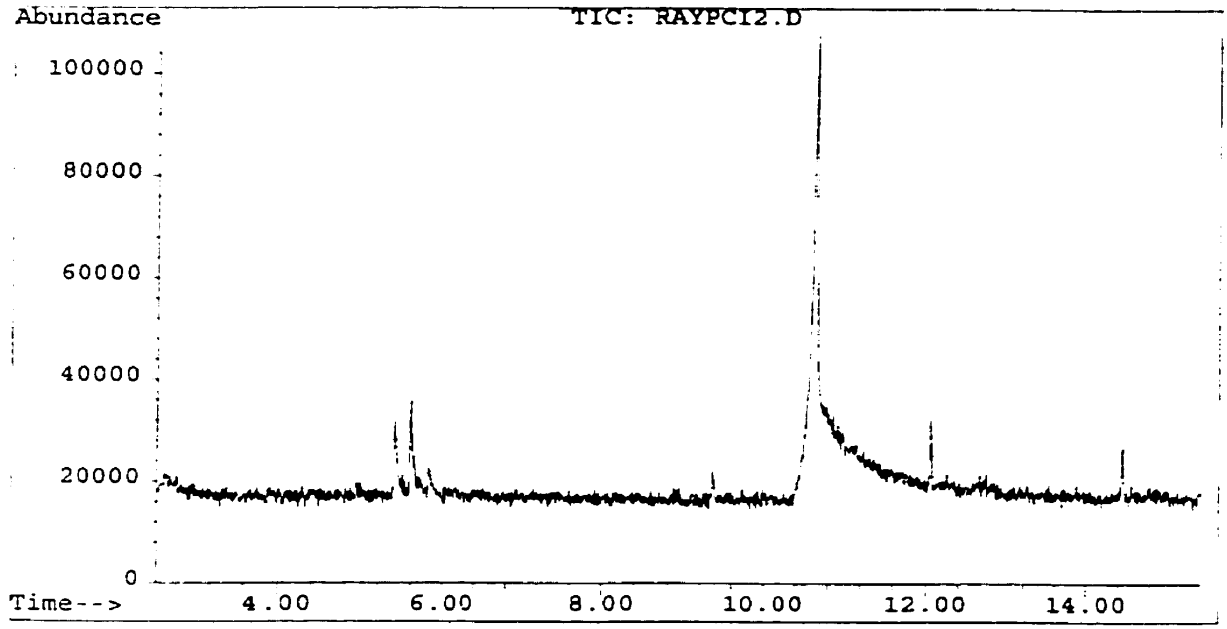

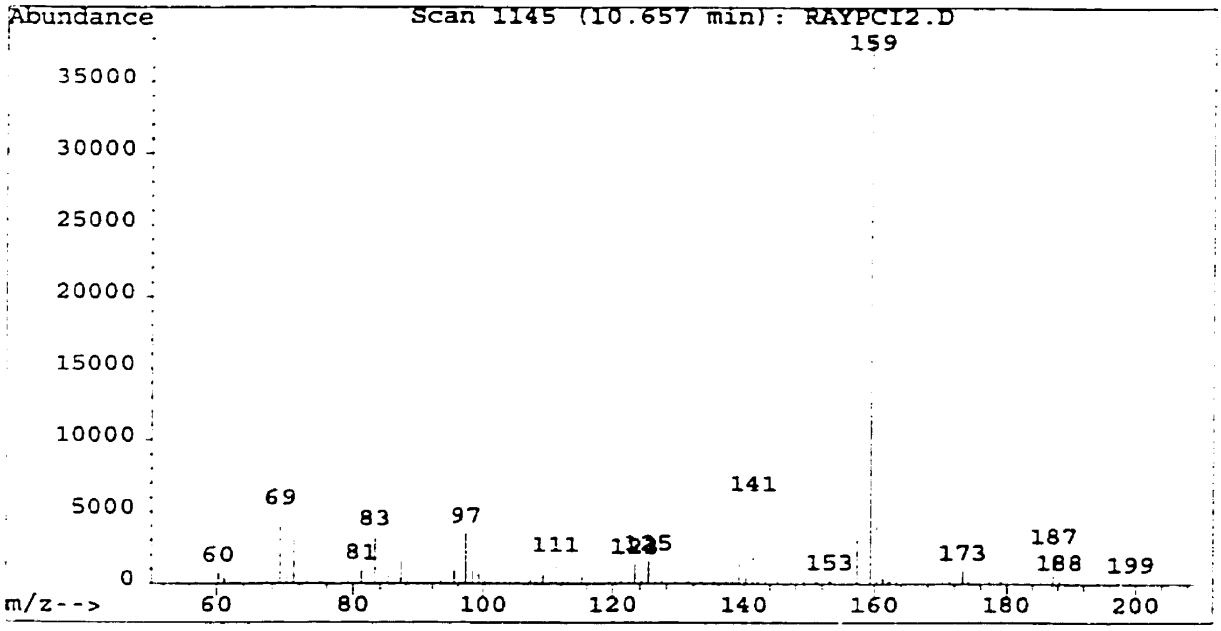

APPENDIX 2 D: Methyl 3-methyloctanoate mass spectrum (PCI)

Scan 1145 (10.657 min): RAYPCI2.D
Sample 2 (Methyl 3-methyloctanoate)
Modified:scaled

m/z	abund.	m/z	abund.	m/z	abund.	m/z	abund.
60.25	2	67.2	1	77.95	0	90.8	0
61.1	1	67.7	0	79.2	1	91.2	0
62.1	0	69.2	12	81.2	3	92.45	0
62.5	0	70.2	2	83.2	9	93.3	1
62.85	0	71.2	8	84.3	1	94.3	0
63.1	0	73.2	2	85.2	2	95.3	3
64.25	0	74.35	0	87.2	4	97.15	9
64.6	0	74.6	0	88.2	0	98.3	3
65	1	75.1	1	89.2	0	99.3	2
65.25	1	75.95	0	90.05	0	100.15	0
66.6	0	77.6	0	90.55	0	100.4	0

Scan 1145 (10.657 min): RAYPCI2.D

m/z	abund.	m/z	abund.	m/z	abund.	m/z	abund.
101.15	2	110.4	0	121.25	1	133.25	1
102.15	0	111.25	4	122.35	0	134.1	0
103.3	3	112.4	1	123.25	4	135.25	1
104.15	1	113.25	1	124.25	1	136.1	0
105.3	0	115.25	2	125.25	4	137.2	1
105.9	0	116	0	126.35	0	138.2	1
106.3	0	117.25	2	127.25	1	139.2	10
106.55	0	118.15	0	128.25	0	140.35	1
107.3	1	119.4	0	129.35	0	141.35	15
108.15	0	120.25	0	131.25	1	142.2	1
109.25	2	120.5	0	132.6	0	143.35	3

Scan 1145 (10.657 min): RAYPCI2.D

m/z	abund.	m/z	abund.	m/z	abund.	m/z	abund.
144.1	0	155.2	1	166.4	0	176.4	0
145.2	0	156.3	0	167.4	0	177.4	1
146.2	0	157.3	8	168.65	0	178.3	0
147.2	0	159.3	100	169.3	0	179.15	1
148.35	0	160.3	11	170.15	0	180.15	0
149.2	0	161.3	1	171.3	1	181.25	0
150.2	0	162.2	1	172.15	0	182	0
151.2	0	163.3	1	173.3	2	183.5	0
152.45	0	164.3	0	174.15	1	184.25	0
153.2	1	164.55	0	175.05	0	185.25	0
154.45	0	165.4	0	175.4	0	186.25	0

APPENDIX 3 A: 3-Methyloctanol ^{1}H NMR spectrum

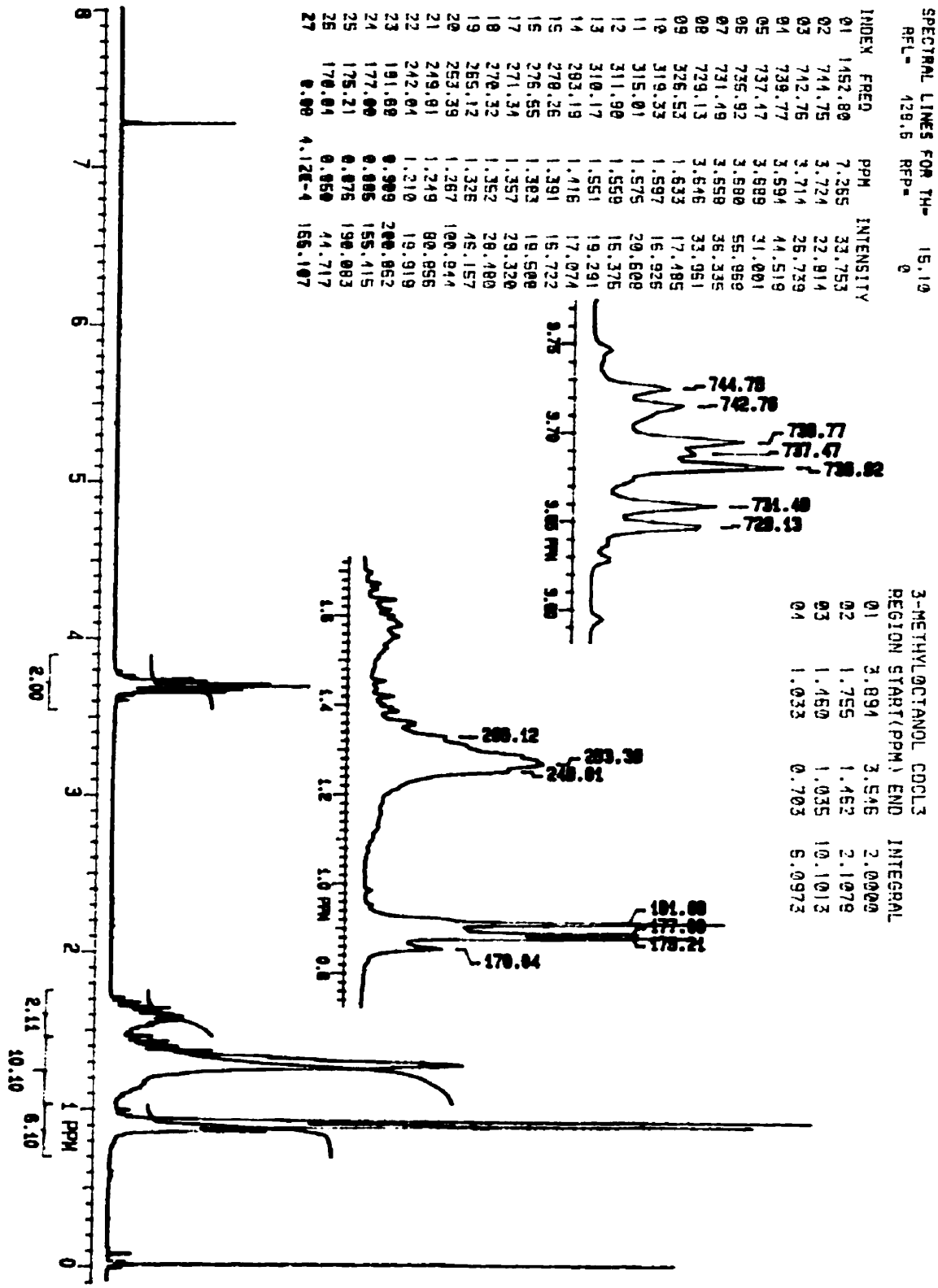

APPENDIX 3 B: 3-Methyloctanol ^{13}C NMR spectrum

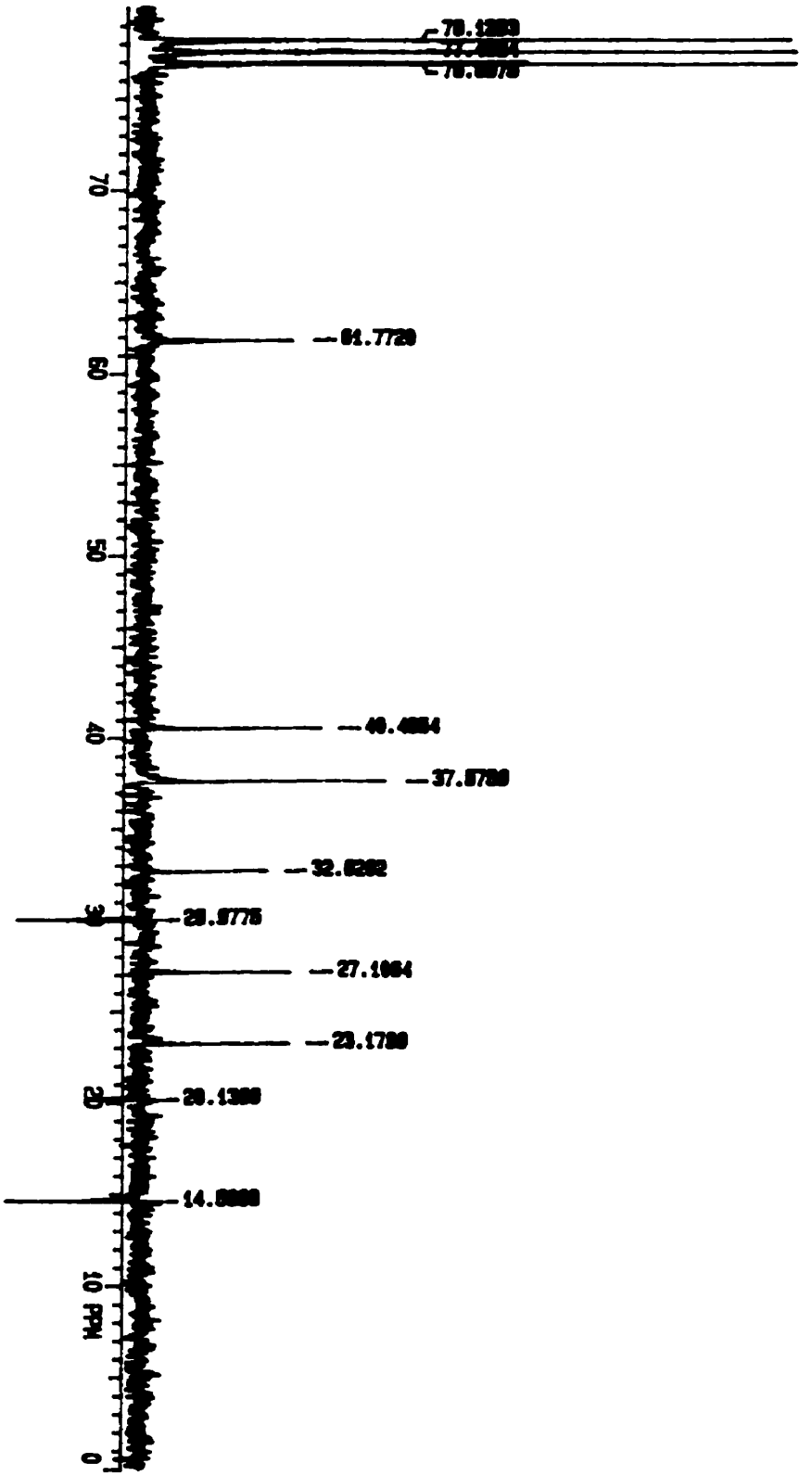

APPENDIX 3 C: 3-Methyloctanol mass spectrum (EI)

```
File         : C:\HPCHEM\1\DATA\JL14S3A.D
Operator     : Ray Bacala
Acquired     : 14 Jul 98  12:15 pm using AcqMethod RAY10JL
Instrument   :    5989B-MS
Sample Name: Sample 3 (3-methyloctanol)
Misc Info    : 1 ul inj(50.0 ng/ul) ran:40-175, fw=144.257
Vial Number: 1
```

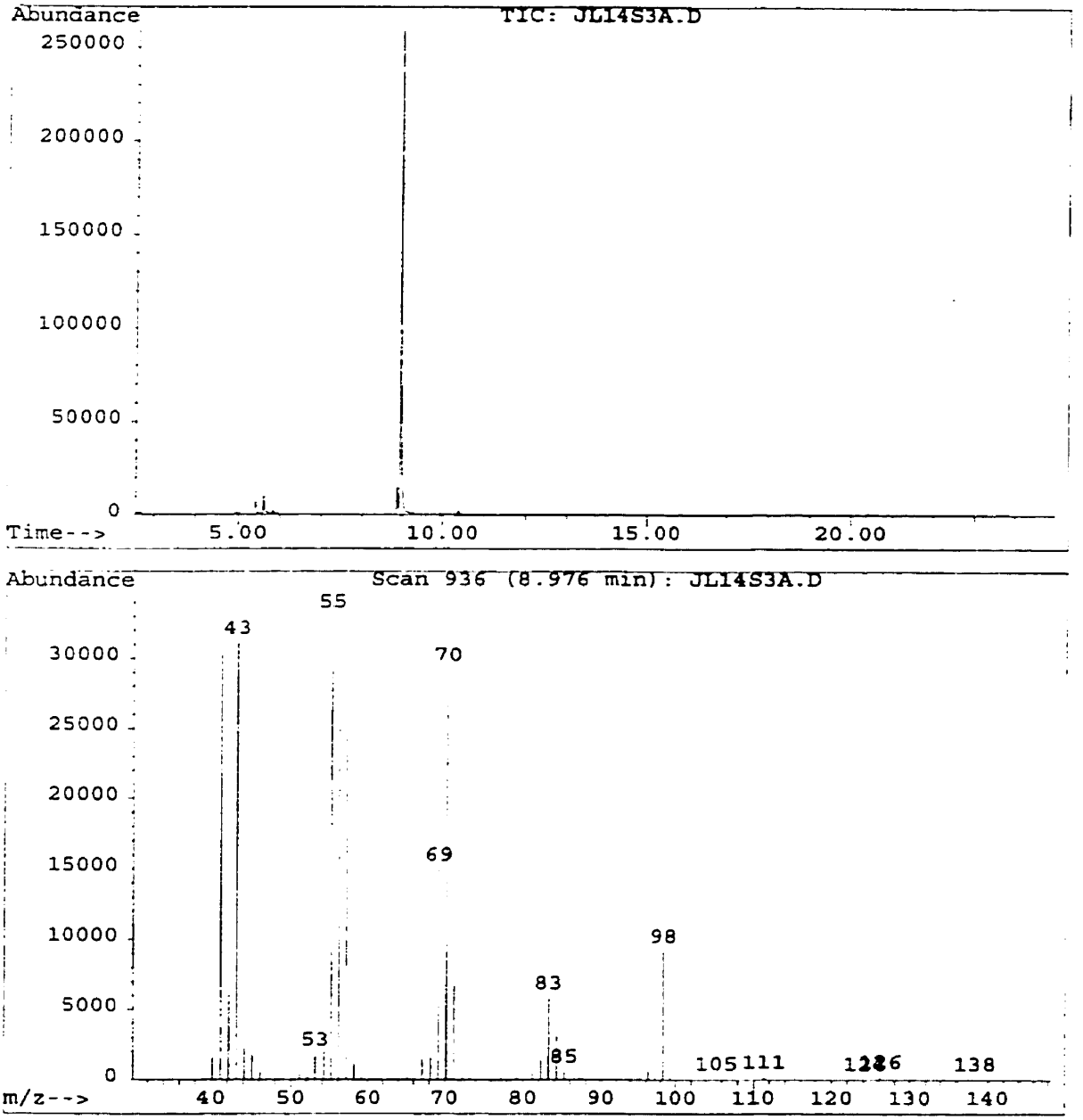

APPENDIX 3 C: 3-Methyloctanol mass spectrum (EI)

Scan 936 (8.976 min): JL14S3A.D
Sample 3 (3-methyloctanol)
Modified:scaled

m/z	abund.	m/z	abund.	m/z	abund.	m/z	abund.
40.1	5	52.1	1	65.2	1	78.2	0
41.1	88	53.1	5	66.2	0	79.2	1
42.1	31	54.2	6	67.1	5	80.2	0
43.1	90	55.1	100	68.2	5	81.2	2
44.1	7	56.1	89	69.2	43	82.2	4
45.1	5	57.1	73	70.2	84	83.2	17
46.1	2	58.1	3	71.2	20	84.2	10
47.1	0	59.1	1	72.2	2	85.2	2
48.2	0	60.1	0	73.2	1	86.2	0
50.1	0	63.1	0	74.2	0	87.2	0
51.1	1	64.2	0	77.2	0	91.2	0

Scan 936 (8.976 min): JL14S3A.D

m/z	abund.	m/z	abund.	m/z	abund.
92.2	0	108.3	0	127.25	0
93.3	0	109.15	0	136.25	0
95.15	1	110.3	0	138.35	0
96.3	2	111.3	0		
97.3	13	112.3	0		
98.3	26	113.15	0		
99.3	2	114.3	0		
100.3	0	121.15	0		
101.3	0	122.25	0		
103.15	0	124.25	0		
105.3	0	126.25	1		

APPENDIX 3 D: 3-Methyloctanol mass spectrum (PCI)

```
File         : C:\HPCHEM\1\DATA\RAYPCI3.D
Operator     : Ray Bacala
Acquired     :  6 Oct 98   1:17 pm using AcqMethod RAYPCI
Instrument   :    5989B-MS
Sample Name: Sample 3 (3-Methyloctanol)
Misc Info    : 1 ul inj. (50 ng/ul), mass 60-175, fw=144.25
Vial Number: 1
```

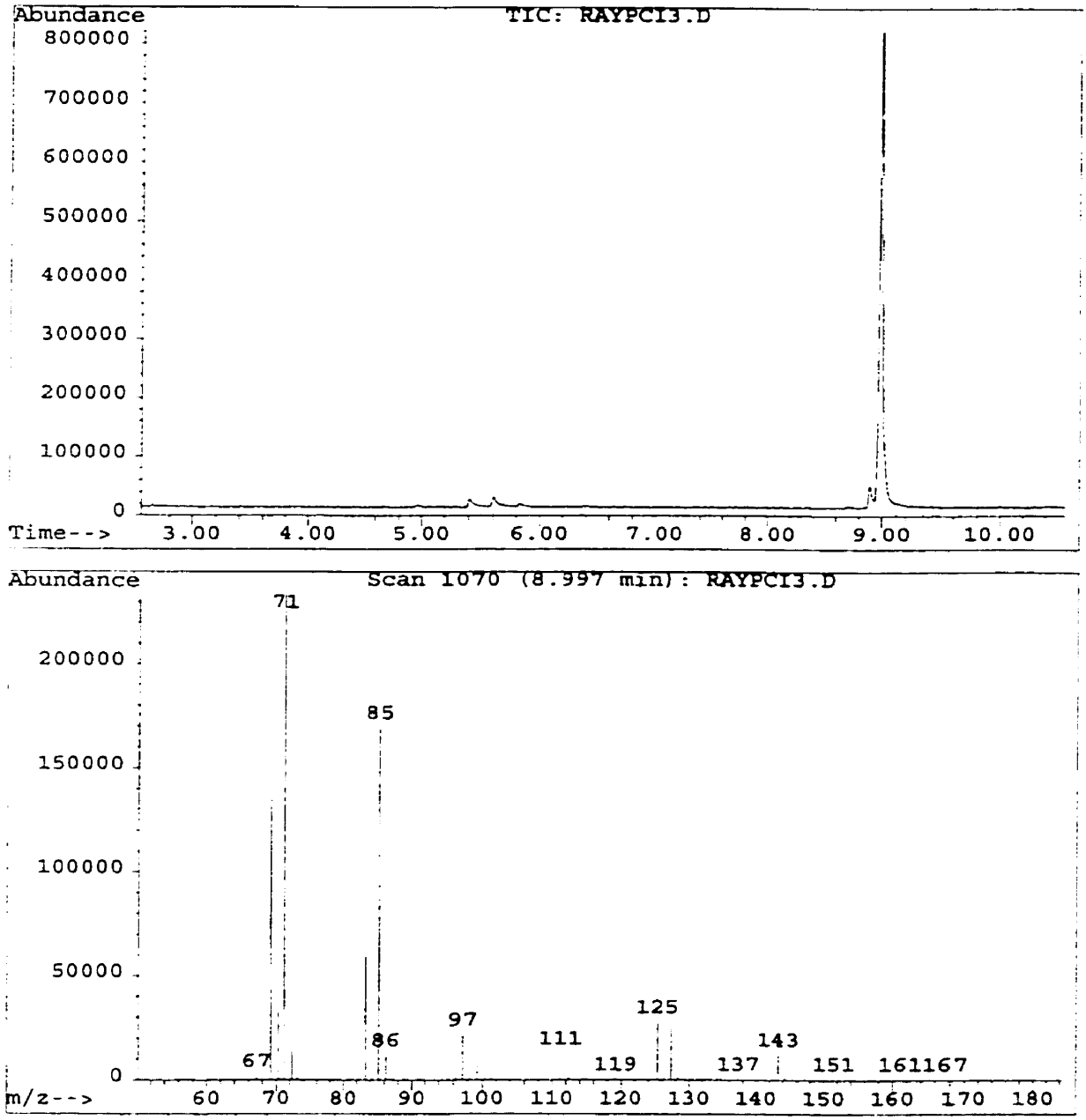

APPENDIX 3 D: 3-Methyloctanol mass spectrum (PCI)

Scan 1070 (8.997 min): RAYPCI3.D
Sample 3 (3-Methyloctanol)
Modified:scaled

m/z	abund.	m/z	abund.	m/z	abund.	m/z	abund.
60.15	0	69.15	58	78.25	0	91	0
60.8	0	70.3	14	79.25	0	92.1	0
61.3	0	71.15	100	79.9	0	92.75	0
62.05	0	72.3	6	81.25	1	93.25	0
62.3	0	73.15	1	83.25	26	94.25	0
63.15	0	74	0	84.25	5	95.35	0
64.15	0	74.25	0	85.25	72	96.35	1
65.05	0	74.65	0	86.25	5	97.25	9
65.65	0	75	0	87.25	0	98.25	8
66.4	0	76.15	0	88.25	0	99.25	3
67.15	1	76.9	0	89.6	0	100.35	0

Scan 1070 (8.997 min): RAYPCI3.D

m/z	abund.	m/z	abund.	m/z	abund.	m/z	abund.
101.2	0	113.35	0	125.3	12	135.3	0
102.45	0	114.35	0	126.3	3	135.9	0
103.6	0	115.45	0	127.3	11	136.4	0
104.2	0	116.95	0	128.3	1	137.3	0
105.2	0	117.45	0	129.3	0	138.3	0
106.45	0	118.3	0	130.4	0	139.4	0
107.2	0	119.2	0	130.65	0	140.3	0
107.95	0	120.05	0	131.3	0	141.3	0
109.2	0	121.45	0	132.15	0	143.3	5
111.2	5	122.3	0	133.05	0	144.25	1
112.35	1	123.3	0	134.15	0	145.25	0

Scan 1070 (8.997 min): RAYPCI3.D

m/z	abund.	m/z	abund.
146.5	0	158.35	0
147.25	0	159.25	0
148.25	0	160.25	0
149.4	0	161.1	0
150.15	0	162	0
151.4	0	162.35	0
152.15	0	163.35	0
153.25	0	164.25	0
155.15	0	165.25	0
156.4	0	166.25	0
157.15	0	167.35	0

APPENDIX 4 A: 3-Methylbromooctane ^{1}H NMR spectrum

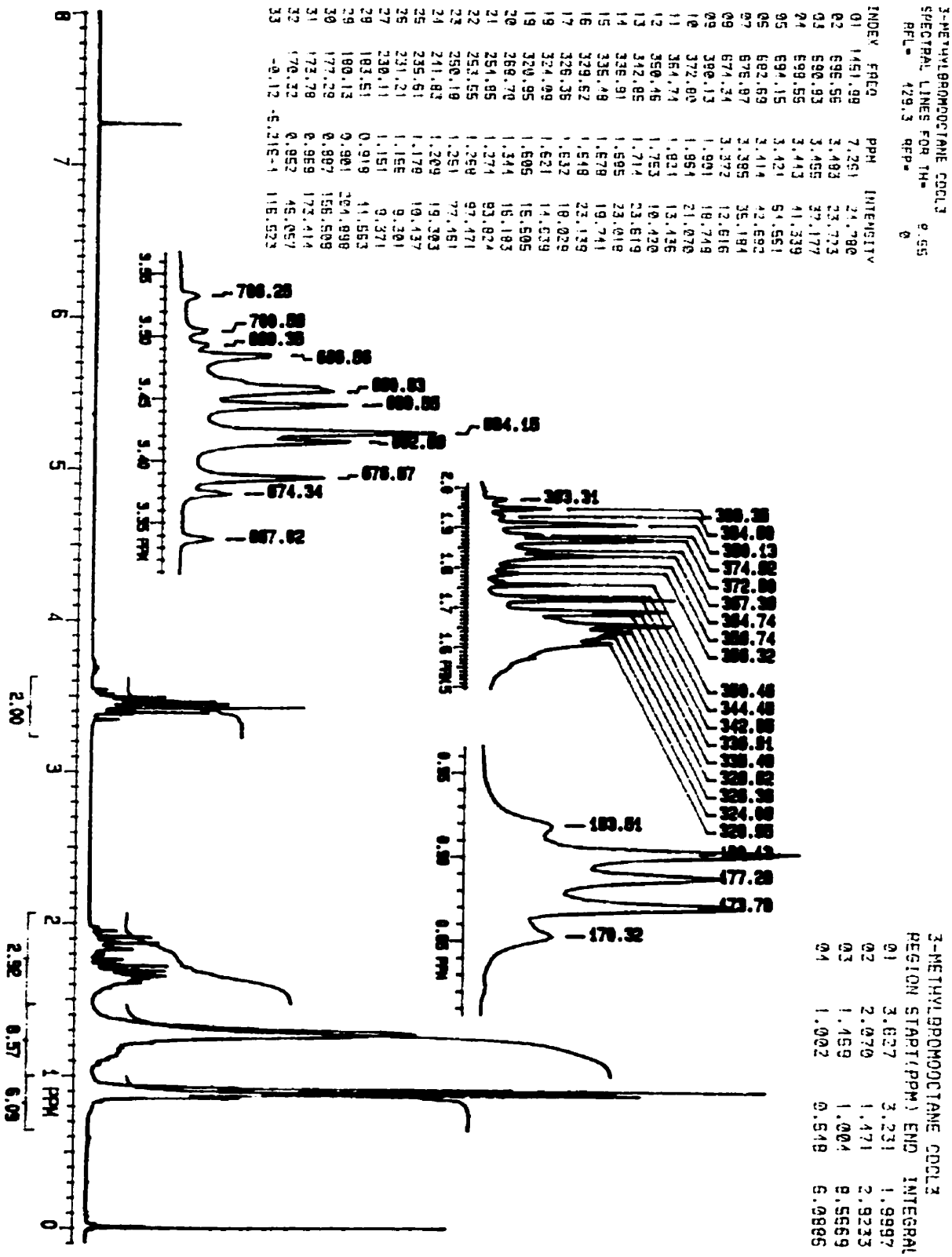

APPENDIX 4 B: 3-Methylbromooctane ^{13}C NMR spectrum

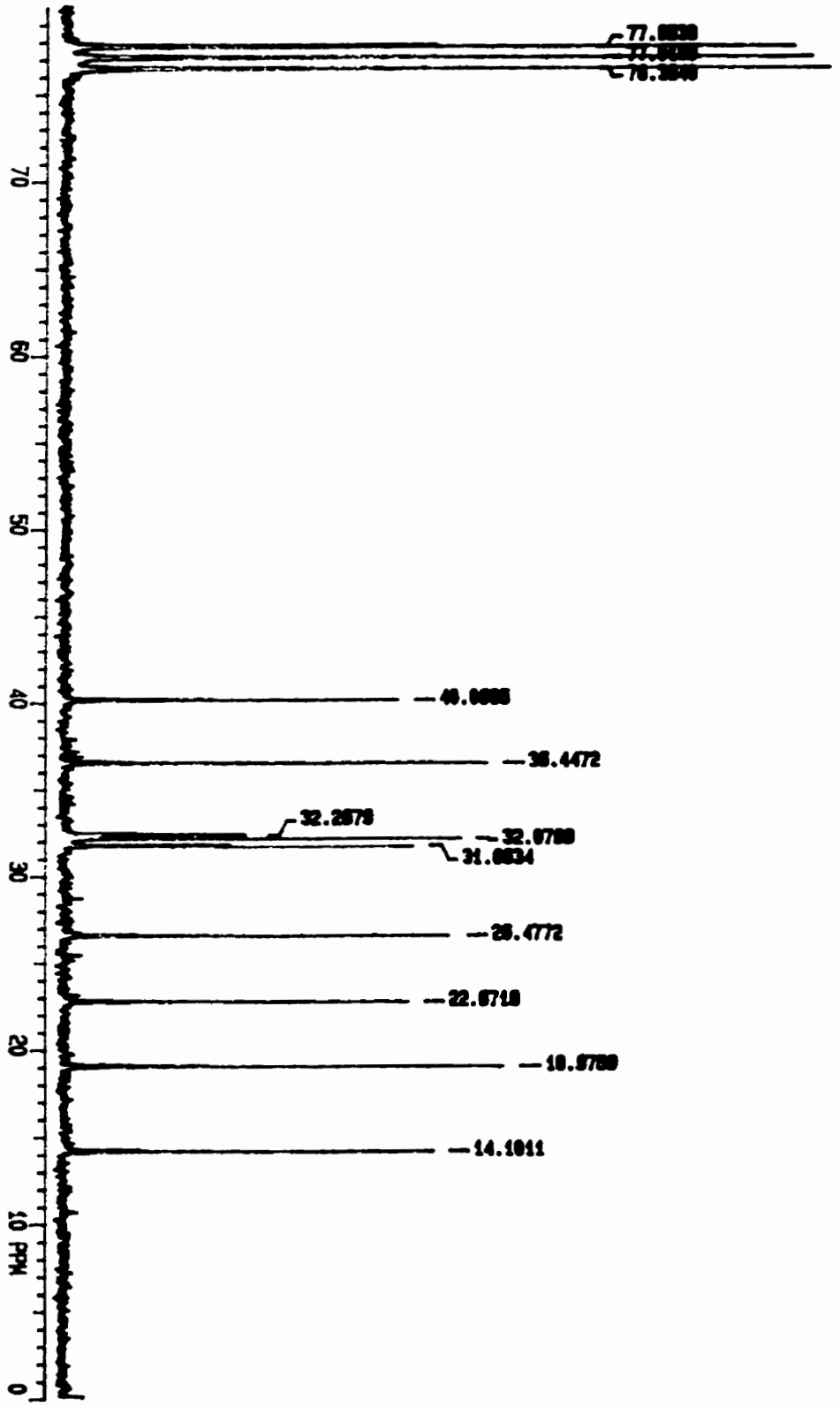

APPENDIX 5 A: 4-Methylnonanoic acid ^{1}H NMR spectrum

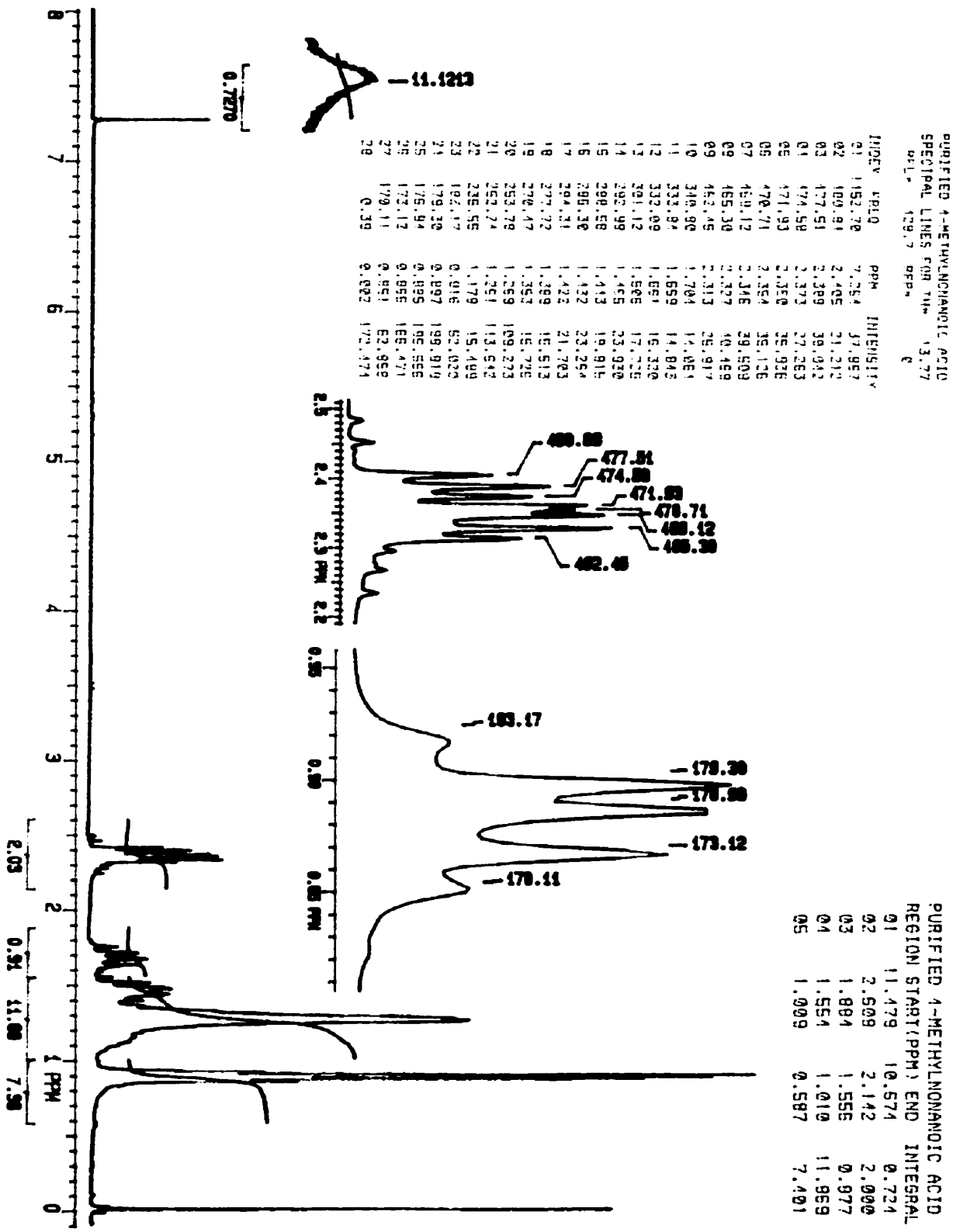

APPENDIX 5 B: 4-Methylnonanoic acid ^{13}C NMR spectrum

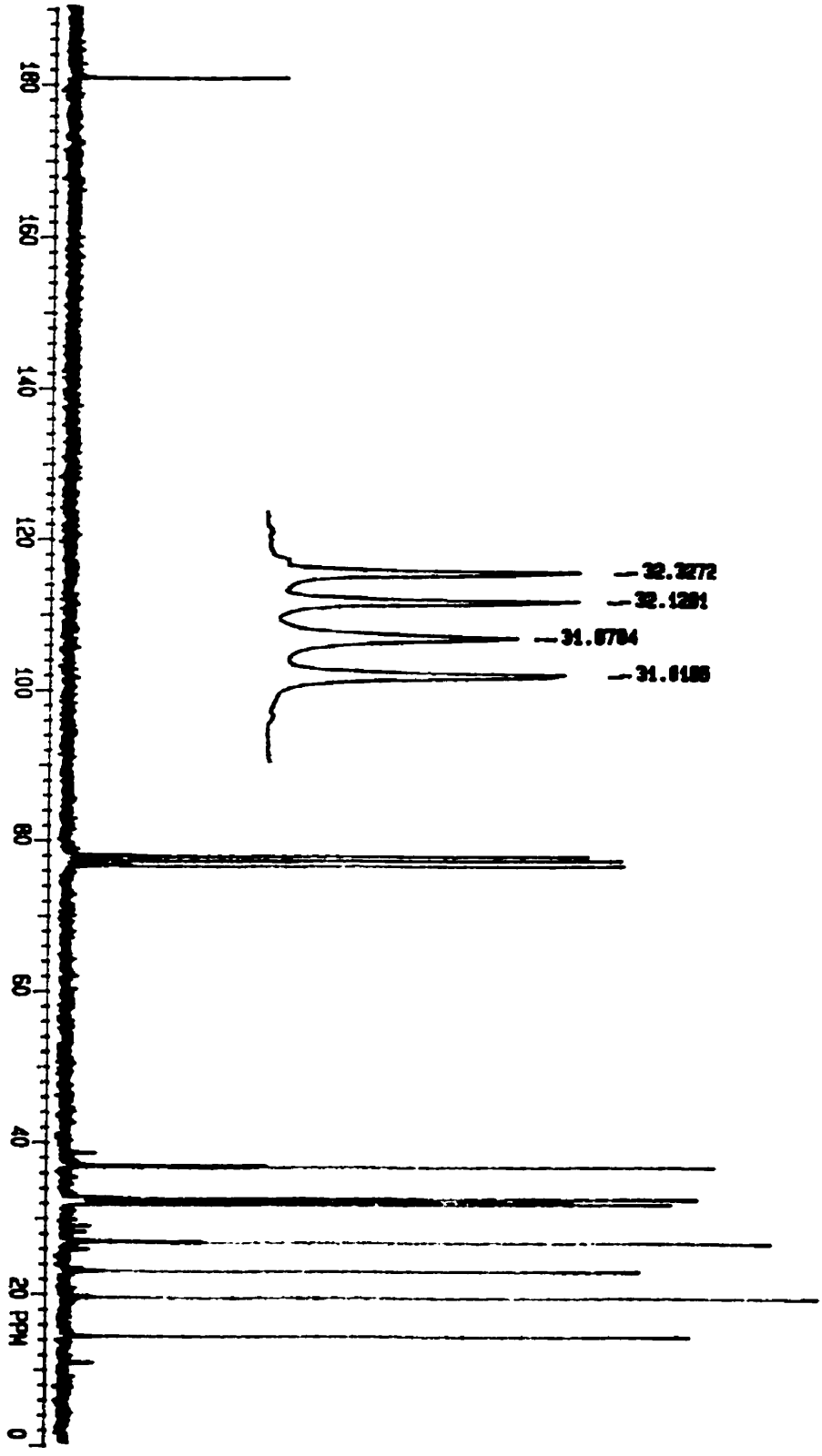

APPENDIX 6 A: 4-Methylnonanol ^{1}H NMR spectrum

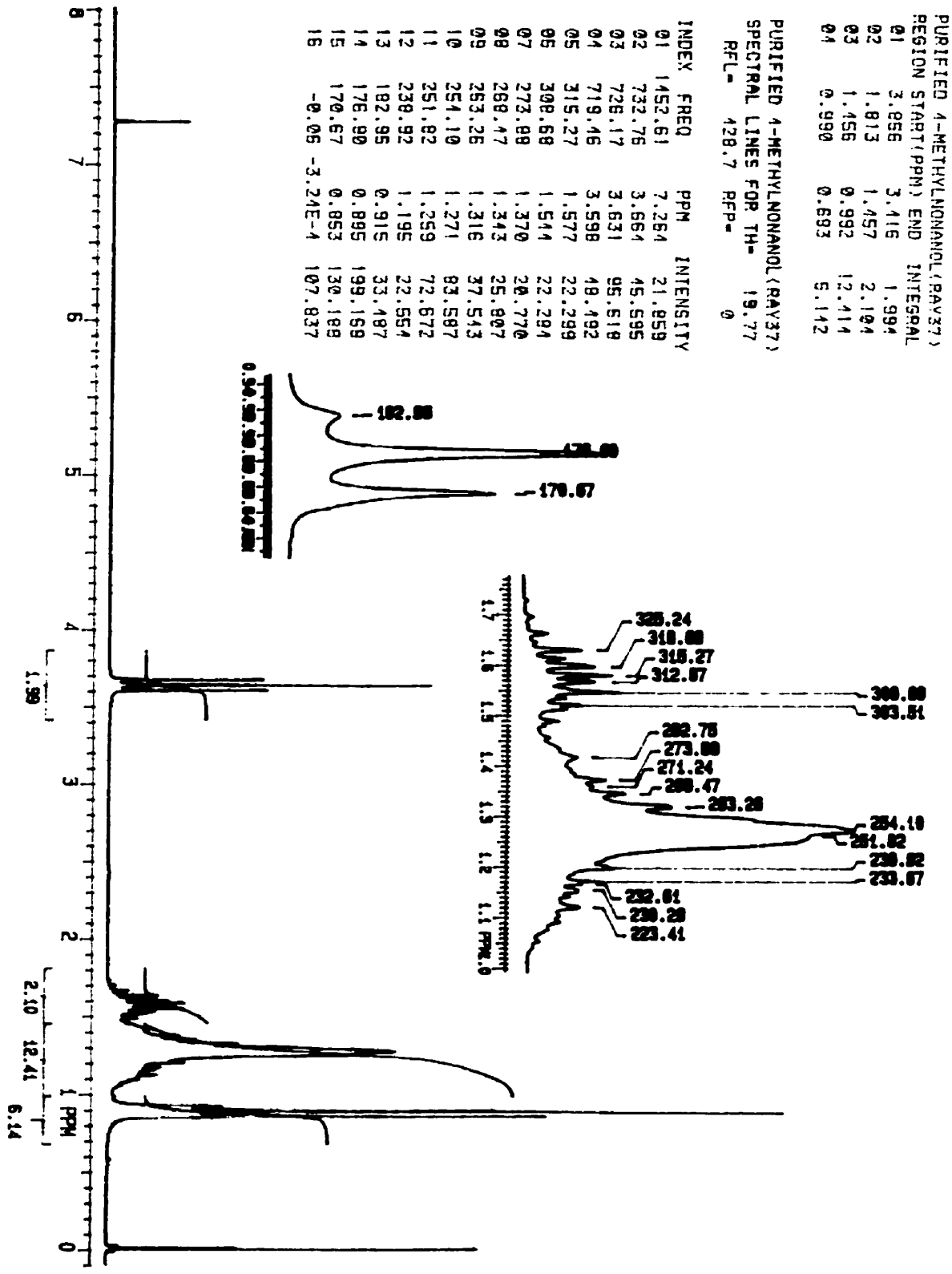

APPENDIX 6 B: 4-Methylnonanol ^{13}C NMR spectrum

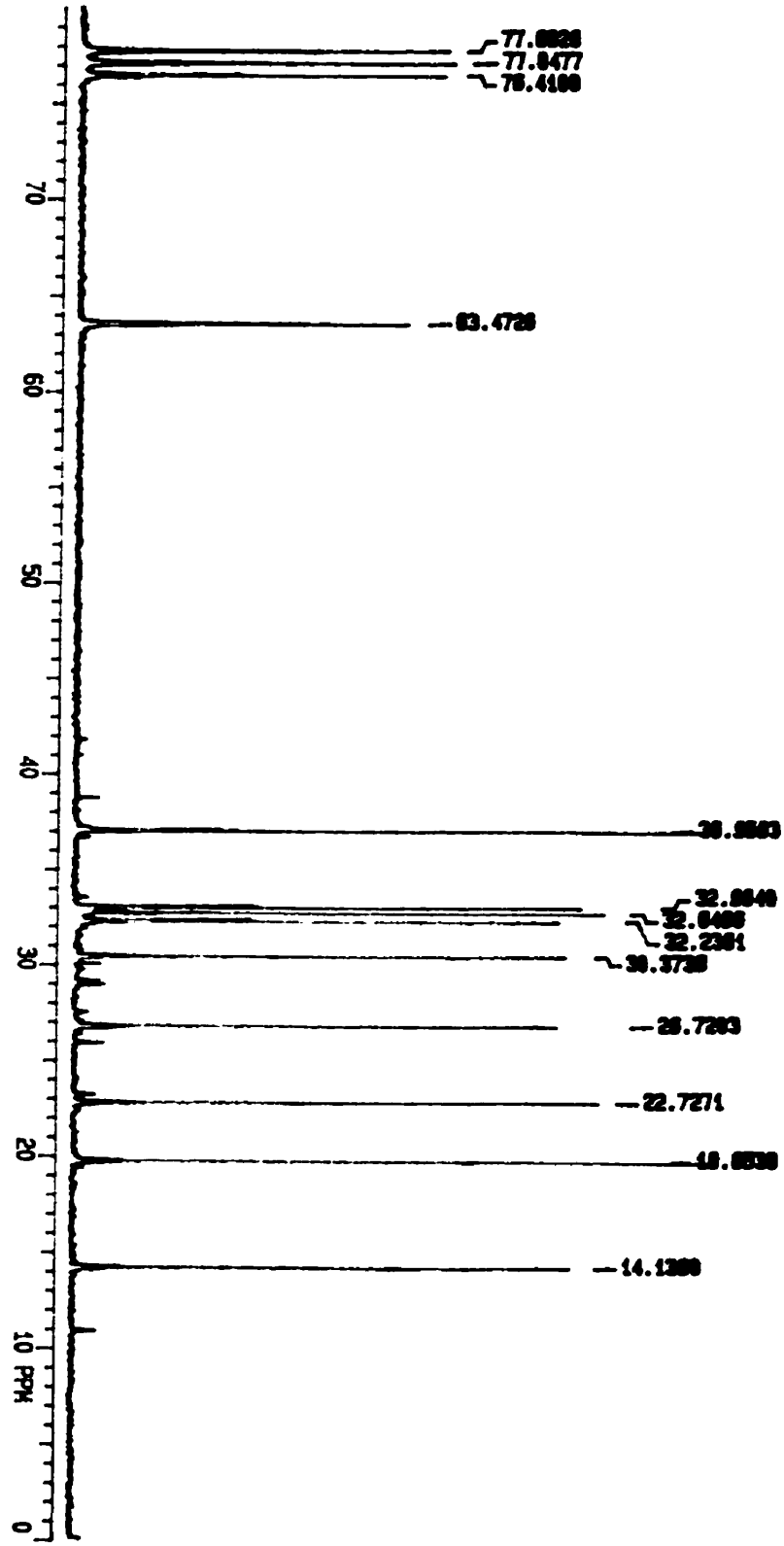

APPENDIX 6 C: 4-Methylnonanol mass spectrum (EI)

```
File        : C:\HPCHEM\1\DATA\OC5S6A.D
Operator    : Ray Bacala
Acquired    :  5 Oct 98  12:29 pm using AcqMethod RAY10JL
Instrument  :    5989B-MS
Sample Name: Sample 6 (4-methylnonanol)
Misc Info   : 1 ul inj. (50 ng/ul), mass 40-180, fw=158.28
Vial Number: 1
```

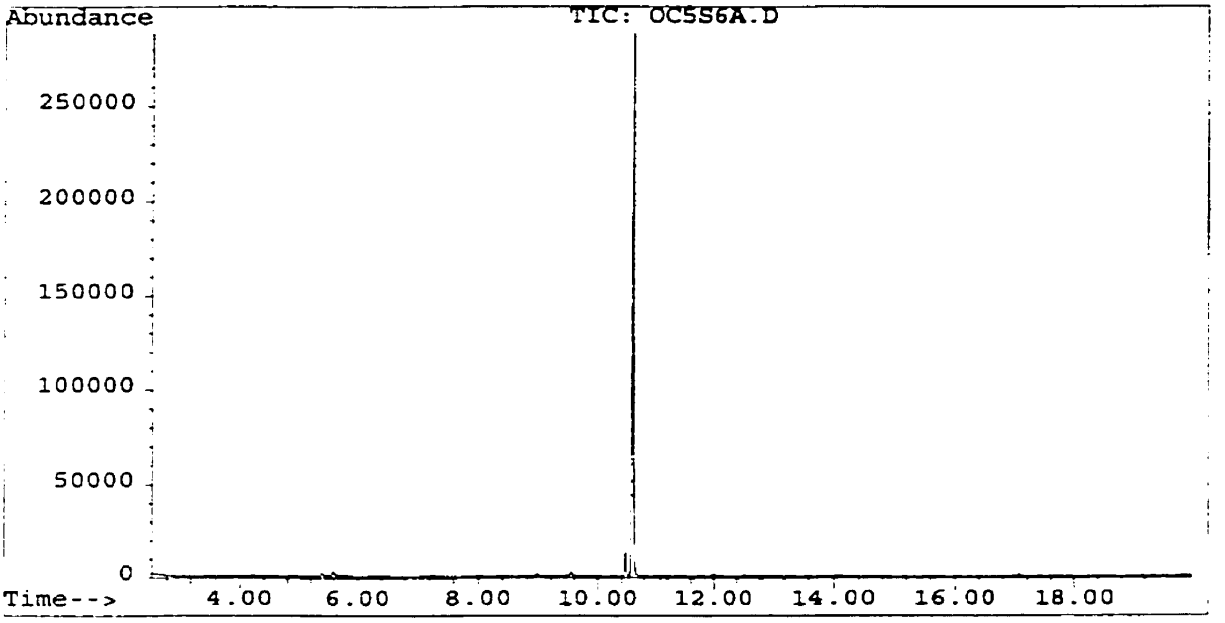

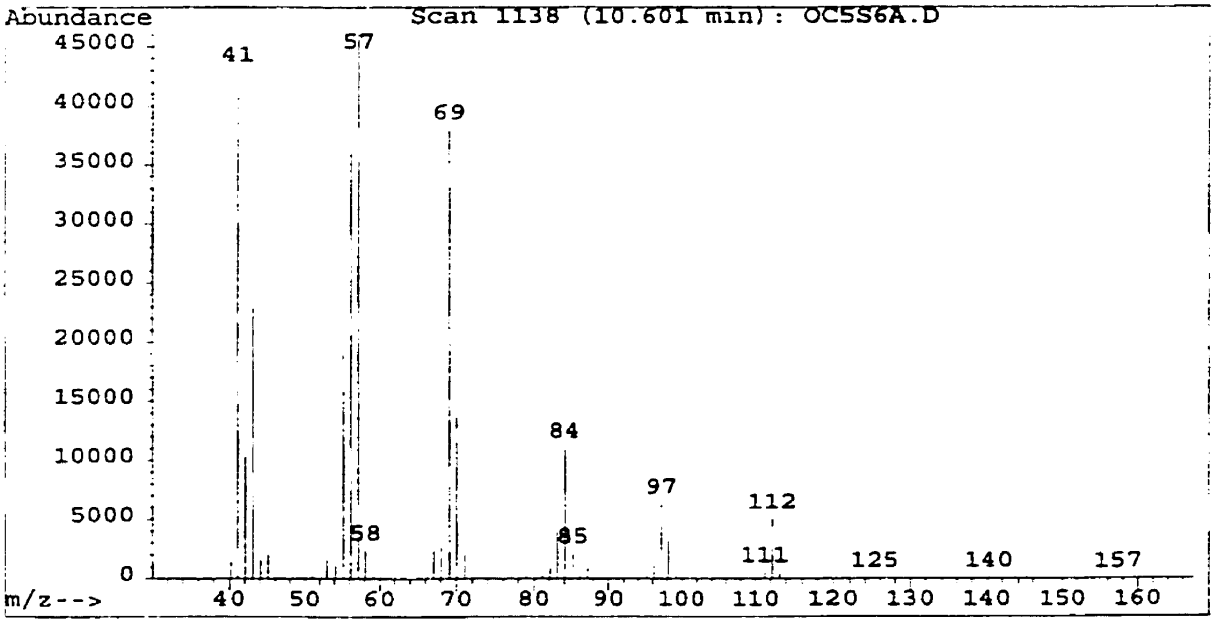

APPENDIX 6 C: 4-Methylnonanol mass spectrum (EI)

Scan 1138 (10.601 min): OC5S6A.D
Sample 6 (4-methylnonanol)
Modified:scaled

m/z	abund.	m/z	abund.	m/z	abund.	m/z	abund.
40.15	3	51	1	62	0	77.1	0
41.05	93	52.15	0	63	0	78.1	0
42.05	22	53	4	65.1	1	79.1	0
43.05	51	54.15	2	66.25	0	80.1	0
44.05	4	55.15	41	67.1	5	81.1	1
45.05	5	56.15	79	68.1	6	82.1	2
46	0	57.15	100	69.1	82	83.1	11
47	0	58.15	5	70.1	30	84.1	24
48	0	59.15	0	71.1	5	85.2	5
49.15	0	60.15	1	72.1	0	86.2	0
50	0	61.15	0	73.1	0	87.2	2

Scan 1138 (10.601 min): OC5S6A.D

m/z	abund.	m/z	abund.	m/z	abund.
88.2	0	100.2	0	125.3	0
89.35	0	101.3	0	126.3	0
91.2	0	105.05	0	128.4	0
92.1	0	109.2	0	140.25	0
93.1	0	110.2	0	141.25	0
94.2	0	111.2	1	157.35	0
95.2	0	112.2	11		
96.2	2	113.2	1		
97.2	14	114.3	0		
98.2	7	115.15	0		
99.2	1	123.3	0		

APPENDIX 6 D: 4-Methylnonanol mass spectrum (PCI)

```
File        : C:\HPCHEM\1\DATA\RAYPCI6.D
Operator    : Ray Bacala
Acquired    :  6 Oct 98    2:14 pm using AcqMethod RAYPCI
Instrument :     5989B-MS
Sample Name: Sample 6 (4-methylnonanol)
Misc Info   : 1 ul inj. (50 ng/ul), mass 60-180, fw=158.28
Vial Number: 1
```

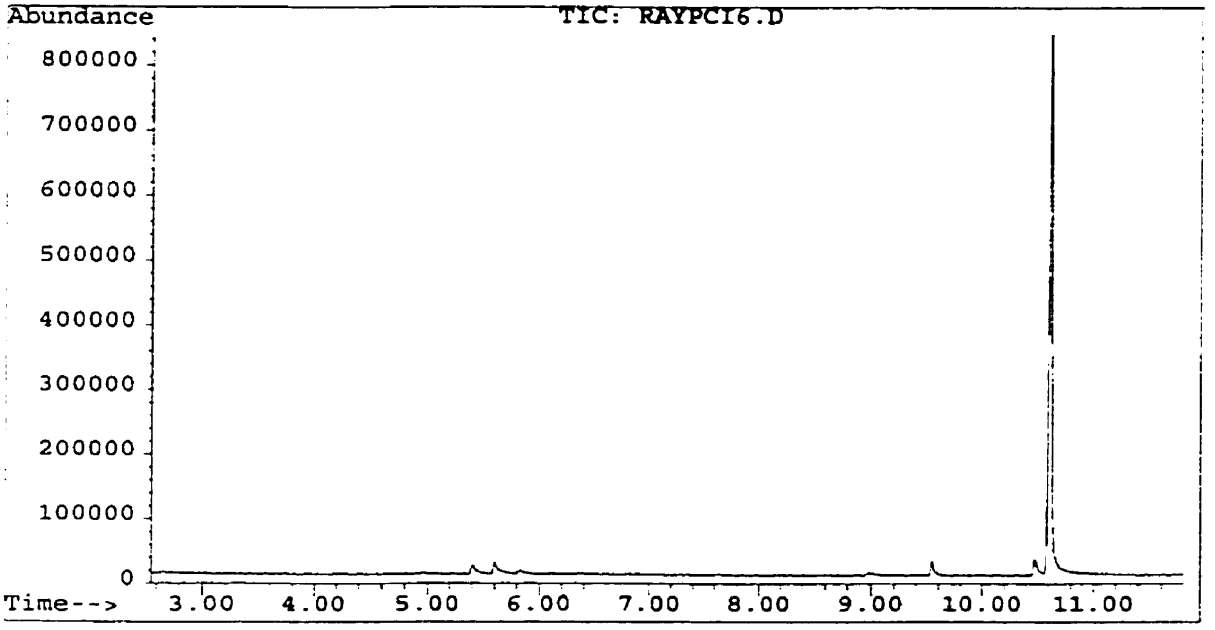

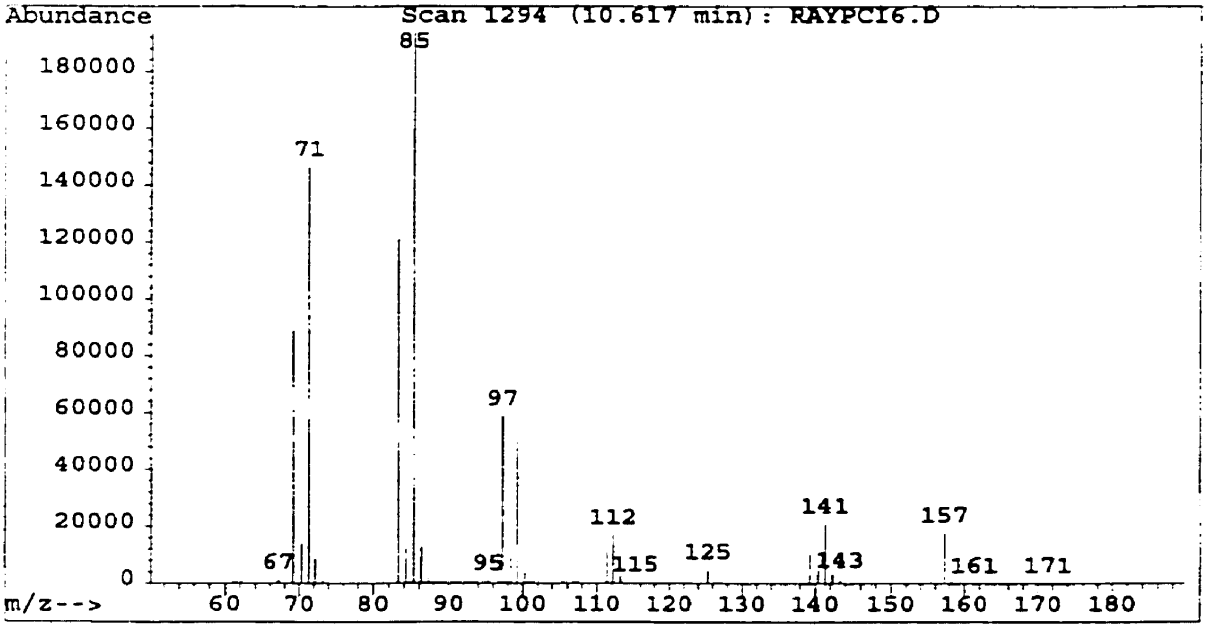

APPENDIX 6 D: 4-Methylnonanol mass spectrum (PCI)

Scan 1294 (10.617 min): RAYPCI6.D
Sample 6 (4-methylnonanol)
Modified:scaled

m/z	abund.	m/z	abund.	m/z	abund.	m/z	abund.
60.3	0	73.25	0	84.25	10	95.35	0
61.05	0	74	0	85.25	100	97.25	30
62.3	0	74.25	0	86.25	7	98.35	5
63.05	0	75	0	87.25	1	99.25	27
65.15	0	75.9	0	88.25	0	100.25	2
66.4	0	77.25	0	89.25	0	101.35	0
67.15	1	78.25	0	90.25	0	102.35	0
69.15	46	79.15	0	91.25	0	102.95	0
70.3	7	79.9	0	92.35	0	103.6	0
71.3	76	81.25	2	93.1	0	103.95	0
72.15	5	83.25	63	93.85	0	104.35	0

Scan 1294 (10.617 min): RAYPCI6.D

m/z	abund.	m/z	abund.	m/z	abund.	m/z	abund.
105.2	0	116.3	0	127.3	0	137.3	0
106.45	0	117.2	0	128.05	0	139.3	5
107.35	0	118.3	0	128.45	0	140.4	2
108.35	0	119.3	0	129.2	0	141.3	11
109.35	0	120.3	0	130.55	0	142.3	2
111.35	6	121.2	0	131.3	0	143.3	1
112.2	9	122.05	0	132.4	0	144.25	0
113.2	1	123.3	0	133.15	0	144.9	0
114.35	0	124.3	0	134.15	0	145.5	0
114.7	0	125.3	3	135.4	0	146.4	0
115.3	0	126.2	0	136.4	0	147	0

Scan 1294 (10.617 min): RAYPCI6.D

m/z	abund.	m/z	abund.
148.15	0	153.5	0
149.25	0	154.25	0
150	0	155.4	0
151.4	0	157.25	9
152.5	0	158.25	1
153.25	0	159.25	0

APPENDIX 7 A: 4-Methyl-1-methoxynonane ^{1}H NMR spectrum

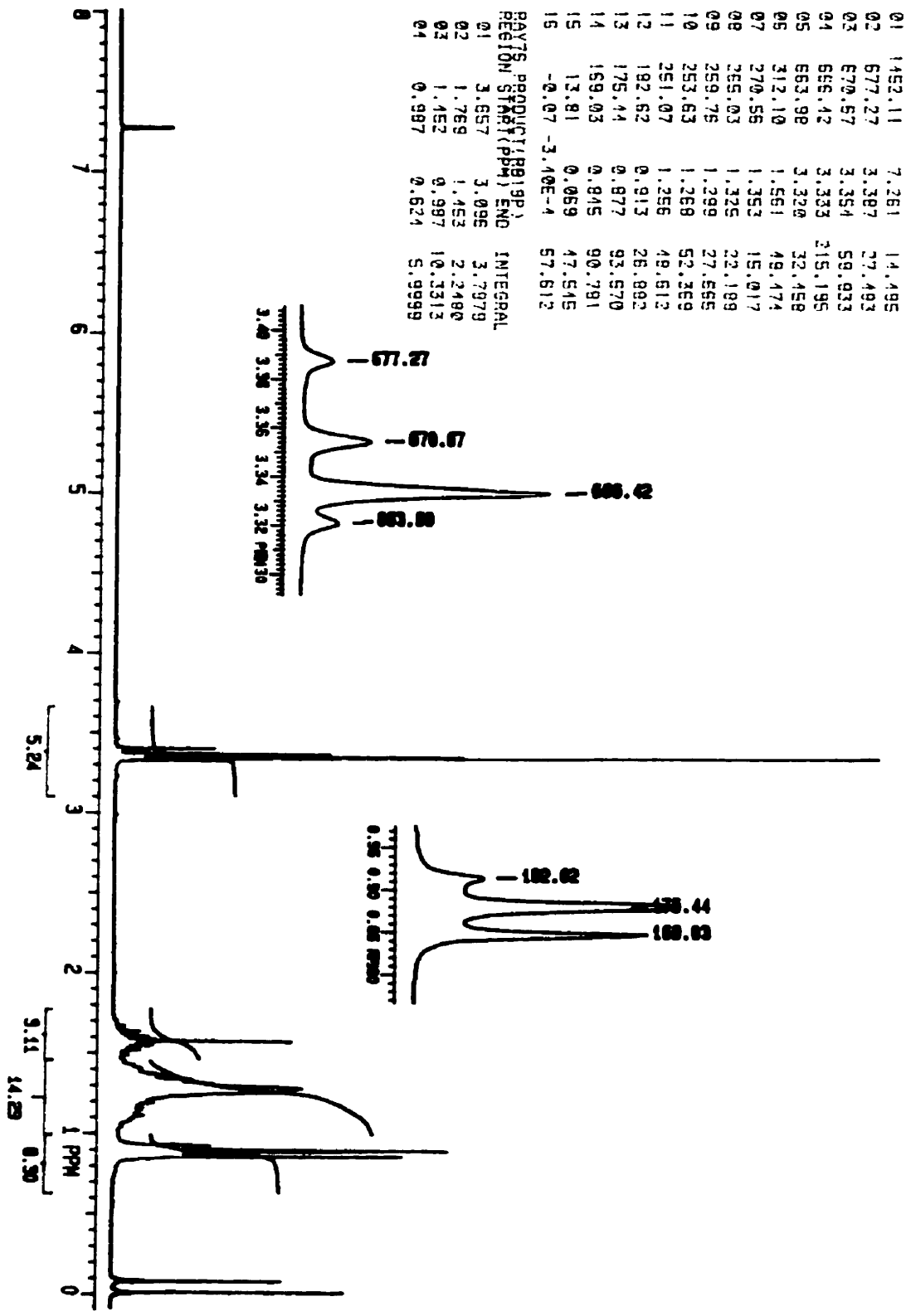

APPENDIX 7 B: 4-Methyl-1-methoxynonane ^{13}C NMR spectrum

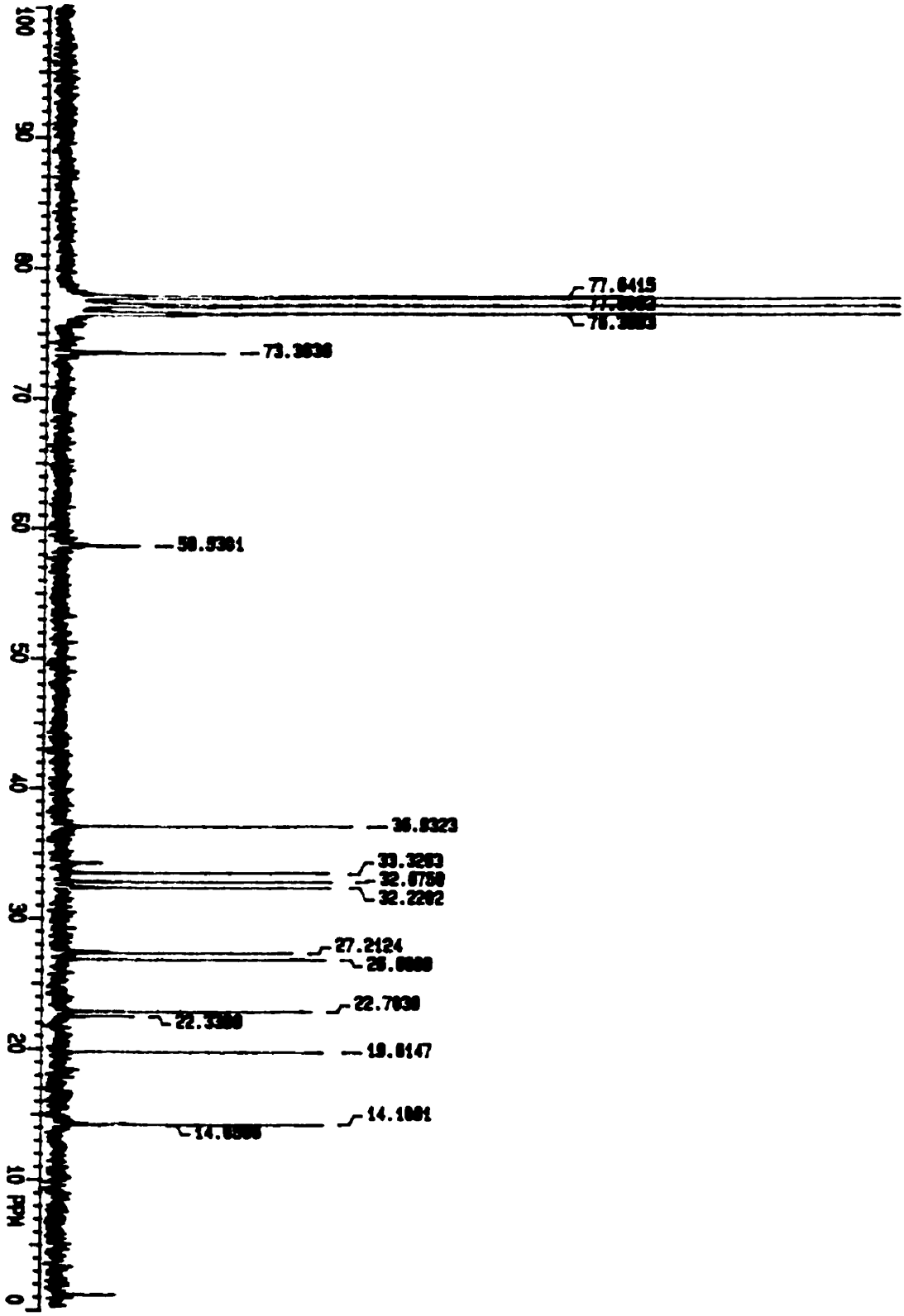

APPENDIX 7 C: 4-Methyl-1-methoxynonane mass spectrum

```
File        : C:\HPCHEM\1\DATA\OC5S7A.D
Operator    : Ray Bacala
Acquired    :  5 Oct 98   2:14 pm using AcqMethod RAY10JL
Instrument  :    5989B-MS
Sample Name: Sample 7 (Methyl 4-methylnonanyl ether)
Misc Info   : 1 ul inj. (50 ng/ul), mass 40-200, fw=172.31
Vial Number: 1
```

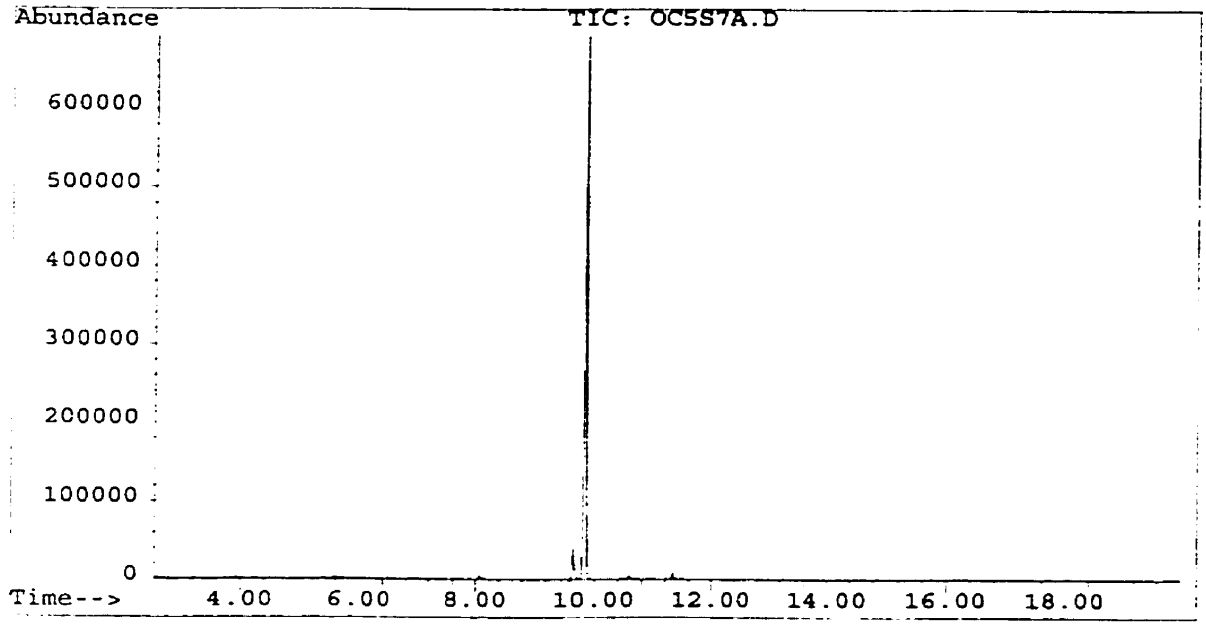

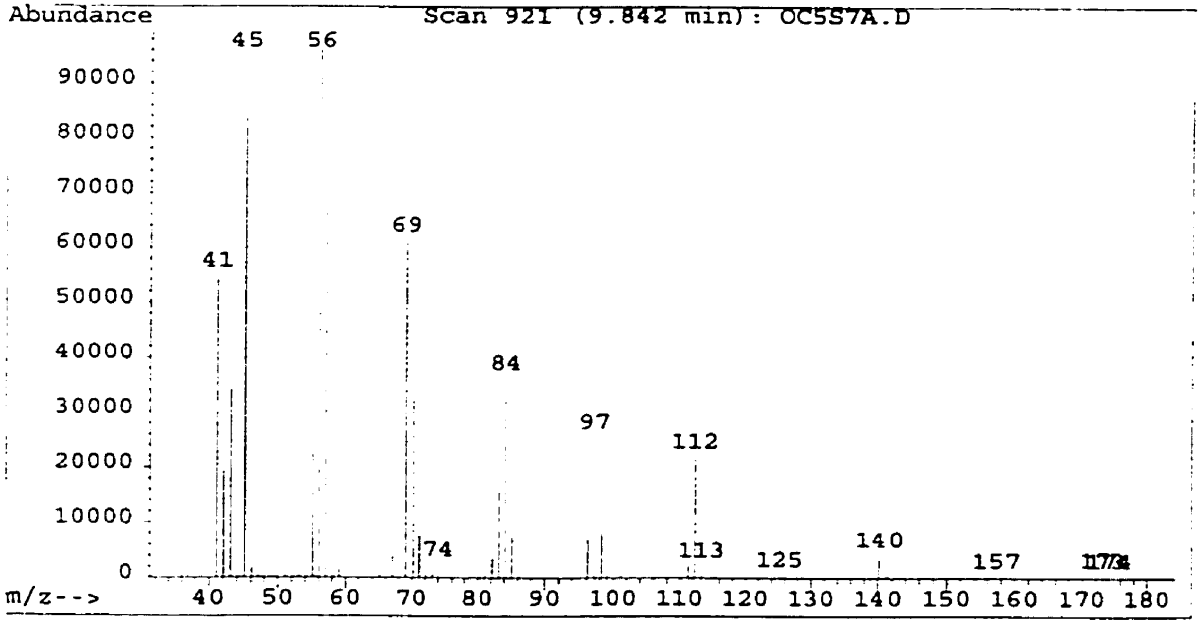

APPENDIX 7 C: 4-Methyl-1-methoxynonane mass spectrum (EI)

Scan 921 (9.842 min): OC5S7A.D
Sample 7 (Methyl 4-methylnonanyl ether)
Modified:scaled

m/z	abund.	m/z	abund.	m/z	abund.	m/z	abund.
41.1	55	53.1	3	65.05	1	75.9	0
42.1	19	55.05	41	66.2	0	77.05	0
43.1	35	56.05	97	67.05	4	78.15	0
45.1	100	57.05	81	68.2	5	79.15	0
46.1	2	58.05	6	69.05	61	80.15	0
47.1	0	59.05	2	70.2	34	81.15	1
48.1	0	60.05	0	71.15	8	82.15	4
48.95	0	61.05	0	72.15	1	83.15	16
50.1	0	62.05	0	73.15	1	84.15	36
51.1	0	63.05	0	74.05	2	85.15	8
52.2	0	64.05	0	75.15	0	86.15	0

Scan 921 (9.842 min): OC5S7A.D

m/z	abund.	m/z	abund.	m/z	abund.	m/z	abund.
87.15	0	99.15	1	114.25	0	141.3	1
88.25	0	101.15	1	115.25	0	142.3	0
89	0	102.15	0	119	0	157.3	0
91.15	0	103	0	123.35	0	171.3	0
92.25	0	105.1	0	124.35	0	172.3	0
93.15	0	107.1	0	125.2	0	173.25	0
94.25	0	109.25	0	126.2	0	174.25	0
95.25	0	110.25	0	128.35	0		
96.15	7	111.25	2	129.2	0		
97.15	25	112.25	22	138.2	0		
98.25	8	113.25	2	140.2	4		

APPENDIX 7 D: 4-Methyl-1-methoxynonane mass spectrum (PCI)

```
File         : C:\HPCHEM\1\DATA\RAYPCI7.D
Operator     : Ray Bacala
Acquired     :  6 Oct 98   2:29 pm using AcqMethod RAYPCI
Instrument   :    5989B-MS
Sample Name: Sample 7 (Methyl 4-methylnonanyl ether)
Misc Info    : 1 ul inj. (50 ng/ul), mass 60-200, fw=172.3
Vial Number: 1
```

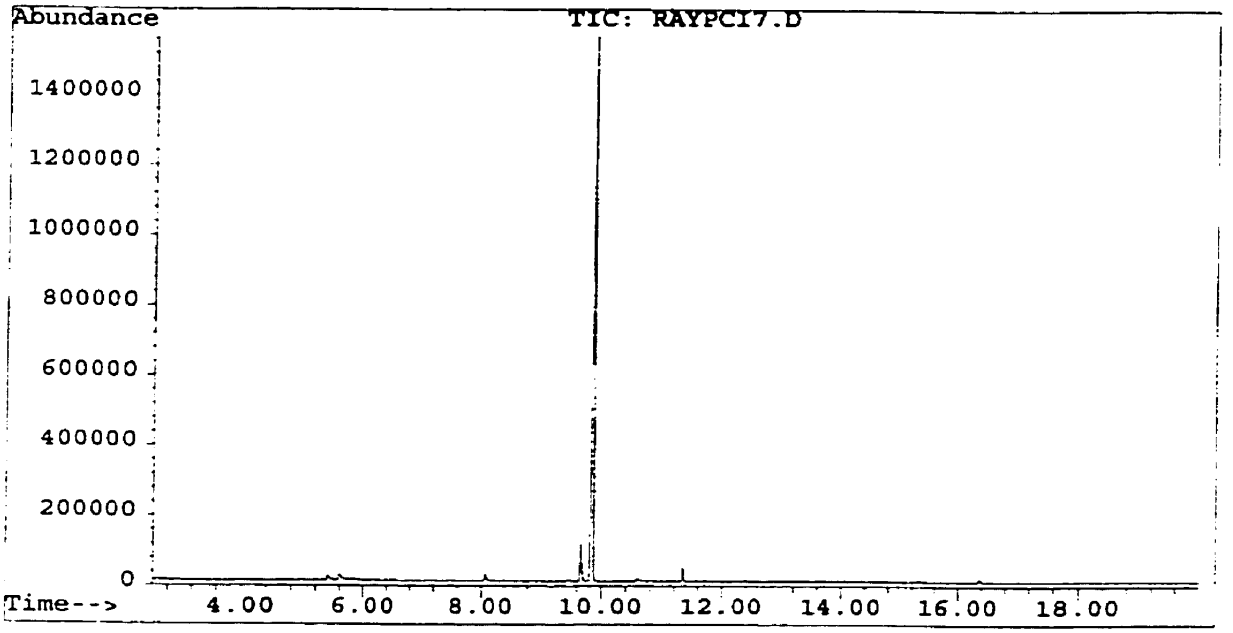

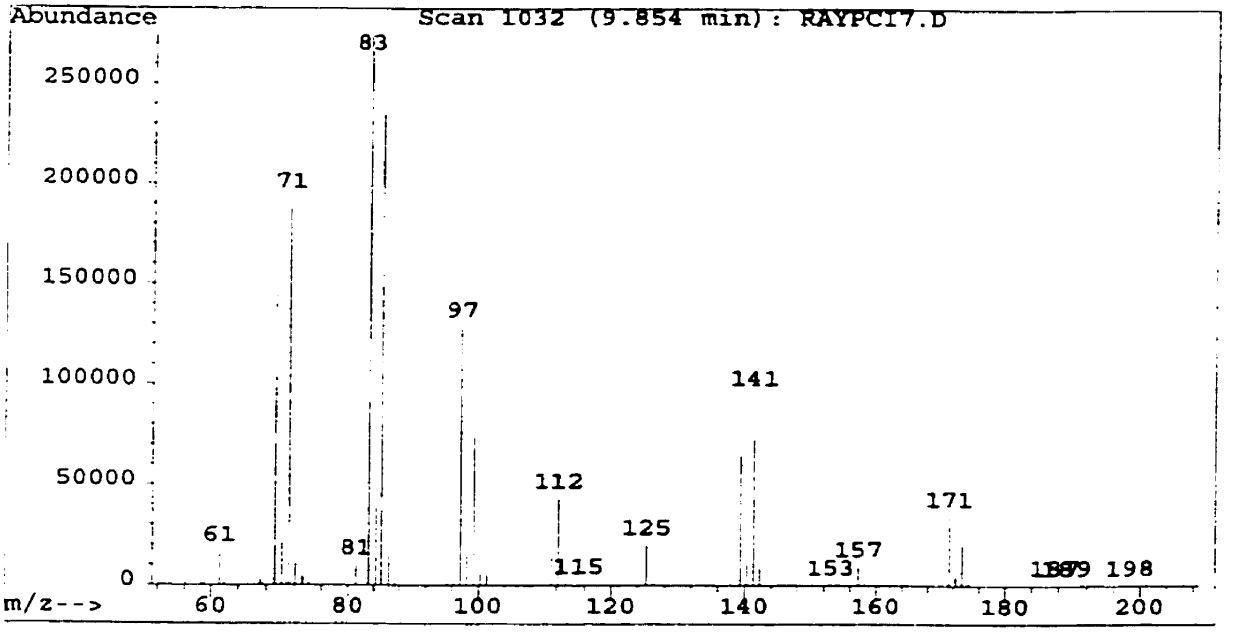

APPENDIX 7 D: 4-Methyl-1-methoxynonane mass spectrum (PCI)

Scan 1032 (9.854 min): RAYPCI7.D
Sample 7 (Methyl 4-methylnonanyl ether)
Modified:scaled

m/z	abund.	m/z	abund.	m/z	abund.	m/z	abund.
61.25	6	72.2	4	85.2	85	96.3	3
62	0	73.2	2	86.3	5	97.3	47
63.1	0	74.2	0	87.2	0	98.3	6
64	0	75.2	0	88.2	0	99.3	27
64.35	0	76.45	0	88.95	0	100.3	2
65.25	0	76.95	0	89.55	0	101.3	2
66.2	0	78.35	0	91.05	0	102.15	0
67.2	1	79.1	0	92.2	0	103.3	0
69.2	53	81.2	4	93.3	0	105.3	0
70.2	8	83.2	100	94.3	0	106.3	0
71.2	70	84.3	14	95.3	0	106.65	0

Scan 1032 (9.854 min): RAYPCI7.D

m/z	abund.	m/z	abund.	m/z	abund.	m/z	abund.
107.3	0	119.25	0	131.25	0	144.1	0
108.15	0	120	0	132.5	0	144.35	0
109.25	0	121	0	133.5	0	144.7	0
111.25	5	122.15	0	134.5	0	145.1	0
112.25	16	123.25	0	135.25	0	145.35	0
113.4	1	125.25	7	137.35	0	145.7	0
114.25	0	126.25	1	139.35	24	146.35	0
115.25	0	127	0	140.35	11	147.2	0
116.25	0	127.85	0	141.35	34	148.35	0
117.15	0	129.35	0	142.35	4	149.35	0
118.4	0	130.6	0	143.35	0	150.35	0

Scan 1032 (9.854 min): RAYPCI7.D

m/z	abund.	m/z	abund.	m/z	abund.
151.3	0	160.55	0	171.3	12
152.05	0	161.2	0	172.3	2
152.7	0	162.2	0	173.3	7
153.05	0	163.45	0	174.3	1
153.3	0	164.65	0		
154.55	0	165.3	0		
155.3	0	166.05	0		
157.3	3	166.4	0		
158.3	0	167.55	0		
159.7	0	168.65	0		
159.95	0	169.3	0		

APPENDIX 8 A: 2-Methyl-1-hepten-3-ol mass ^{1}H NMR spectrum

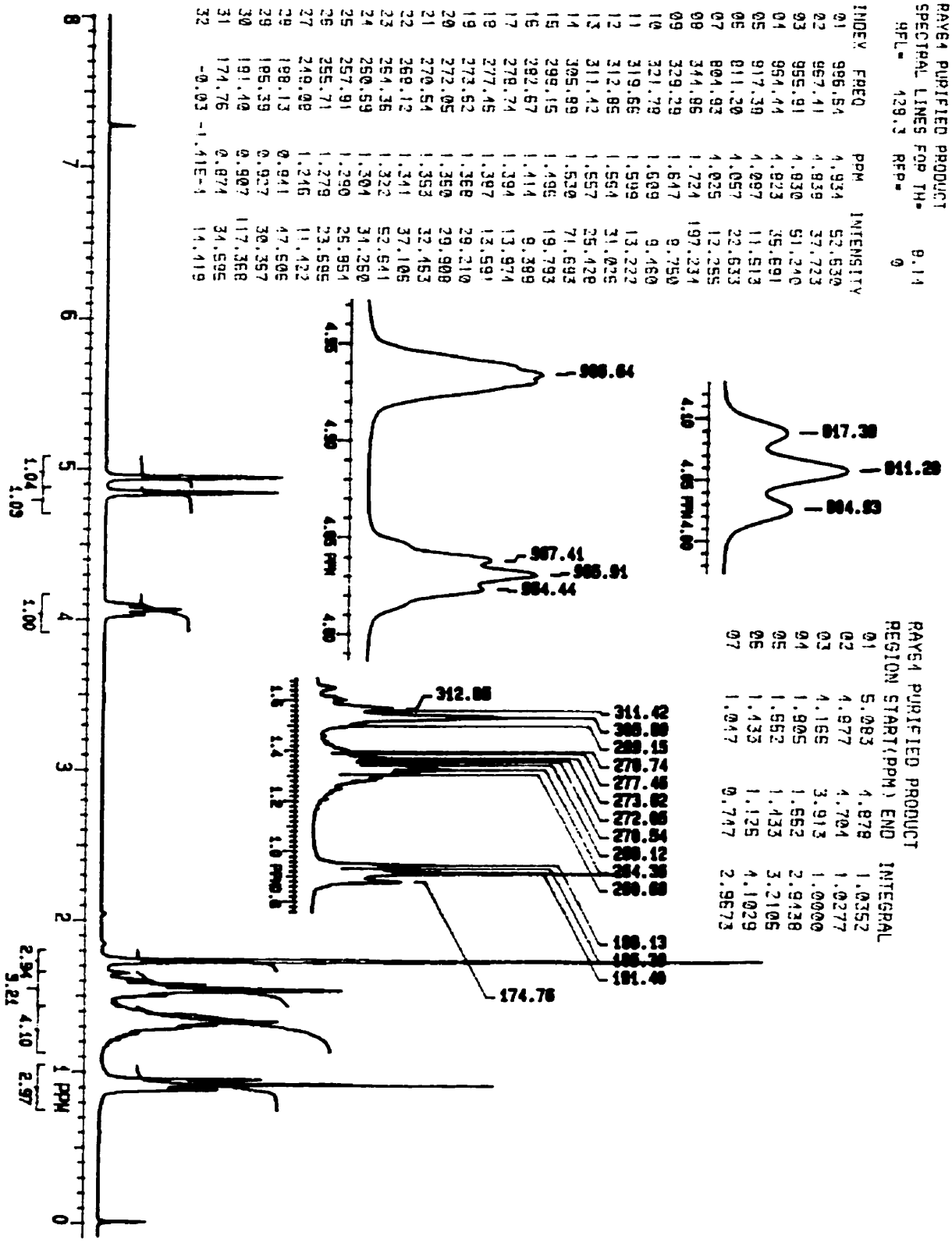

APPENDIX 8 B: 2-Methyl-1-hepten-3-ol mass ^{13}C NMR spectrum

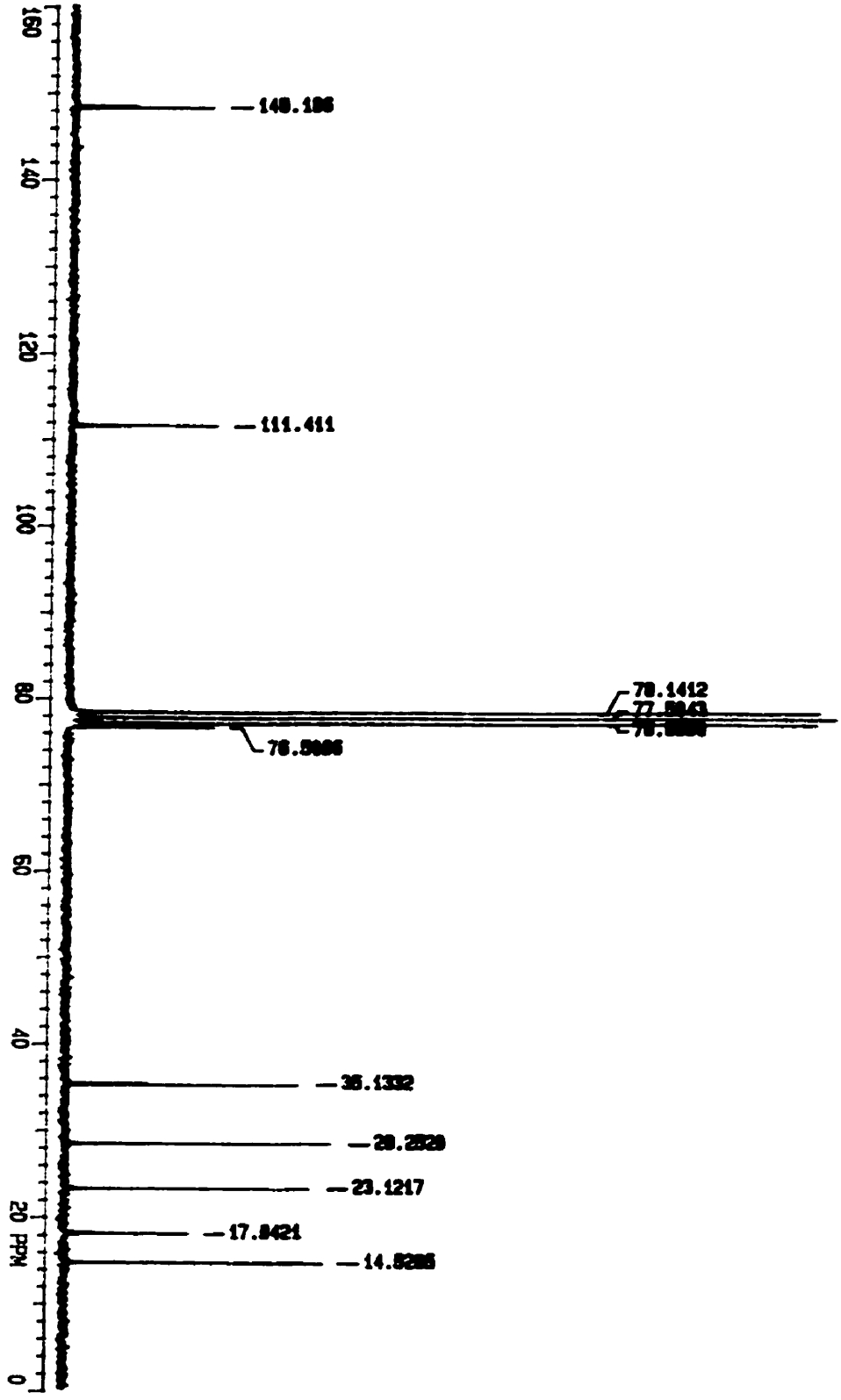

APPENDIX 8 C: 2-Methyl-1-hepten-3-ol mass spectrum (EI)

```
File         : C:\HPCHEM\1\DATA\OC5S9A.D
Operator     : Ray Bacala
Acquired     :  5 Oct 98    4:10 pm using AcqMethod RAY10JL
Instrument   :     5989B-MS
Sample Name: Sample 9 (2-Methylhept-1-en-3-ol)
Misc Info    : 1 ul inj. (50 ng/ul), mass 40-150, fw=128.21
Vial Number: 1
```

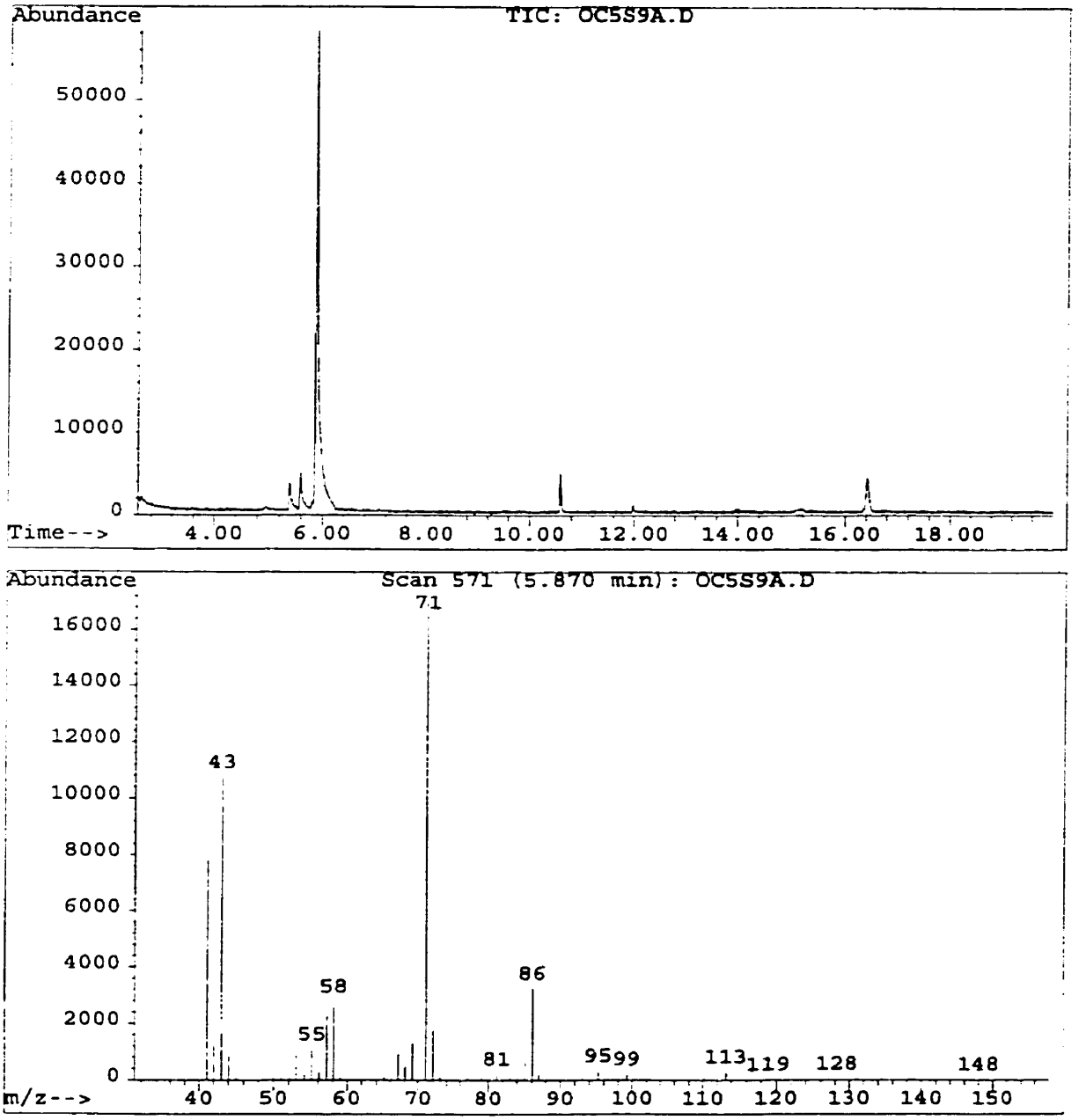

APPENDIX 8 C: 2-Methyl-1-hepten-3-ol mass spectrum (EI)

Scan 571 (5.870 min): OC5S9A.D
Sample 9 (2-Methylhept-1-en-3-ol)
Modified:scaled

m/z	abund.	m/z	abund.	m/z	abund.	m/z	abund.
41.05	45	52.15	1	62.25	0	76.1	0
42.05	7	53	5	63	0	77.1	0
43.05	62	54.15	1	64.1	0	78.35	0
44.05	5	55.15	6	65.1	1	79.1	1
45.05	3	56.15	2	67.1	5	80.2	0
45.9	0	57.15	15	68.1	3	81.2	1
46.9	0	58.15	16	69.1	8	82.1	0
47.75	0	59.15	1	71.1	100	83.1	1
49	0	60	0	72.1	10	84.1	1
50	1	60.9	0	73.1	1	85.1	5
51	1	61.75	0	74.1	0	86.1	19

Scan 571 (5.870 min): OC5S9A.D

m/z	abund.	m/z	abund.	m/z	abund.
87.1	1	103.05	0	127.3	0
88.2	0	108.3	0	128.3	0
91.2	0	109.05	0		
92.2	0	110.2	0		
93.1	0	111.3	0		
95.2	2	112.05	0		
96.1	0	113.2	2		
97.2	0	114.15	0		
98.2	0	118.9	0		
99.2	1	126.55	0		
100.2	0	126.9	0		

APPENDIX 8 D: 2-Methyl-1-hepten-3-ol mass spectrum (PCI)

```
File        : C:\HPCHEM\1\DATA\RAYPCI9.D
Operator    : Ray Bacala
Acquired    :  6 Oct 98  11:18 am using AcqMethod RAYPCI
Instrument :    5989B-MS
Sample Name: Sample 9 (2-Methylhept-1-en-3-ol)
Misc Info   : 1 ul inj. (50 ng/ul), mass 60-150, fw=128.21
Vial Number: 1
```

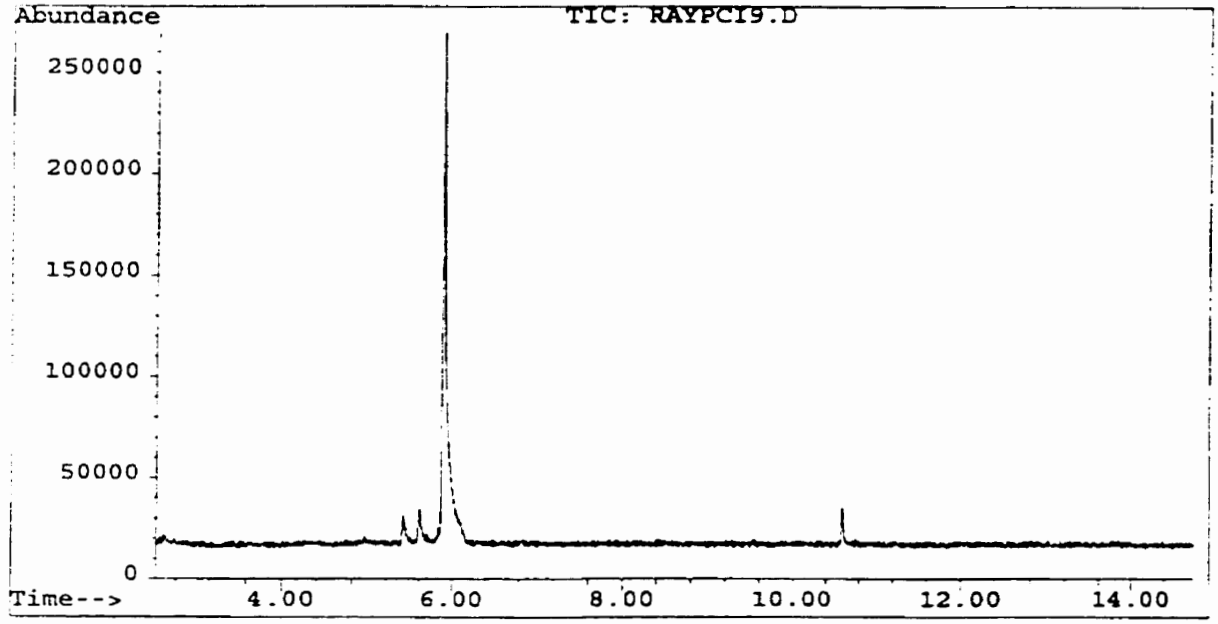

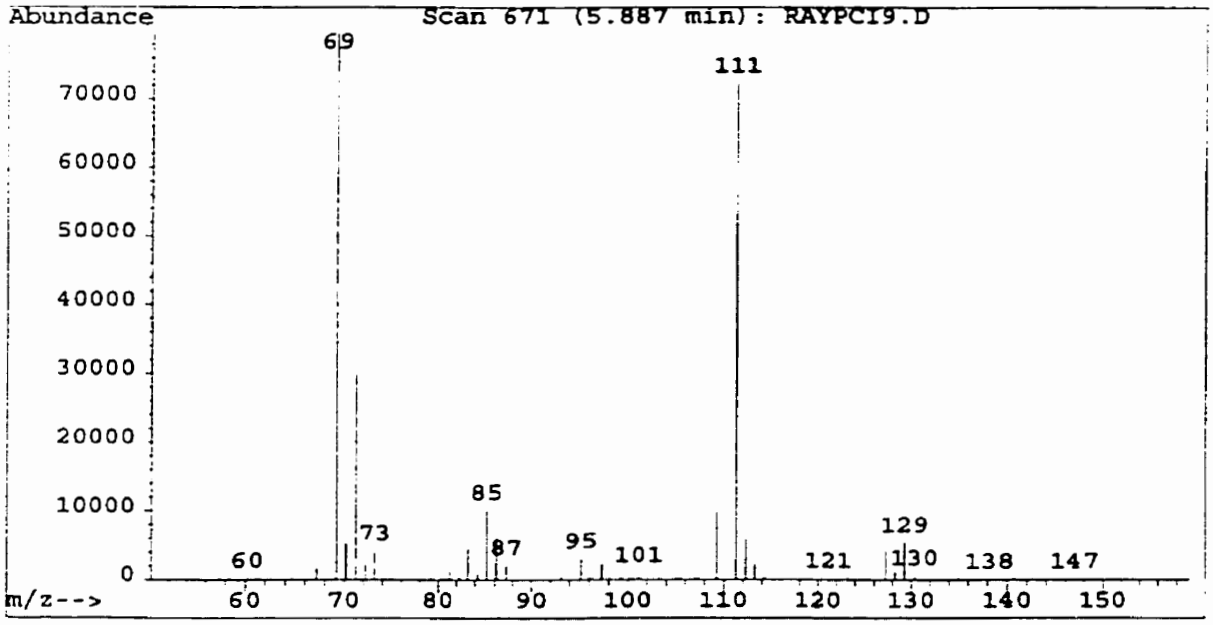

APPENDIX 8 D: 2-Methyl-1-hepten-3-ol mass spectrum (PCI)

Scan 671 (5.887 min): RAYPCI9.D
Sample 9 (2-Methylhept-1-en-3-ol)
Modified:scaled

m/z	abund.	m/z	abund.	m/z	abund.	m/z	abund.
60.25	0	73.2	5	84.3	1	95.15	4
61.25	0	74.1	0	85.2	13	96.05	0
62	0	74.95	0	86.2	8	97.3	3
63.1	0	75.95	0	87.3	3	98.15	0
64.25	0	77.1	0	88.3	0	99.3	1
65.1	0	77.85	0	89.2	0	100.15	0
67.2	2	79.2	0	90.05	0	101.15	1
69.2	100	80.2	0	91.2	0	102.05	0
70.2	7	81.2	2	92.05	0	103.15	0
71.2	38	82.3	1	93.2	1	104.05	0
72.2	3	83.2	6	94.15	0	105.15	0

Scan 671 (5.887 min): RAYPCI9.D

m/z	abund.	m/z	abund.	m/z	abund.
106.3	0	117.25	0	128.25	1
107.15	0	118.15	0	129.25	7
109.25	12	119.25	0	130.35	1
111.25	91	120.4	0		
112.25	8	121.15	0		
113.25	3	122.25	0		
114.25	0	123.25	1		
114.9	0	124.35	0		
115.15	0	125.35	0		
115.5	0	126.1	0		
116.25	0	127.25	6		

APPENDIX 9 A: Methyl 4-methylnon-4-enoate ^{1}H NMR spectrum

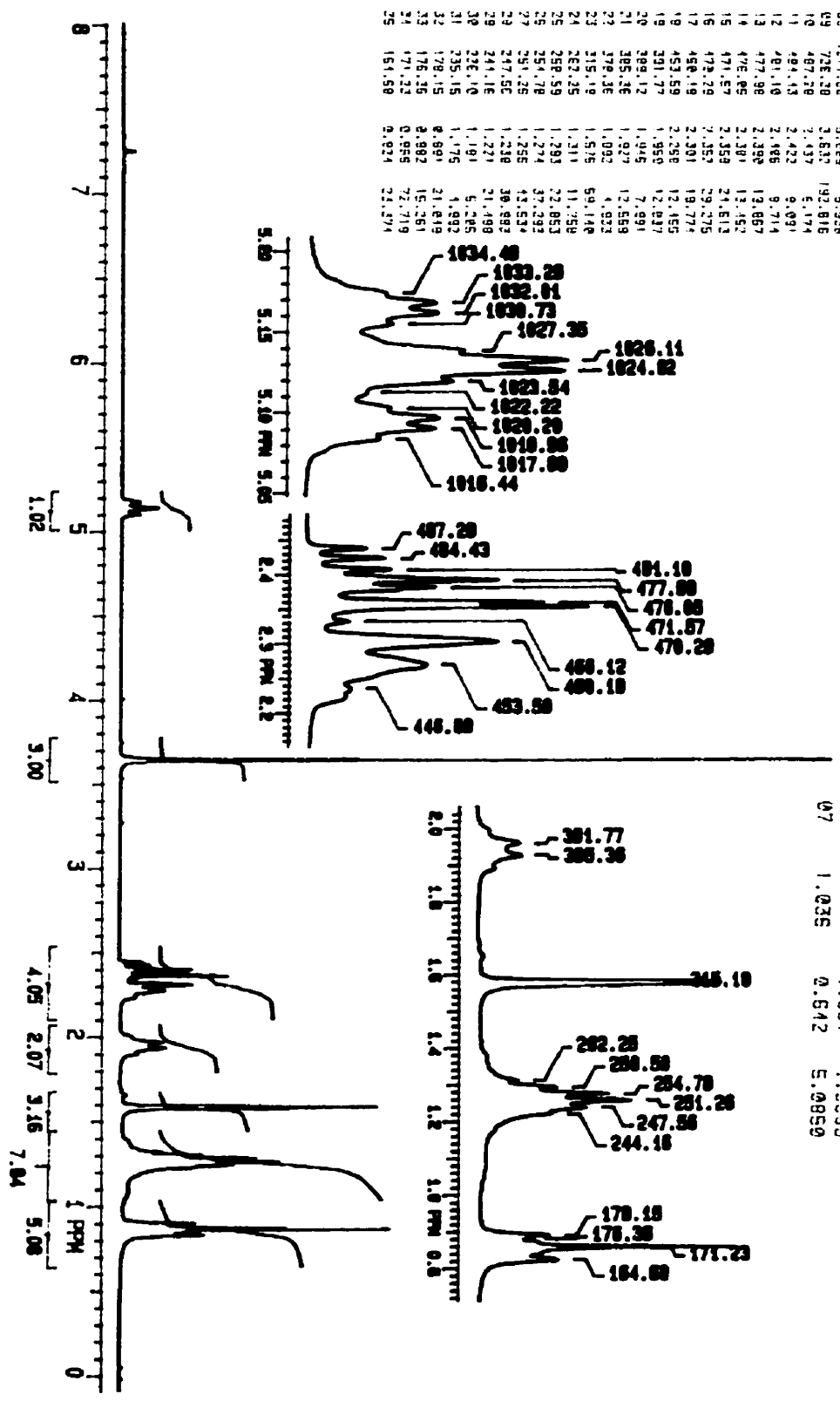

APPENDIX 9 B: Methyl 4-methylnon-4-enoate ^{13}C NMR spectrum

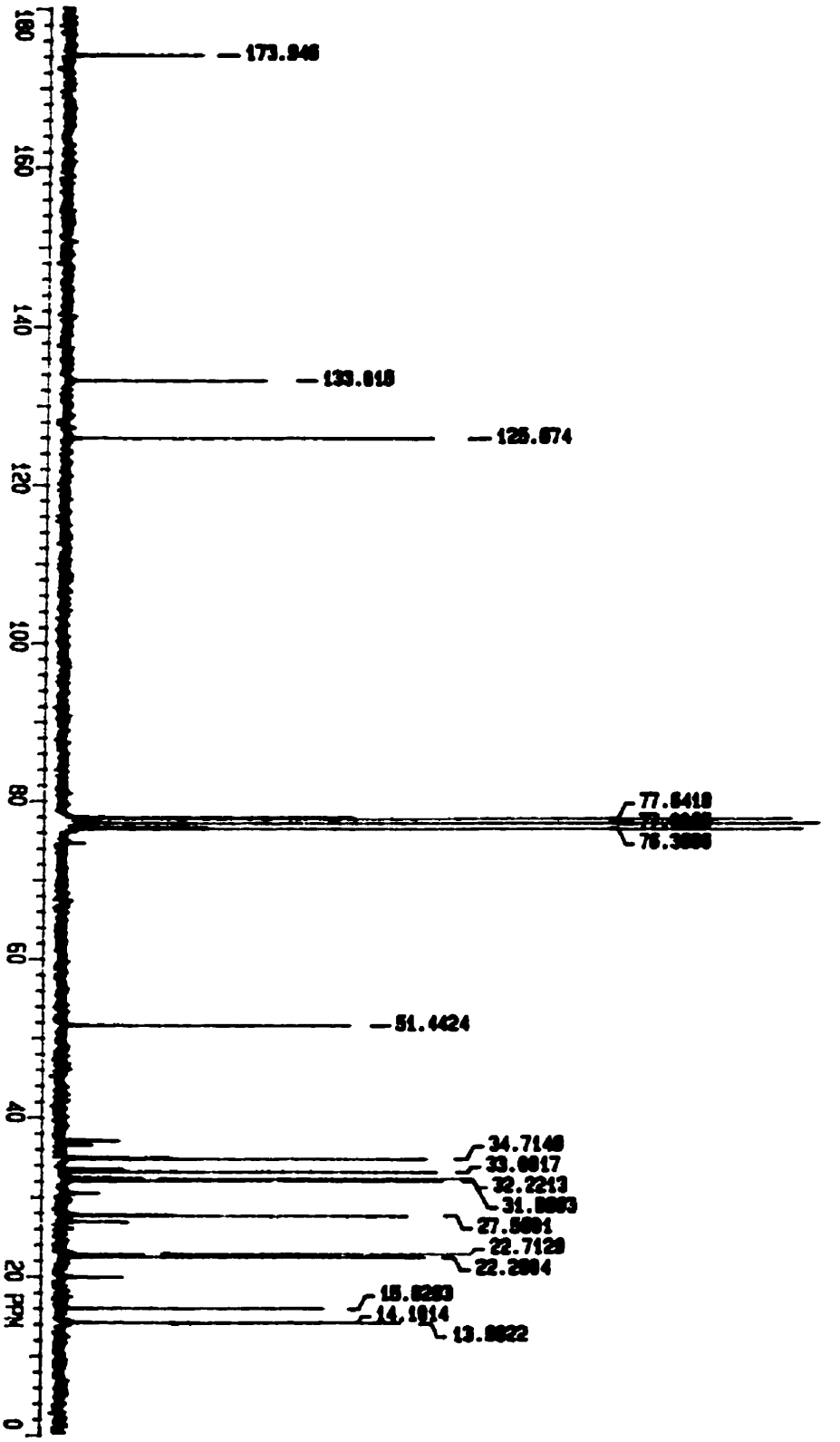

APPENDIX 10 A: Methyl 4-methylnonanoate ^{1}H NMR spectrum

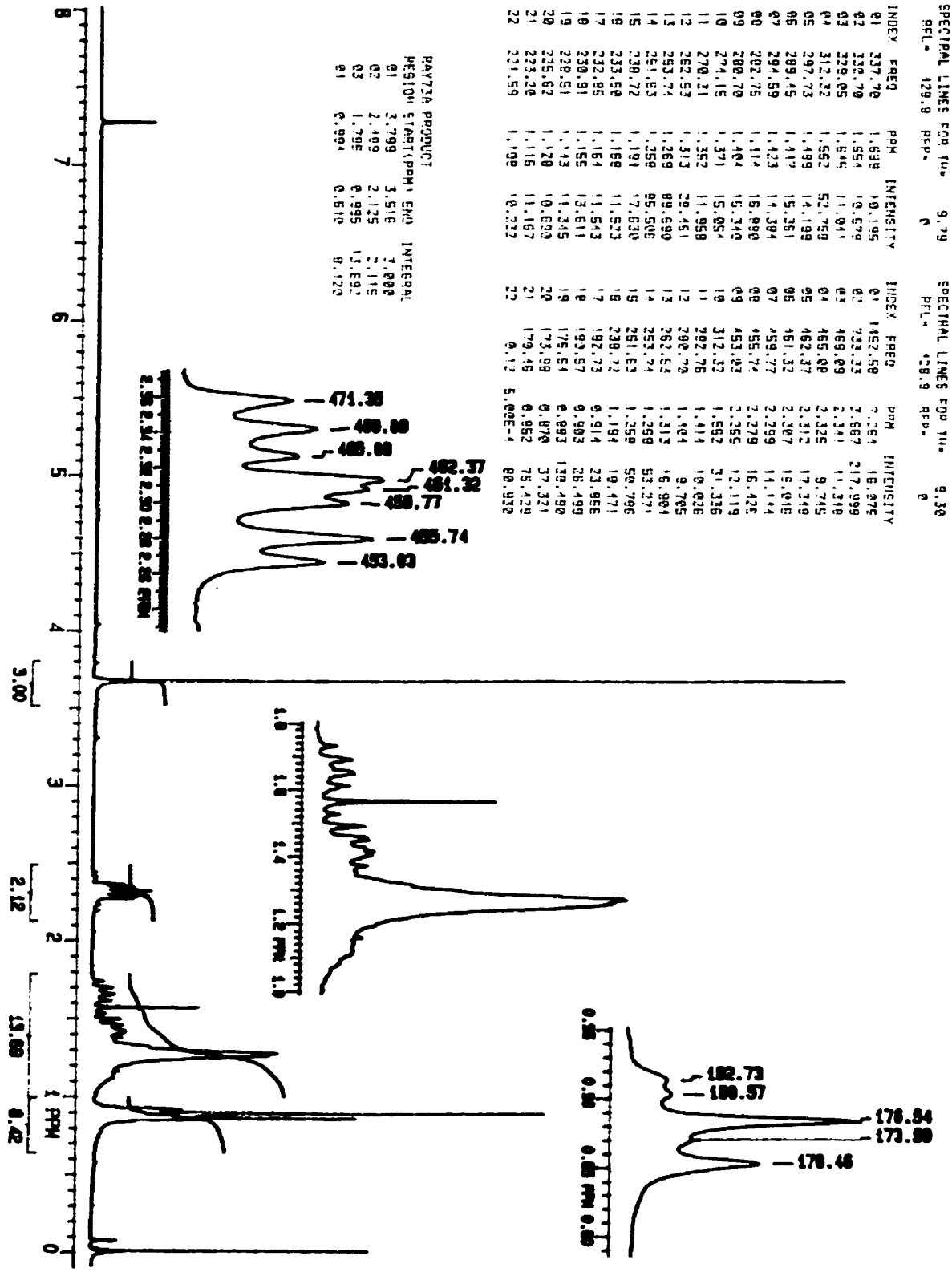

APPENDIX 10 B: Methyl 4-methylnonanoate ^{13}C NMR spectrum

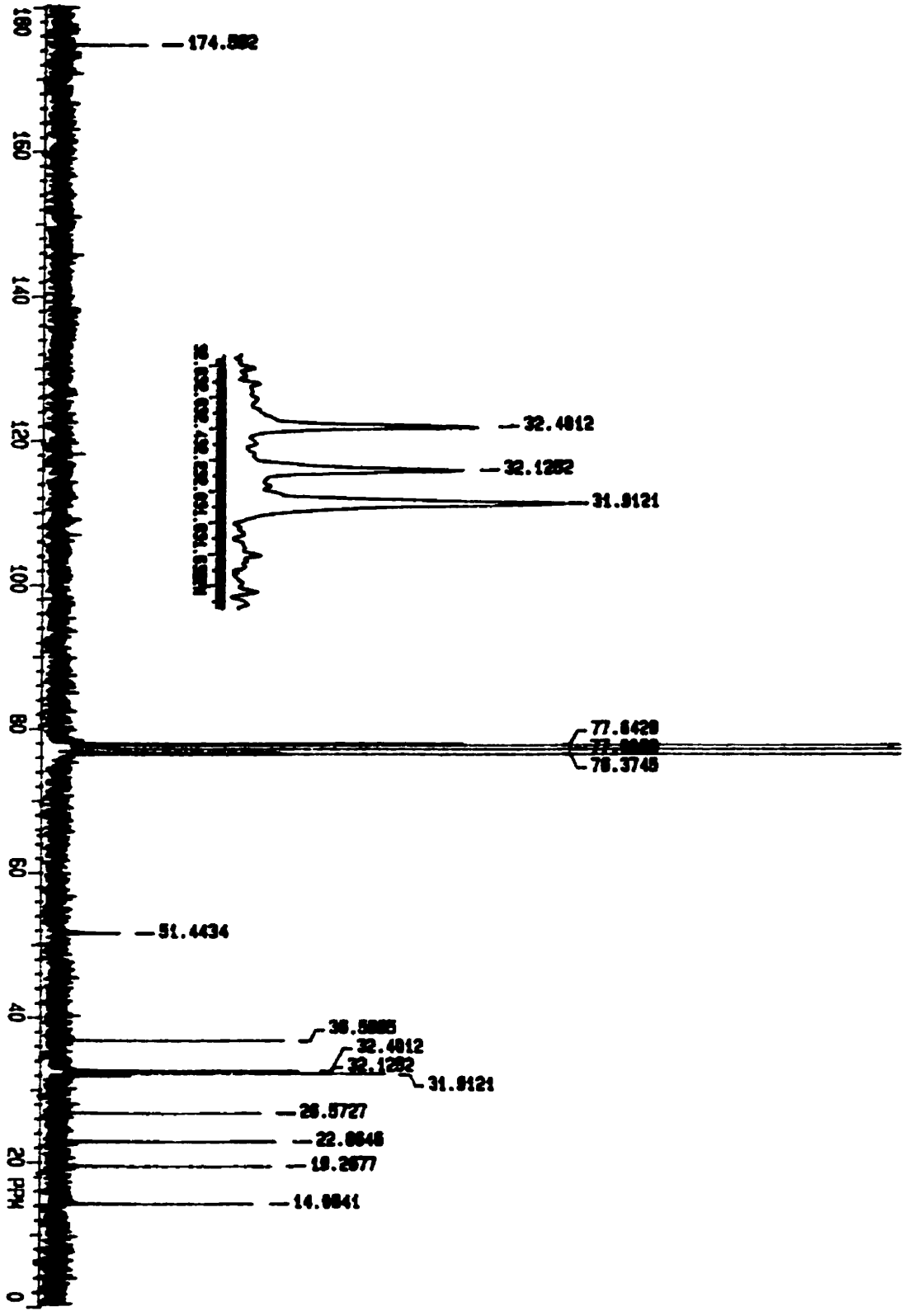

APPENDIX 10 C: Methyl 4-methylnonanoate mass spectrum (EI)

```
File         : C:\HPCHEM\1\DATA\JL14S5A.D
Operator     : Ray Bacala
Acquired     : 14 Jul 98    3:22 pm using AcqMethod RAY10JL
Instrument   :     5989B-MS
Sample Name: Sample 5 (methyl 4-methylnonanoate)
Misc Info    : 1 ul inj (50.0 ng/ul), mass 40-200, fw=186.2
Vial Number: 1
```

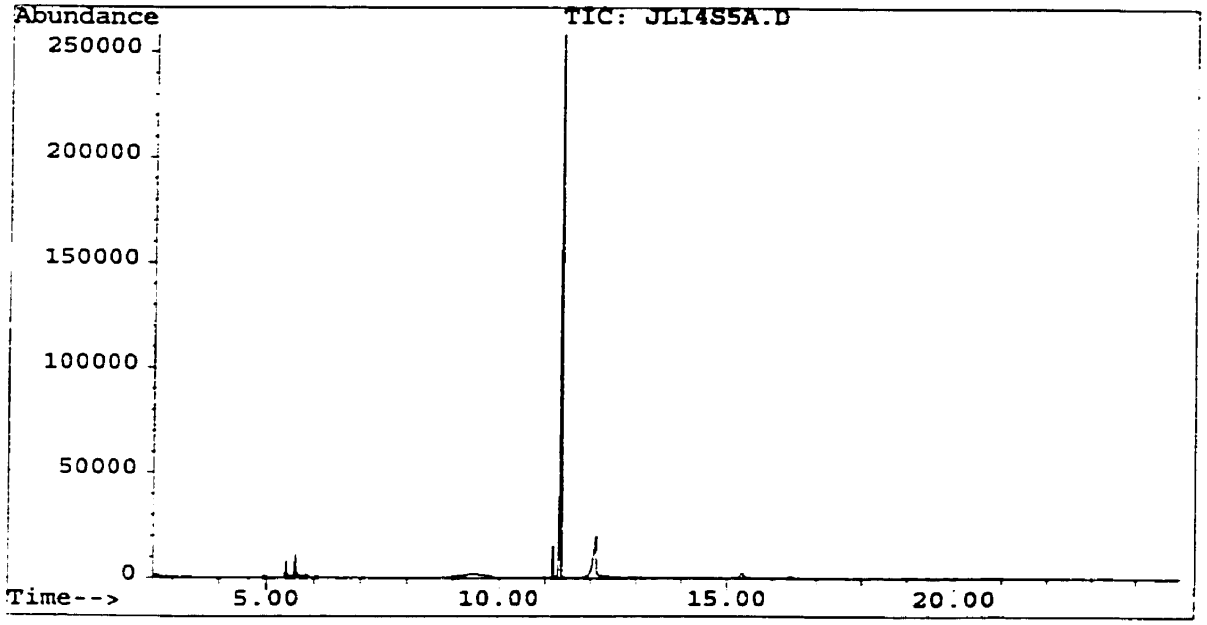

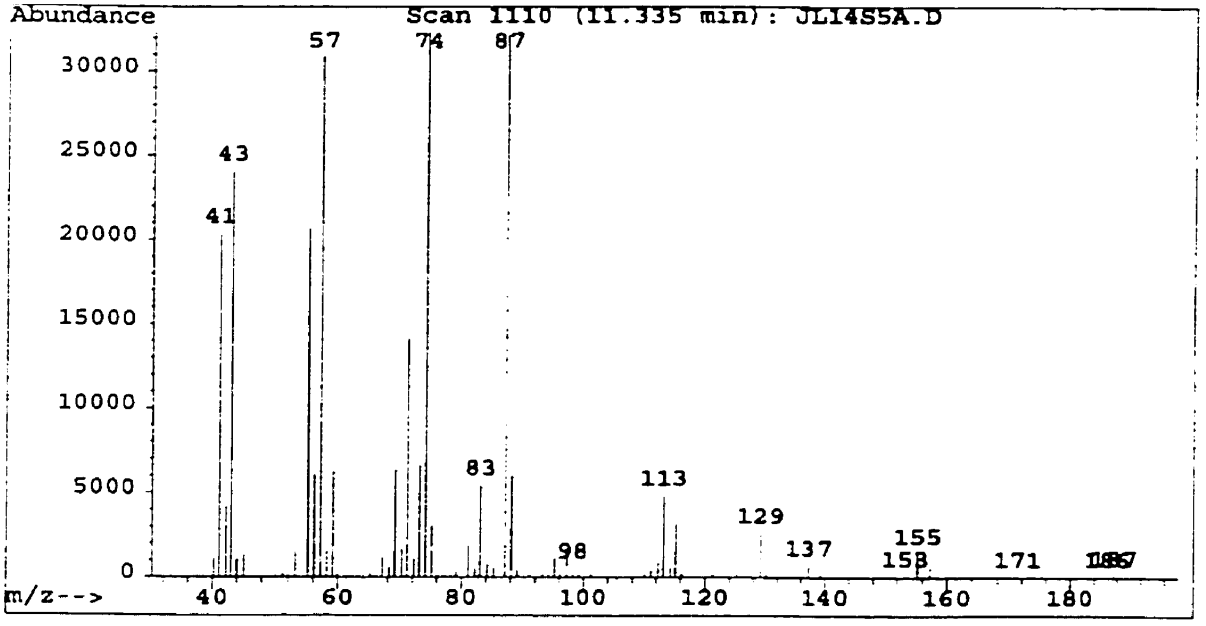

APPENDIX 10 C: Methyl 4-methylnonanoate mass spectrum (PCI)

Scan 1110 (11.335 min): JL14S5A.D
Sample 5 (methyl 4-methylnonanoate)
Modified:scaled

m/z	abund.	m/z	abund.	m/z	abund.	m/z	abund.
40.15	4	51.15	1	62.25	0	74.15	100
41.05	63	52.15	0	63.15	0	75.15	10
42.15	13	53.15	5	65.15	1	76.15	1
43.05	74	55.15	64	66.15	0	77.15	1
44.05	3	56.15	19	67.15	4	78.25	0
45.05	4	57.15	96	68.25	2	79.15	1
46.15	0	58.15	5	69.15	20	81.15	6
46.9	0	59.15	19	70.25	5	82.25	2
48.05	0	60	1	71.15	44	83.1	17
49.15	0	61.15	0	72.25	3	84.25	2
50.05	0	62	0	73.15	21	85.25	2

Scan 1110 (11.335 min): JL14S5A.D

m/z	abund.	m/z	abund.	m/z	abund.	m/z	abund.
87.1	100	98.25	2	113.2	15	129.2	8
88.1	19	99.25	0	114.35	2	130.2	1
89.1	1	100.5	0	115.2	10	135.3	0
90.25	0	101.25	1	116.2	1	136.3	0
91.1	0	102.25	0	117.2	0	137.3	2
92.25	0	107.2	0	121.35	0	138.3	0
93.25	1	108.2	0	122.35	0	139.3	1
94.25	0	109.2	0	123.2	0	140.45	0
95.25	4	110.2	1	125.2	0	143.3	0
96.25	1	111.2	1	126.2	0	144.2	0
97.25	5	112.35	3	127.3	0	152.4	0

Scan 1110 (11.335 min): JL14S5A.D

m/z	abund.
153.3	0
155.3	4
156.3	1
157.3	2
158.3	0
171.3	0
186.25	0
187.4	0
188.4	0

APPENDIX 10 D: Methyl 4-methylnonanoate mass spectrum (PCI)

```
File        : C:\HPCHEM\1\DATA\RAYPCI5.D
Operator    : Ray Bacala
Acquired    :  6 Oct 98   1:55 pm using AcqMethod RAYPCI
Instrument :     5989B-MS
Sample Name: Sample 5 (Methy 4-methylnonanoate)
Misc Info   : 1 ul inj. (50 ng/ul), mass 60-200, fw=186.2
Vial Number: 1
```

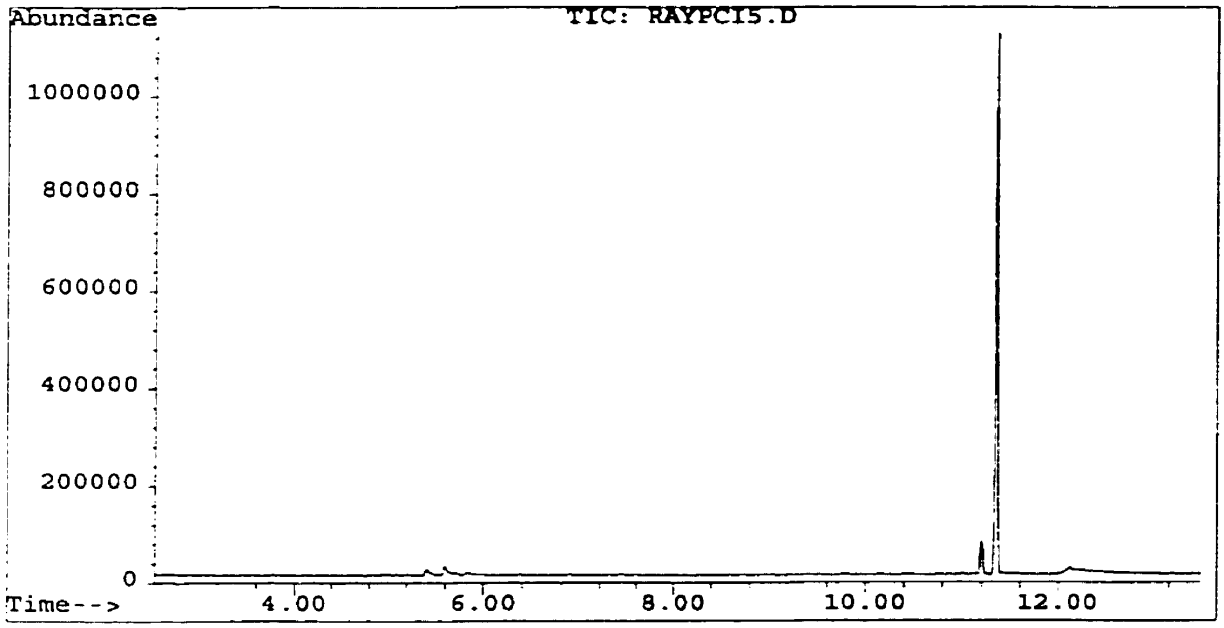

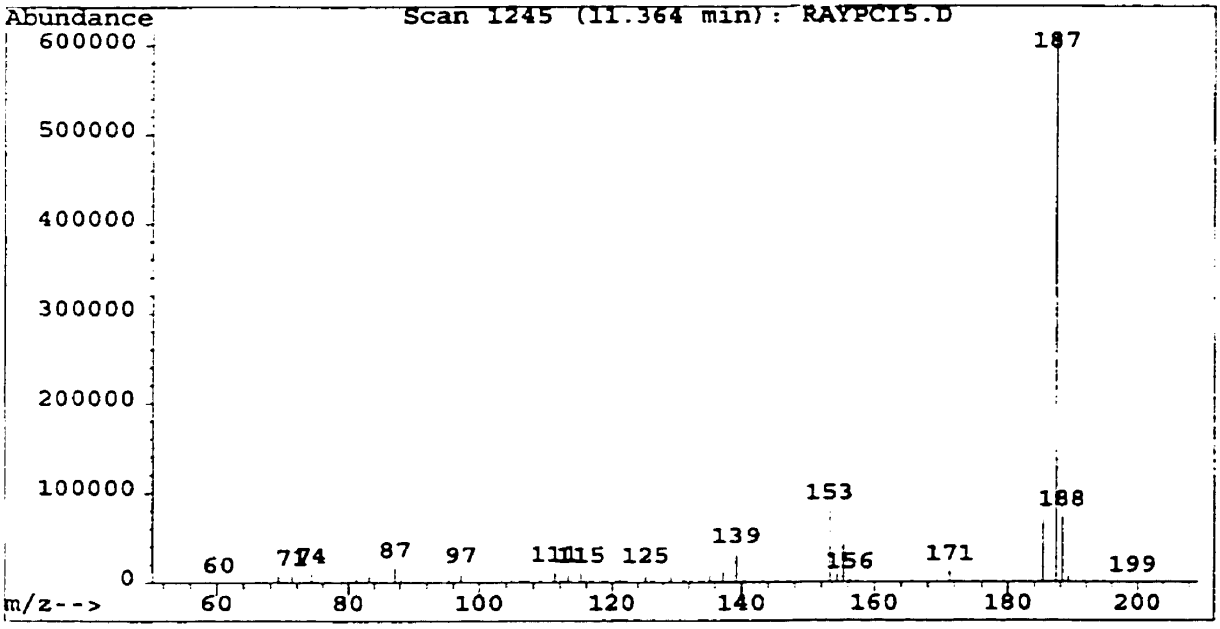

APPENDIX 10 D: Methyl 4-methylnonanoate mass spectrum (PCI)

Scan 1245 (11.364 min): RAYPCI5.D
Sample 5 (Methy 4-methylnonanoate)
Modified:scaled

m/z	abund.	m/z	abund.	m/z	abund.	m/z	abund.
60.35	0	70.2	0	80.3	0	91.8	0
61.1	0	71.2	1	81.2	1	93.3	0
62.25	0	72.35	0	82.2	0	94.15	0
63.1	0	73.2	0	83.2	1	95.3	1
63.75	0	74.2	2	84.2	0	97.15	2
64	0	75.2	0	85.3	0	98.15	0
65.35	0	76.1	0	87.2	3	99.3	0
66.35	0	77.35	0	88.2	0	100.15	0
67.1	0	77.85	0	89.2	0	101.15	0
68.1	0	78.35	0	90.2	0	102.15	0
69.2	1	79.1	0	91.2	0	103.3	0

Scan 1245 (11.364 min): RAYPCI5.D

m/z	abund.	m/z	abund.	m/z	abund.	m/z	abund.
104.15	0	117.25	0	131.25	0	144.45	0
105.15	0	118.15	0	132.25	0	145.35	0
106.05	0	119.4	0	133.25	0	146.35	0
107.3	0	121.25	0	133.75	0	147.2	0
108.05	0	122.25	0	135.25	1	148.35	0
109.15	0	123.25	0	136.25	0	149.35	0
111.25	2	125.25	2	137.2	2	150.45	0
112.25	0	126.25	0	139.2	5	151.2	0
113.25	1	127.35	0	140.35	0	153.2	13
115.25	2	129.25	1	141.2	0	154.3	1
116.25	0	130.35	0	143.2	0	155.3	7

Scan 1245 (11.364 min): RAYPCI5.D

m/z	abund.	m/z	abund.	m/z	abund.	m/z	abund.
156.3	1	167.8	0	179.4	0	191	0
157.3	0	168.55	0	180.25	0	191.9	0
158.3	0	169.3	0	181.4	0	192.85	0
159.3	0	171.3	2	182.15	0	194.25	0
160.05	0	172.3	0	182.65	0	195.35	0
161.2	0	173.4	0	183.25	0	196.25	0
162.55	0	174.05	0	185.25	11	197.35	0
163.2	0	175.15	0	187.25	100	198.25	0
164.55	0	176.15	0	188.25	12	199.25	0
165.15	0	177.4	0	189.25	1		
167.15	0	178.05	0	190.4	0		